Characterizing the cargo binding and regulatory function of the tail domain in Ncd motor protein

Natalie E. Lonergan

Thesis submitted to the faculty of the Virginia Polytechnic Institute and State University
in partial fulfillment of the requirements for the degree of

Master of Science
In
Biological Sciences

Richard A. Walker, Ph.D., Chair
Jill C. Sible, Ph.D.
Eric A. Wong, Ph.D.

October 9, 2009
Blacksburg, VA

Keywords: Non-claret disjunctional; Kinesin-14 motor proteins; nuclear localization signal

Characterizing the cargo binding and regulatory function of the tail domain in Ncd motor protein

Natalie E. Lonergan

(ABSTRACT)

Non-claret disjunctional (Ncd) is a Kinesin-14 microtubule motor protein involved in the assembly and stability of meiotic and mitotic spindles in *Drosophila* oocytes and early embryos, respectively. Ncd functions by cross-linking microtubules through the tail and motor domains. It was originally believed that the role of the Ncd tail domain was to only statically bind microtubules. However, the Ncd tail domain has recently been shown to have properties that stabilize and bundle microtubules, and contribute to the overall motility of the Ncd protein. Continued characterization of the Ncd tail domain is essential to understanding the complete role of Ncd in cell division. This work explored the regulatory function and microtubule binding properties of the Ncd tail domain.

Ncd activity is regulated during interphase by nuclear sequestration. GFP-Ncd fusion proteins, containing full length Ncd, individual Ncd domains, or combinations of Ncd domains, were used to identify the presence of a nuclear localization signal (NLS) in the Ncd polypeptide. The nuclear localization of only the GFP fusion proteins incorporating the Ncd tail domain sequence indicates that the NLS is contained within the tail domain. Subsequent experiments performed with GFP fusion proteins containing segments of the tail domain indicated that essential NLS amino acid residues are located along the length of the tail domain sequence.

Attempts to characterize the microtubule binding properties of the Ncd tail domain, using bacterially expressed MBP2-Ncd tail-stalk, were unsuccessful. MBP2-Ncd tail-stalk proteins aggregated under binding assay conditions, preventing an accurate determination of the stoichiometric binding relationship between Ncd and the tubulin dimer.

Acknowledgements

I consider myself fortunate to have experienced graduate life at Virginia Tech, and I would like to express my gratitude to the faculty, staff, and fellow graduate students who were responsible for shaping that experience. Firstly, I want to sincerely thank my committee members, Drs. Jill Sible and Eric Wong, and especially my committee chair Dr. Richard Walker for their efforts and patience. I am eternally grateful that Dr. Walker kindly brought me into his laboratory with little to no research experience. Dr. Walker's investment of time and effort in introducing me to biological research was tremendous, and I have and will continue to appreciate his role in my professional development.

I would also like to express my appreciation to Mrs. Sue Rasmussen, who made my degree completion possible by patiently answering my numerous questions, and by tirelessly helping me submit the necessary degree documentation. Of course, my graduate experience was enhanced by the Walker lab members. Thank you to the Lindsey Fierer and Brie Barnes who both tediously scanned and categorized SDS-PAGE gels, which made the process of writing my thesis off-campus much easier, and to Elizabeth Lamb for her assistance and friendship. These women brightened days in the laboratory with laughter and easy spiritedness, both of which are essential given the highs and lows of scientific research. I would also like to thank Matthew Arnold for his camaraderie and endless banter, without which the lab would have been much less entertaining.

Funding was partly provided through the Graduate Research Development Project, for which I would like to acknowledge and thank the Virginia Tech Graduate Student Assembly.

To my good friends, Amy Lewis, Nicole Ganzala, and Jennifer Pressley, I want to extend my warmest thanks and affection. I feel blessed to have met you during my graduate school experience and I look forward to many more years of your friendship.

At Eastern Virginia Medical School I would especially like to thank Dr. Claretta Sullivan, whose technical and culinary guidance has been invaluable, and Dr. David Taylor–Fishwick for his guidance and constant encouragement. I would also like to express my warmest thanks to Dr. Banumathi Cole for her friendship and technical support, and to Kim Akinyanju, who supported me more than any friend should ever have to while I completed this thesis.

Most importantly, I want to express my love and appreciation to my parents, Pamela and Robert Lonergan, and brother, Hal Lonergan, whose love and encouragement have never waivered. The knowledge of their unconditional support has allowed me to freely celebrate my successes and graciously accept my defeats, and it would be impossible for me to fully express my gratitude towards them.

Table of Contents

List of Figures

List of Tables

List of Abbreviations

ADP: adenosine diphosphate

BSA: bovine serum albumin

AMP-PNP: adenosine 5'-(β,γ-imino)-triphosphate

ATP: adenosine triphosphate

B_{max}: stoichiometric binding ratio

cand: Ncd null mutant

CFP: cyano fluorescent protein

CIAP: calf intestinal alkaline phosphatase

GFP: green fluorescent protein

GST: glutathione S-transferase

IPTG: isopropylthio-β-D-galactoside

KLP61F: kinesin-like protein 61F

MBP: maltose binding protein

MBP2: modified maltose binding protein

mRFP: monomeric red fluorescent protein

Msps: mini-spindle proteins

MT: microtubule

Ncd: non-claret disjunctional protein

NES: nuclear export signal

NLS: nuclear localization signal

NT6: monomeric Ncd tail protein

PCR: polymerase chain reaction

P_i: inorganic phosphate

SDS-PAGE: sodium dodecyl sulfate polyacrylamide gel electrophoresis

TMTs: taxol-stabilized microtubules

TRX: thioredoxin

Chapter 1: Literature Review of Non-Claret Disjunctional Protein (Ncd)

Introduction

Propagation of germ cells and somatic cells occurs through meiotic and mitotic cell division, respectively. The accurate execution of these sophisticated and intricately orchestrated processes is the key to healthy and viable cells. The two major participants in meiosis and mitosis are microtubules (MTs) and microtubule motor proteins, specifically, kinesin-like motors and dyneins [1]. Both motor proteins and MTs are integral to the assembly and stability of meiotic and mitotic spindles.

MTs are dynamic, polar polymers, which are composed of α- and β- tubulin subunits. Each MT has a highly dynamic end (plus end) and a less dynamic end (minus end) where polymerization and depolymerization of α-β tubulin heterodimers occur at rapid and slow rates, respectively. The ability of MTs to rapidly change in length is termed dynamic instability, and is exhibited as solely polymerization, solely depolymerization, or a combination of both where polymerization occurs at one end and depolymerization occurs at the other [2]. Therefore, the dynamic nature of MTs provides an excellent structuring scaffold for equally dynamic processes like cell division, in which changes in spindle arrangement requires both rapid reorganization and isometric periods of rest.

Motor proteins travel unidirectionally along MTs and microfilaments in order to transport cellular material within individual cells. To perform this function, motor proteins typically possess a MT or microfilament binding site, a cargo-binding site, and

an ATPase site. ATP hydrolysis provides the required energy for MT or microfilament translocation [2, 3]. Motor proteins crosslink MTs and microfilaments with motor protein specific cargo. Common types of motor protein cargo include membrane vesicles, chromosomes, MTs, microfilaments, and other cellular components. Each motor protein binds a specific cargo type. Two examples of well documented motor proteins are Kinesin-1, which is responsible for transporting membrane vesicles along axonal MTs, and myosin II, which glides along actin microfilaments in addition to binding them as cargo [2].

There is pronounced gene conservation between *Drosophila melanogaster* and human cells, including that of cell proliferation genes. Therefore, *Drosophila* cells have proven to be a convenient model for the study of cell division and the machinery that mediates cell division [4]. Furthermore, *Drosophila* cells have only four chromosomes, which permits easier observation of chromosome movement during cell division and facilitates easy manipulation of the genome. Consequently, a large bank of single gene mutations has been established [5, 6]. This, in conjunction with the advances in spindle visualization techniques (i.e. fluorescence assays), has led to advances in understanding the meiotic and mitotic processes in *Drosophila* [5]. The focus of this literature review is to outline the structure and function of the Kinesin-14 *Drosophila* motor protein, non-claret disjunctional (Ncd), and to explore the implications of Ncd activity in the meiotic oocytes and mitotic early embryos of *Drosophila melanogaster*.

Ncd organization and function

Ncd is a minus-end directed microtubule motor protein and is a Kinesin-14 member of the kinesin superfamily. Through maintenance of meiotic and mitotic spindles, Ncd ensures proper chromosome segregation during meiotic cell division in *Drosophila* oocytes and early mitotic cell division in *Drosophila* early embryos [6]. Recombinant Ncd has been purified as a homodimer, in which each monomer (700 amino acids) is composed of a tail domain, stalk domain, and motor (head) domain (Figure 1.1). The tail domain spans ~200 amino acids at the N-terminus, and possesses two MT-binding sites, which allows the tail to transport MTs as cargo [3]. In addition to cargo binding functions, the Ncd tail domain has been implicated in MT stabilization [7]. The stalk domain, which spans amino acids 199-355 of the Ncd polypeptide, mediates Ncd dimerization through a coiled-coil secondary structure. Lastly, the motor domain (amino acids 356-700) is located at the C-terminus of the Ncd polypeptide. Like the tail domain, it has MT binding capability, but in addition, possesses a highly conserved ATPase site. Thus, the motor domain performs the mechanochemical activity required for MT gliding. The Ncd motor domain sequence is ~40% homologous to the motor domain sequence in Kinesin-1, a plus end directed motor protein [3]. Regardless of sequence homology, in contrast to Kinesin-1, Ncd is a non-processive, minus-end directed motor protein [3, 8].

Ncd motors work in groups to assemble and maintain bipolar spindles, and have been localized in high numbers at spindle poles and in lower numbers on spindle MTs [9]. Ncd stabilizes spindles by crosslinking parallel MTs at spindle poles and regulates

spindle length by crosslinking and sliding anti-parallel polar MTs at the spindle mid-body [9]. Recently, for the first time it was demonstrated, *in vivo*, that Ncd mediates sliding of anti-parallel MTs at a rate similar to that demonstrated by *in vitro* motility assays [10]. Consequently, the significance of past and future *in vitro* work is increased in respect to *in vivo* application [10].

Mitosis in *Drosophila* early embryos

In mitotic embryos, Ncd crosslinks polar MTs that originate from opposing centrosomes so that the polar MT bound by the tail domain is carried as cargo and the polar MT bound by the motor domain is used as a gliding pathway. The MTs are arranged with the minus ends pointed toward the polar centrosomes. As Ncd pulls one MT as cargo and glides toward the minus end of the motor bound MT, the opposing spindle poles are pulled together [11]. Since Ncd produces an inward pull on spindle poles, it is apparent that other proteins are required to exert opposite pull in order to maintain a normal bipolar mitotic spindle. In fact, Ncd is a member of an antagonistic team of motor proteins that work in a coordinated fashion to form and maintain a bipolar spindle. Other members of this team include cytoplasmic dynein and the kinesin, KLP61F. Cytoplasmic dynein is securely attached to the cell cortex and travels toward the minus end of astral MTs. KLP61F is a member of the Kinesin-5 family. Members of this family are plus end directed, bipolar motor proteins. Like Ncd, KLP61F crosslinks polar MTs. Together cytoplasmic dynein and KLP61F generate forces that distance the two spindle poles in the mitotic bipolar spindle. The outward force placed on the spindle

poles by cytoplasmic dynein and KLP61F, is opposed by the inward force generated by Ncd (Figure 1.2.) [12]. During various stages of mitosis in early *Drosophila* embryos , the inward and outward forces are balanced to create an isometric bipolar spindle. Isometric spindles may represent checkpoints that ensure proper formation of the spindle. It is also speculated that isometric spindles offer a delay in the mitotic process to allow polymerization of polar MTs. Lengthened polar MTs increase the efficiency of spindle pole separation [13]. The time course and varying rate of spindle pole separation indicates that the three members of this antagonistic motor protein team are selectively functional at the various mitotic stages.

During prophase of mitosis, the spindle poles are separated by ~6 μm [12]. At this stage, KLP61F is still contained within the nuclear envelope; therefore, dynein is the major source of the outward force that separates the spindle poles. Ncd, while also stored in the nucleus, has been released and opposes the outward force implemented by dynein. By late prophase, Ncd eventually counteracts dynein. The balance of inward and outward forces results in an isometric state in which the spindle pole separation is maintained at ~6 μm [12, 14]. Sharp et al. utilized anti-dynein antibodies and human p50 dynamitin to inhibit dynein. Both serological inhibition and p50 inhibition of dynein produced mono-polar spindles in *Drosophila* embryos. The mono-polar spindles formed due to the loss of the outward force provided by dynein. To examine the effects of the loss of Ncd function on spindle organization, Sharp et al. [12] observed spindle formation in Ncd null-mutant embryos (ca^{nd}). The mutant embryos exhibited an increased rate of spindle pole separation and increased spindle length. There also appeared to be spindle malformation, indicated by the appearance of

“spurs”. Spurs are MTs that extend outside of the normal spindle realm. Spurs are thought to increase the probability of chromosomal loss and/or non-disjunction. Mutant (*ca*nd) embryos treated with anti-dynein antibodies demonstrated proper spindle formation, supporting the belief that there is a force balance between Ncd and dynein [12].

After nuclear envelope breakdown, KLP61F is released into the cytosol. During metaphase, KLP61F increases the outward force placed on the spindle, and the spindle poles separate to ~10 μm. Embryo cells treated with anti-KLP61F antibodies develop unstable spindles that slowly collapse and become mono-polar [12]. An isometric spindle length is obtained during metaphase and anaphase A. Although the outward forces provided by KLP61F and dynein are greater than the inward force applied by Ncd, the isometric spacing of the spindle poles results from MT polymerization and depolymerization at the plus and minus ends, respectively [13]. The joint action of the motor proteins and MT polymerization-depolymerization trends establishes the isometric state.

During anaphase B, rapid spindle pole elongation occurs [13]. The spindle poles are distanced ~14 μm apart [12]. KLP61F and MT polymerization are responsible for the rapid spindle pole separation [13]. Ncd activity during Anaphase B is almost nonexistent. Mutant embryos (*ca*nd) show similar spindle elongation in anaphase B as wild type embryos [12].

The loss of Ncd function in early, mitotic embryos results in a greater distancing between the spindle poles [15]. In Ncd null mutants (cand) and siRNA mediated knockouts, the mitotic spindles are unfocused at the poles and display MT protrusions

emitting from the spindle area [10, 15]. Chromosomes are usually bound to these extraneous MT protrusions and are consequently lost during cell division. In another effort to demonstrate the involvement of Ncd in mitotic spindle maintenance, Endow et al. [15] constructed a partial Ncd mutant, MC2, created with a deletion within the stalk domain. The MC2 mutant embryos exhibited wild-type movement and MT binding capability but had a significantly lower performance quality than wild- type Ncd, demonstrating instances of centrosome loss and centrosome splitting. However, null mutants that were augmented with MC2 showed a slight improvement in chromosomal disjunction [15]. The findings from the aforementioned experiments support the theory that spindle maintenance by Ncd prevents the loss of chromosomes and ensures normal chromosomal disjunction. The loss of Ncd function results in the loss and/or non-disjunction of chromosomes. Consequently, aneuploidy and subsequent cell death may occur [6].

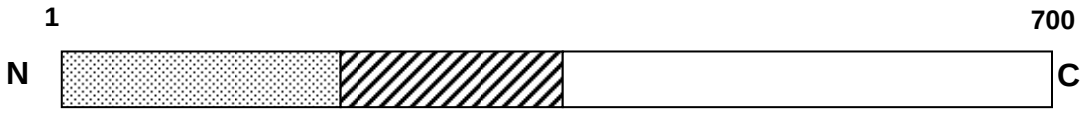

Figure 1.1. The Ncd polypeptide is composed of three functional domains.
The three designated domains of the Ncd polypeptide include: an N-terminal tail domain spanning residues ~1-200 (stippled pattern), a stalk domain spanning residues ~199-355 (diagonal stripes), and a C-terminal motor domain spanning residues 356-700 (white). The tail domain binds MTs as cargo, the stalk domain is an alpha helical segment that mediates dimerization of Ncd polypeptides via coiled-coil interactions, and the motor domain binds and glides along MTs in an ATP-dependent manner.

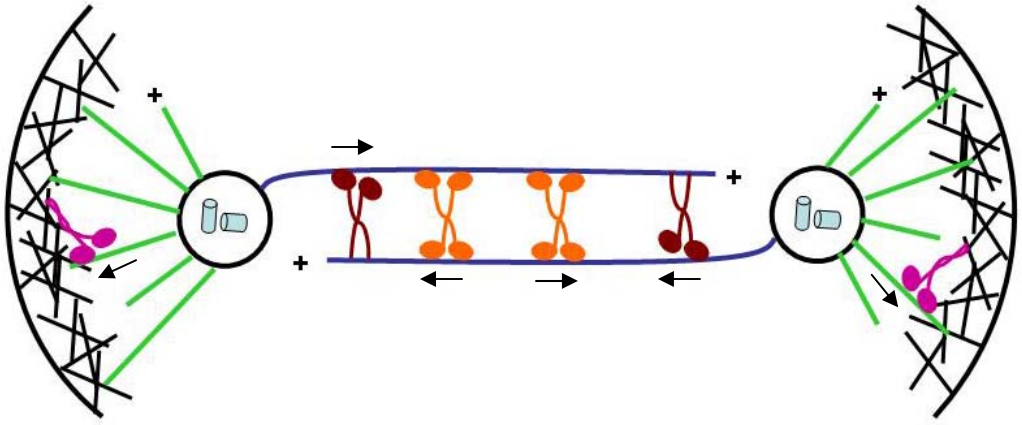

Figure 1.2. The force balance model of Ncd, KLP61F, and cytoplasmic dynein motor proteins in mitotic *Drosophila* embryos.

Ncd (red) exerts an inward force on the spindle poles in opposition to the outward forces exerted by cytoplasmic dynein (purple) and KLP61F (orange). Arrows indicate respective inward and outer forces placed on the bipolar spindle by individual motors. Ncd binds polar MTs (blue) as cargo via the tail domain and glides towards the minus-ends of motor bound polar MTs. KLP61F also binds polar MTs as cargo, but glides towards the plus-ends of polar MTs via the motor domain. Cytoplasmic dynein attaches to the cell cortex and glides towards the minus-end of astral MTs (green). The presence and quantity of each motor protein varies as a function of the cell cycle, thereby resulting in a controlled separation of the spindle poles.

Meiosis in *Drosophila* oocytes

Meiotic spindles in *Drosophila* oocytes differ from mitotic spindles in *Drosophila* early embryos in that they lack centrosomes. While *Drosophila* is one of several eukaryotic species that have been shown to form oocyte spindles without the use of a MT organizing center, the mechanism of anastral/ acentrosomal spindle formation has not been fully outlined. In many anastral meiosis spindle models, including those of *Xenopus* and mouse oocytes, the presence of centrosomal proteins like γ- tubulin and CP-60 are believed to nucleate the spindle array [16, 17]. The *Drosophila* oocyte meiosis I spindle is an example of an anastral spindle where the presence of γ-tubulin and CP-60 centrosomal proteins has not been detected, although it has been demonstrated that *Drosophila* oocytes containing γ-tubulin mutations (γ-Tub37C) produce irregularly sized asters in meiosis I spindles [18, 19]. Instead, spindle formation and maintenance in *Drosophila* oocytes is proposed to occur by Ncd mediated focusing of MTs into foci-like asters in conjunction with the stabilizing support of mini-spindle proteins (Msps) and the centrosomal protein, D-TACC [16, 20]. While the details of the process are not well defined, Ncd is believed to transport Msps (mini-spindle proteins) to the minus-end MTs at the poles of the meiotic spindle, where they are anchored by D-TACC [20]. In *Drosophila* embryos, it was demonstrated that a decrease in D-TACC levels resulted in fewer Msps being localized to the mitotic spindle pole, which in turn led to spindle destabilization. Although it is believed that in order to stabilize only those MTs associated with the astral pole, Msps primarily associate with the minus-ends of MTs, Msps have been shown to illicit MT polymerization at MT

positive-ends [20, 21]. Msps and D-TACC mediated stabilization of both anastral and astral spindle poles is highly conserved throughout evolution, which may indicate mechanistic significance [21].

Meiotic spindle assemblies are less characterized than mitotic spindle assemblies, which is in part due to the complex assembly of anastral meiotic spindles found in some species. Fortunately, with the use of wild-type Ncd fused to GFP at the C-terminus, Sköld et al. [16] made advances towards outlining meiosis I spindle assembly in *Drosophila* oocytes from the point of nuclear envelope breakdown as follows: 1) formation of “aster”-like foci by Ncd and short MTs; 2) movement of Ncd-MT “asters” towards the condensed chromosomes; 3) MT nucleation at the endobody 4) MT elongation in varying directions and subsequent re-organization and pole focusing by Ncd; 5) MT and bivalent chromosome association; 6) Ncd mediated MT crosslinking, and consequent lateral associations between bivalent chromosomes; 7) MT polymerization and subsequent Ncd mediated spindle elongation (Figure 1.3.). It is unclear what initiates nucleation of aster MTs; however, in *Xenopus* egg extracts, it has been proposed that nucleation occurs due to favorable conditions caused by the presence of chromatin in the cytoplasm [22]. Sköld et al. [16] suggests that MT nucleation may occur from the short “astral”-like MTs which act as nucleation centers, or that given the location of “asters” at the endobody, bivalent chromosome binding may be responsible.

After the conclusion of meiosis I, meiotic II spindles originate from the reorganization of the anastral meiotic I spindle poles and the *de novo* synthesis of two astral poles. Therefore, the meiotic II spindle is an anastral-astral hybrid with the

original anastral spindle separated distally and paired with the newly synthesized, central, astral poles. This arrangement results in a meiotic II spindle that is composed of two newly synthesized central spindle poles and two salvaged, distal spindle poles (Figure 1.4.). The formation of the meiotic II spindle is initiated when the central spindle pole body, a ring shaped cluster of MTs, is formed in the mid-body of the meiotic I spindle from the spindle MTs. A motor protein other than Ncd is believed to be responsible for the central spindle pole formation; however, Ncd is required to localize γ-tubulin to the central spindle pole body, via protein specific binding, where γ-tubulin nucleates and stabilizes central, astral spindle MTs [17]. Accordingly, γ-tubulin and CP-60 proteins have only been detected in regions of the *Drosophila* oocyte meiosis II spindle that are formed from spindle de novo, not from spindle material salvaged from the earlier formed meiosis I spindle [16]. In addition, Ncd stabilizes and focuses the newly nucleated MT minus-ends into poles. The proposed relationship between Ncd and γ-tubulin is further supported by the coordinated cell cycle-dependent association with the central spindle pole body, where the presence of both is detected at metaphase II and is diminished by telophase II [17].

With the loss of Ncd, the MTs polymerized for the production of the meiotic I spindle are unfocused, thereby preventing the formation of a bipolar spindle [6, 16, 17]. In contrast, during meiosis II, Ncd null mutants (ca^{nd}) demonstrate that γ-tubulin fails to localize to the mid-body of the meiotic I spindle and that MTs in the region where the spindle pole body forms begin to depolymerize [17]. Consequently, due to indirect and direct involvement of Ncd in formation and maintenance of meiotic I and II spindles, Ncd mutant oocytes exhibit irregularly formed spindles that are diffuse, multipolar, and

atypically wide. Furthermore, there is a high incident of bivalent chromosomes existing free of spindle MTs [6].

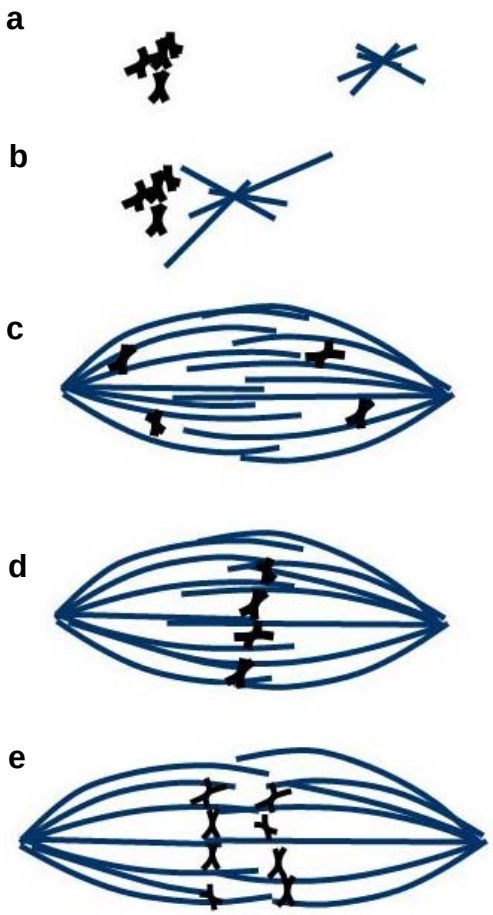

Figure 1.3. The assembly of meiotic I anastral spindles in *Drosophila* oocytes.
Illustration of the meiotic I spindle assembly: a) formation of “aster”-like foci by Ncd and short MTs; b) MT nucleation and elongation in proximity of condensed chromosomes, followed by re-organization and spindle pole focusing; c) MT and bivalent chromosome association; d) MT cross-linking and consequent lateral associations between bivalent chromosomes; e) MT polymerization and subsequent spindle elongation.

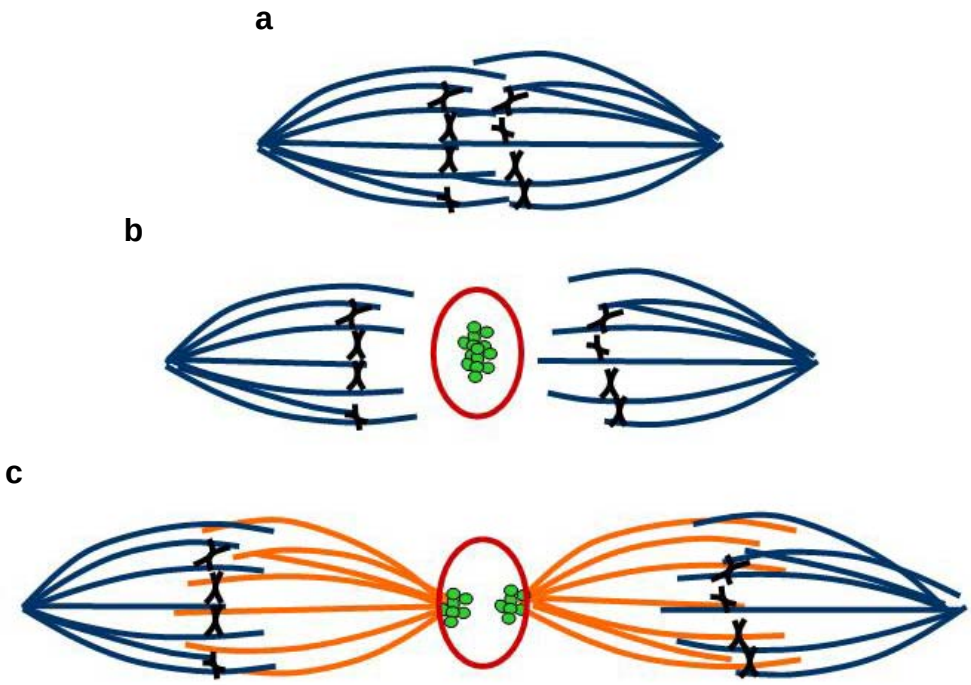

Figure 1.4. The assembly of meiotic II anastral-astral hybrid spindles in *Drosophila* oocytes. Illustration of the meiotic II spindle assembly: a) meiotic I anastral spindle; b) central spindle pole body is formed in the mid-body of the meiotic I spindle (red), where γ-tubulin (green) is then localized; c) γ-tubulin nucleates and stabilizes new central spindle MTs (orange), resulting in two anastral-astral hybrid spindles.

Interactions between the Ncd tail domain and MTs

The role of Ncd on stability and formation of the spindle MTs is integral to the successful execution of mitosis and meiosis. The mode in which Ncd affects MT dynamics is based on the binding properties between the Ncd tail domain and MTs. Cargo binding responsibility requires that the tail domain binds continuously to MTs. Fittingly, Wendt et al. [23] speculated that the rigid nature of the motor and stalk requires that the tail domain be flexible enough to maintain contact with cargo MTs. Furthermore, without the tail domain, Ncd stalk-motor constructions fail to localize to the oocyte meiosis I spindle and localize sparsely to the mitotic spindles in early embryos [24]. Therefore, the tail domain is integral to the formation maintenance of meiotic and mitotic spindles by means of MT assembly, MT stability, and MT sliding.

Two MT binding sites have been identified within the tail domain, a high affinity site at residues 83-100, and a low affinity binding site at residues 115-187 [25]. Both sites are rich in basic and proline amino acid residues, which are believed to interact electrostatically, as verified with EDC crosslinking experiments, with acidic residues found within four Ncd binding sites on the tubulin dimer [7, 23, 25, 26]. NT6, a monomeric Ncd tail protein (residues 83-187) that encompasses both low and high affinity tubulin binding sites was shown to facilitate MT assembly, bundling, and stability. NT6 induced the polymerization of free tubulin into MTs, stabilized them in depolymerizing ionic conditions, and bound MTs in co-sedimentation assays. Conversely, the failure of another monomeric Ncd tail protein, NT8 (residues 115-187), which includes only the low affinity binding site, to perform similarly to NT6 indicates that a cooperative action of both MT binding sites occurs [7]. Out of the four Ncd

binding sites on the tubulin dimer, two are internal and two are exposed on the external surface; all four sites are recognized by NT6 [23]. Consequently, NT6 monomeric Ncd tail proteins can bind to tubulin dimers at a 4:1 ratio, although this may be sterically prohibited for Ncd tail dimers. The two external Ncd binding sites are comprised of the last ~ 15 amino acids on the C-terminus of both α- and β- tubulin, a position known as the E-hook [26, 27]. Subtilisin digestion of MTs removed the E-hook, resulting in a reduced 2:1 binding ratio of NT6 to tubulin dimer, thereby confirming the presence of four binding sites [26].

While the Ncd tail domain does not confer mechanochemical derived motility to the Ncd motor protein, Fink et al. [9] recently demonstrated that Ncd tail binding to MTs may not be static, but may occur as a dynamic interaction that leads to diffusion of the tail domain along MTs. This property was demonstrated using a newly designed motility assay that eliminates issues of steric hindrance produced in conventional motility assays by binding motor proteins to a glass surface. In lieu of a glass surface, motor proteins were bound to “template” MTs arranged on a surface, thereby providing a natural binding environment. The “template” MT motility assay performed with full length, headless, and tailless Ncd-GFP constructions demonstrated that full length Ncd, and headless Ncd diffused along MTs, while tailless Ncd bound to MTs unstably and did not diffuse. This indicated that the diffusive movement is a function of the dynamic interaction between the tail domain and MTs. The addition of AMP-PNP to the motility assay resulted in loss of diffusion by full length Ncd, which suggests that strong binding of the motor domain abrogates tail diffusion as the ATPase cycle predominates. In addition to providing a more physiologically relevant motility assay, the “template” model

facilitated the discovery that the dynamic interaction of the tail domain with MTs permits transfer of Ncd dimers from one MT to another. Consequently, the force of motor activity can be coordinated by the exchange of motors proteins between anti-parallel and parallel MTs to generate coordinated-force sliding of MTs or opposing-force static crosslinking of MTs, respectively. The theory of MT transfer explains how groups of Ncd motors coordinate motor activity for precise MT positioning, as a function of the cell cycle. Cumulatively, this data suggests that full length Ncd is not only needed for crosslinking MTs but for effective translocation along MTs, and further suggests that Ncd motility is a balanced and combinative effect of both active movement by the motor and diffusion by the tail domain [9].

Interactions between the Ncd motor domain and MTs

In an effort to understand the interactions between the Ncd motor domain and MTs, EDC crosslinking studies involving bacterially expressed monomeric Ncd motor domains (MC6) and tubulin dimers were performed. Results from these experiments demonstrated that like the tail domain, the motor domain is able to bind the E-hooks of both α- and β- tubulin, but that binding of the motor domain to the tubulin dimer occurs at a 1:1 ratio [23, 28]. It is believed that a single Ncd motor simultaneously binds α- and β- subunits either between tubulin dimers or within tubulin dimers. Similarly, Kinesin-1 also exhibits a 1:1 binding ratio with the tubulin dimer and accordingly, binds MTs with 8 nm spacing or roughly the length of a tubulin dimer. Competitive binding experiments involving Kinesin-1 and Ncd indicate that Kinesin-1 binds regions on MTs that are also

partially or fully recognized by Ncd. Given these similarities, it is probable that Ncd may also exhibit an 8 nm binding pattern, which results in the 1:1 Ncd to tubulin dimer binding ratio [28].

In order to understand the role of the Ncd motor domain in MT dynamics and stability, binding of the Ncd motor domain to tubulin dimers was explored using a monomeric motor construction of residues 335-700 (Ncd335). Ncd335 was found to interact unstably with tubulin, but the interaction did not stimulate ATPase activity. Furthermore, Ncd335 completely dissociated from the tubulin dimer in the presence of ATP, making an *in vivo* interaction of the motor domain with tubulin dimers unlikely. The lack of ATPase activity by the monomeric motor domain was not a function of sequence or dimerization since a dimeric Ncd motor domain construction (residues 250-700) also demonstrated both weak tubulin dimer binding and no ATPase activity in the presence of tubulin dimers. Therefore, while it has been shown that Ncd assembles and stabilizes MTs these actions do not directly involve the motor domain [29].

Unlike Kinesin-1, which moves processively along the MT axis in a “hand over hand” coordinated fashion with both motor domains attached to the MT, Ncd moves non-processively along the MT axis with only one head attached at a time [30-32]. Thus, Kinesin-1 is a faster motor than Ncd, with a motility rate of 500-800 nm/s as compared to the 100-200 nm/s motility rate demonstrated by Ncd [33]. Slower, non-processive motility is believed to be essential for the coordinate activity of Ncd motor proteins, which work together to focus spindle poles and balance forces for isometric spindles [30, 34]. The MT binding site and the ATPase site of the motor domain are closely associated so that conformational changes at one binding site confer

conformational changes in the other. This coupling is bidirectional in that ADP, in the ATPase pocket of unbound Ncd, is released upon MT binding, thereby freeing the ATPase site for ATP binding and subsequent hydrolysis, which in turn causes the motor domain to dissociate from the MT [32, 35]. Since Ncd binds ADP stronger than ATP, ADP release has been shown to be the rate limiting step in this cycle. MT and ATP binding by the motor domain are intricately orchestrated to confer conformational changes that result in minus end or positive end directed movement of Ncd and Kinesin-1 respectively [29, 35]. An alternative, ATP-independent mode of motor domain mediated motility has been proposed in which the motor domain, stabilized by the interaction between the tail domain and the MT cargo, binds loosely to the E-hooks of tubulin and moves in a processive manner [27]. Although diffusive motility via weak binding of the motor domain has been suggested [36], the aforementioned processive movement theory has not been supported by additional outside research. Consequently, the consensus still establishes Ncd as a solely, non-processive motor.

Directionality of Movement

Directional movement of an individual Ncd motor protein occurs with only a single motor domain bound to the MT at one time. While the Ncd homodimer has a two-fold symmetry, upon binding of the single head to the MT, Ncd takes on an asymmetrical conformation as the unbound Ncd head points away from the MT and towards the minus end of the MT. The function and design of this asymmetry has been extensively studied as an explanation for Ncd minus-end directionality [31, 32, 37, 38]. Given the

high sequence similarity between the motor domains of Ncd and Kinesin-1, it is surprising that the two motor domains translocate along MTs in opposite directions. Obvious differences between Kinesin-1 and Ncd such as, domain placement, tail-stalk domain sequence, and binding patterns were suspect in conferring directionality [8].

Originally, the difference in directional movement was attributed to the respective location of the Ncd and Kinesin-1 motor domains within the polypeptide. It was hypothesized that the N-terminal location of the Kinesin-1 motor domain and the C-terminal location of the Ncd motor domain conferred plus- and minus-end directed movement, respectively. However, displacement of the Kinesin-1 motor domain to the C-terminus of a polypeptide, which was achieved by the fusion of GST to the N-terminus of the Kinesin-1 motor domain, resulted in the retention of plus-end movement. Also, data collected with the use of truncated Ncd and Kinesin-1 GST fusion proteins indicated that the loss of tail and stalk domains does not impact directionality of movement, indicating that the motor domain sequence dictates directionality. However, a direct relationship did exist between increased truncation of the stalk domain and a decrease in motility rate [8]. Accordingly, recent evidence implicates a 13 amino acid coiled-coil structure at the very end of the stalk domain, referred to as the neck, as the direction-determining factor [38]. Interestingly, 6 of the 13 amino acids in the neck are conserved among C-terminal kinesin motors. Through hydrophobic interactions the neck associates with the motor domain region near the catalytic core. The interactions between the neck and catalytic core influence the positioning of the motor domains during MT binding in a way that the unbound motor domain is directed towards the minus end. The Kinesin-1 neck also interacts with the motor domain, but does so in a

way that the unbound motor domain is directed towards the plus end. The different MT binding arrangements of the Kinesin-1 and Ncd motor domains are believed to arise from the difference in neck structure, that is, the interrupted beta strand conformation of the Kinesin-1 neck differs in motor interaction from the coiled-coil conformation of the Ncd neck. Thus, even though both the Kinesin-1 and Ncd neck regions associate at the highly conserved catalytic core, the conformational changes experienced by each motor protein upon MT binding will be differentially relayed, via the necks, to the respective unbound heads [38]. This idea was further supported by the production of Ncd/Kinesin-1 chimeras, in which the Ncd catalytic core interacts with the Kinesin-1 neck, and in which the opposite is true for the Kinesin-1 catalytic core. The chimera proteins exhibited directionality according to the respective neck sequence. Interestingly, site-directed mutagenesis of the Ncd neck eliminated the minus-end directed movement of the Kinesin-1 catalytic core/Ncd neck chimera, indicating that the Ncd neck overrides a natural tendency towards plus-end directed movement [37].

ATPase Mechanism

The accepted theoretical ATPase mechanism of Ncd centers around the belief that only one Ncd motor domain binds to the MT at a time and that a “lever-arm” rotation of the neck initiates Ncd translocation. Prior to binding the MT, Ncd is bound to ADP, and upon MT binding, ADP is released at a rate limiting speed. Yun et al. [31] proposed that upon ADP release a conformational change in the motor disrupts the connections between the catalytic core of the bound motor domain and the neck, thereby inducing a

rotation of necks, the stalk, and the unbound head towards the minus-end of the MT. In contrast, Endres et al. [30] and Wendt et al. [32] suggested that ATP binding results in the conformational change responsible for a neck rotation of ~75-90^{o}. Regardless, after ATP hydrolysis, the head dissociates from the MT with ADP plus P_i bound. Subsequently, P_i is released, and the neck returns to the original conformation, thereby reestablishing tight interactions with the respective catalytic core (Figure 1.5.)[30, 32]. Minus-end movement is achieved by the "lever-arm" rotation of the neck towards the minus-end of the MT.

The theory that the neck acts as a lever-arm is supported not only by crystallography and cryo-electron microscopy, but also by studies with truncated, extended [30, 31], and mutant Ncd proteins [31]. Ncd motor proteins that were truncated or extended at the stalk/neck region demonstrated directly proportional changes in motility rates, as is consistent with a lever-arm mechanism. ATPase levels of each altered protein were not significantly affected, thereby indicating that the alteration did not affect MT binding [30, 31]. Also consistent with the theory of a lever-arm mechanism was the identification of glycine residue 347 (G347) as a pivot point for neck rotation [31].

Contrary to other proposed ATPase mechanisms, an alternate mechanism proposed by Foster et al. [39] describes a cycle in which both motor domains are bound to the MT at the same time. Furthermore, this proposal also surrounds the belief that the two motor domains, although identical in sequence and conformation, differ in their ADP binding capabilities. One head strongly binds ADP while the other binds weakly to ADP. The motor domain that binds to the ADP weakly is the first motor to bind to the

MT. After binding, it releases the ADP quickly (18 s^{-1}) allowing the motor domain to bind ATP. After ATP hydrolysis by the first motor domain, the second motor domain binds to the MT. The conversion of ATP to ADP and P_i is necessary to induce the attachment of the second motor domain to the MT. Likewise, ATP hydrolysis is required for dissociation of the first motor domain from the MT. It is at this point that the binding of both motor domains overlaps for a short period (12 s^{-1}). The second motor domain binds ADP strongly, and upon MT binding ADP is released slowly (1.4 s^{-1}) from this motor domain. The ADP release is the rate-limiting step of this Ncd ATPase mechanism. After the release of ADP, the second motor domain binds ATP, and the subsequent hydrolysis of the ATP molecule permits the dissociation of the second motor domain from the MT. Therefore, this proposed ATPase mechanism requires the expenditure of two ATP molecules for the translocation of the Ncd dimer via both motor domains [39].

Despite findings by Foster et al. [39], which describe a two motor binding conformation of Ncd during the ATPase cycle, crystallography and cryo-electron microscopy data suggest that only one Ncd motor binds to the MT at a time [30-32]. MT binding by only one motor domain is most likely due to strong interactions between the catalytic core and neck of each monomer, which sterically prohibits double motor domain binding [32]. The role of the unbound Ncd motor domain in both motility and directionality is not well understood. Mackey et al. [34] reported that the dissociation of the bound motor domain from the MT is facilitated by the unbound motor domain. However, it is believed that Ncd motor domains cease to interact after neck rotation, and do not reconnect until after the reestablishment of neck-core interactions by MT

release [37, 38]. Additionally, experiments performed with a single-headed Ncd heterodimer showed that the absence of the unbound head had no effect on the motility of the complete monomer [30]. It is unclear whether the two motor domains take turns binding to the MT, or whether there is one motor domain that has a greater MT binding propensity [32]. Perhaps the belief that one motor domain binds ADP weaker than the other [39] correlates to a motor domain that binds MTs most often.

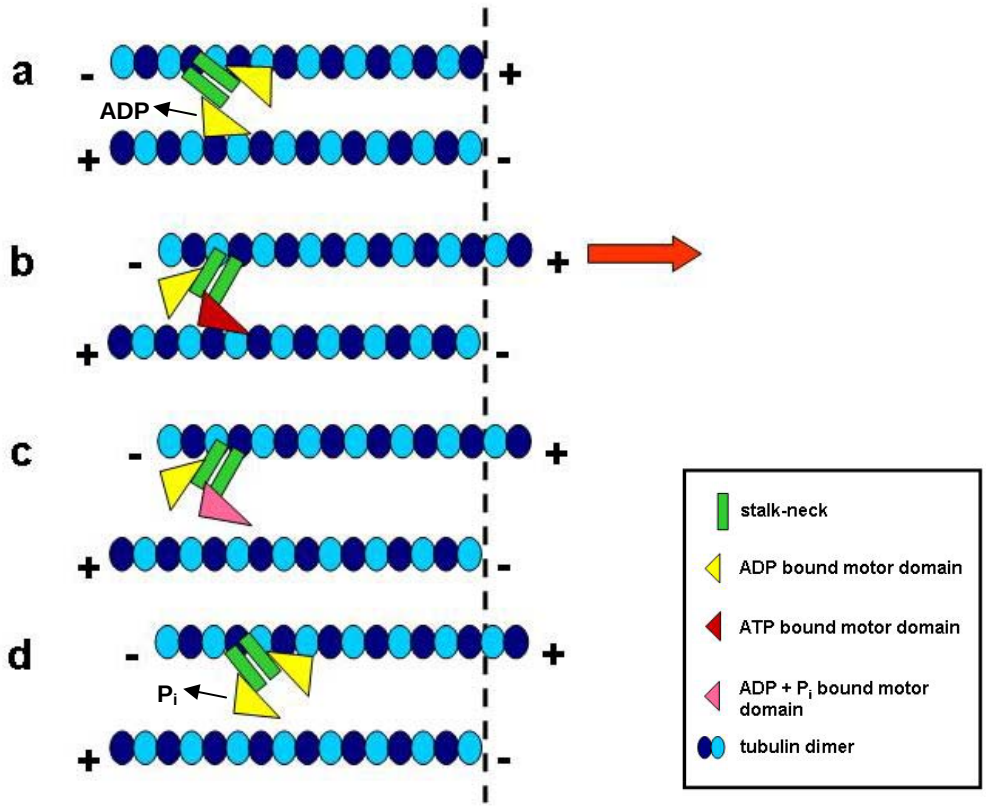

Figure 1.5. The lever arm based model of Ncd minus-end directed movement.
a) A single, ADP bound Ncd head attaches to the MT and ADP is released; b) the unbound head, and the stalk-necks of both the bound and unbound heads rotate ~75-90^{o} upon ADP release or upon ATP binding, and the cargo MT is transported towards the minus end of the motor-bound MT (red arrow); c) ATP is hydrolyzed and the bound head releases from the MT; d) P_i is released and the neck returns to the original conformation.

Conclusion

The Ncd motor domain has been extensively characterized both structurally and biochemically [23]. This is partially due to the sequence homology to Kinesin-1 [3], and perhaps because the motor domain was viewed as more dynamic and integral to the function of the Ncd motor protein than the supposedly static tail domain. However, recent studies involving the tail domain have shattered the viewpoint that the tail is a static and somewhat inert portion of the Ncd motor protein. Instead, the Ncd tail domain has been shown to induce MT polymerization, facilitate MT bundling, and to stabilize MTs in depolymerizing conditions [7]. Additionally, it has been suggested that the attachment between the tail domain and MTs is such that it allows the tail to contribute to the general motility of the motor protein by facilitating motor domain attachment to MTs and by providing a diffusion-like movement of its own [9]. Given this new position on the functional importance of the tail domain, further elucidation of tail binding properties and tail domain function is crucial to fully illustrating the role of Ncd in meiosis and mitosis. The following chapters will detail studies that were aimed at further investigating the regulatory function and binding properties of the Ncd tail domain.

References

1. Barton, N.R. and L.S. Goldstein, *Going mobile: microtubule motors and chromosome segregation.* Proceedings of the National Academy of Sciences of the United States of America, 1996. **93**(5): p. 1735-1742.
2. Lodish, H., Berk, A., Zipursky, S.L., Matsudaira, P., Baltimore, D., & Darnell, J.E., *Molecular Cell Biology*. 4th ed. 2000, New York: W.H. Freeman and Company.
3. Chandra, R., et al., *Structural and functional domains of the Drosophila ncd microtubule motor protein.* J. Biol. Chem., 1993. **268**(12): p. 9005-9013.
4. Reiter, L.T., et al., *A Systematic Analysis of Human Disease-Associated Gene Sequences In Drosophila melanogaster.* Genome Research, 2001. **11**(6): p. 1114-1125.
5. Orr-Weaver, T.L., *Meiosis in Drosophila: seeing is believing.* Proceedings of the National Academy of Sciences of the United States of America, 1995. **92**(23): p. 10443-10449.
6. Hatsumi, M. and S.A. Endow, *The Drosophila ncd microtubule motor protein is spindle-associated in meiotic and mitotic cells.* J Cell Sci, 1992. **103**(4): p. 1013-1020.
7. Karabay, A. and R.A. Walker, *The Ncd Tail Domain Promotes Microtubule Assembly and Stability.* Biochemical and Biophysical Research Communications, 1999. **258**(1): p. 39-43.
8. Stewart, R.J., J.P. Thaler, and L.S. Goldstein, *Direction of microtubule movement is an intrinsic property of the motor domains of kinesin heavy chain and*

Drosophila ncd protein. Proceedings of the National Academy of Sciences of the United States of America, 1993. **90**(11): p. 5209-5213.

9. Fink, G., et al., *The mitotic kinesin-14 Ncd drives directional microtubule-microtubule sliding.* Nat Cell Biol, 2009. **11**(6): p. 717-723.
10. Oladipo, A., A. Cowan, and V. Rodionov, *Microtubule Motor Ncd Induces Sliding of Microtubules In Vivo.* Mol. Biol. Cell, 2007. **18**(9): p. 3601-3606.
11. Sharp, D.J., et al., *Antagonistic microtubule-sliding motors position mitotic centrosomes in Drosophila early embryos.* Nat Cell Biol, 1999. **1**(1): p. 51-54.
12. Sharp, D.J., et al., *Functional Coordination of Three Mitotic Motors in Drosophila Embryos.* Mol. Biol. Cell, 2000. **11**(1): p. 241-253.
13. Brust-Mascher, I. and J.M. Scholey, *Microtubule Flux and Sliding in Mitotic Spindles of Drosophila Embryos.* Mol. Biol. Cell, 2002. **13**(11): p. 3967-3975.
14. Cytrynbaum, E.N., J.M. Scholey, and A. Mogilner, *A Force Balance Model of Early Spindle Pole Separation in Drosophila Embryos.* Biophysical Journal, 2003. **84**(2): p. 757-769.
15. Endow, S.A., et al., *Mutants of the Drosophila ncd microtubule motor protein cause centrosomal and spindle pole defects in mitosis.* J Cell Sci, 1994. **107**(4): p. 859-867.
16. Skold, H.N., D.J. Komma, and S.A. Endow, *Assembly pathway of the anastral Drosophila oocyte meiosis I spindle.* J Cell Sci, 2005. **118**(8): p. 1745-1755.
17. Endow, S.A. and D.J. Komma, *Assembly and dynamics of an anastral:astral spindle: the meiosis II spindle of Drosophila oocytes.* J Cell Sci, 1998. **111**(17): p. 2487-2495.

18. Matthies, H.J., et al., *Anastral meiotic spindle morphogenesis: role of the non-claret disjunctional kinesin-like protein.* J. Cell Biol., 1996. **134**(2): p. 455-464.

19. Tavosanis, G., et al., *Essential role for [gamma]-tubulin in the acentriolar female meiotic spindle of Drosophila.* EMBO J, 1997. **16**(8): p. 1809-1819.

20. Cullen, C.F. and H. Ohkura, *Msps protein is localized to acentrosomal poles to ensure bipolarity of Drosophila meiotic spindles.* Nat Cell Biol, 2001. **3**(7): p. 637-642.

21. Lee, M.J., et al., *Msps/XMAP215 interacts with the centrosomal protein D-TACC to regulate microtubule behaviour.* Nat Cell Biol, 2001. **3**(7): p. 643-649.

22. Heald, R., et al., *Self-organization of microtubules into bipolar spindles around artificial chromosomes in Xenopus egg extracts.* Nature, 1996. **382**(6590): p. 420-425.

23. Wendt, T., et al., *A Structural Analysis of the Interaction between ncd Tail and Tubulin Protofilaments.* Journal of Molecular Biology, 2003. **333**(3): p. 541-552.

24. Hallen, M.A., Z.-Y. Liang, and S.A. Endow, *Ncd motor binding and transport in the spindle.* J Cell Sci, 2008. **121**(22): p. 3834-3841.

25. Karabay, A. and R.A. Walker, *Identification of Microtubule Binding Sites in the Ncd Tail Domain* Biochemistry, 1999. **38**(6): p. 1838-1849.

26. Karabay, A. and R.A. Walker, *Identification of Ncd tail domain-binding sites on the tubulin dimer.* Biochemical and Biophysical Research Communications, 2003. **305**(3): p. 523-528.

27. Furuta, K.y. and Y.Y. Toyoshima, *Minus-End-Directed Motor Ncd Exhibits Processive Movement that Is Enhanced by Microtubule Bundling In Vitro.* Current Biology, 2008. **18**(2): p. 152-157.

28. Walker, R.A., *ncd and kinesin motor domains interact with both alpha- and beta-tubulin.* Proceedings of the National Academy of Sciences of the United States of America, 1995. **92**(13): p. 5960-5964.

29. Smyczynski, C., J. Derancourt, and P. Chaussepied, *Regulation of ncd by the oligomeric state of tubulin.* Journal of Molecular Biology, 2000. **295**(2): p. 325-336.

30. Endres, N.F., et al., *A lever-arm rotation drives motility of the minus-end-directed kinesin Ncd.* Nature, 2006. **439**(7078): p. 875-878.

31. Yun, M., et al., *Rotation of the stalk/neck and one head in a new crystal structure of the kinesin motor protein, Ncd.* EMBO J, 2003. **22**(20): p. 5382-5389.

32. Wendt, T.G., et al., *Microscopic evidence for a minus-end-directed power stroke in the kinesin motor ncd.* EMBO J, 2002. **21**(22): p. 5969-5978.

33. Foster, K.A., J.J. Correia, and S.P. Gilbert, *Equilibrium Binding Studies of Non-claret Disjunctional Protein (Ncd) Reveal Cooperative Interactions between the Motor Domains.* J. Biol. Chem., 1998. **273**(52): p. 35307-35318.

34. Mackey, A.T. and S.P. Gilbert, *Moving a Microtubule May Require Two Heads: A Kinetic Investigation of Monomeric Ncd* Biochemistry, 2000. **39**(6): p. 1346-1355.

35. Morii, H., et al., *Removal of Tightly Bound ADP Induces Distinct Structural Changes of the Two Tryptophan-Containing Regions of the ncd Motor Domain.* J Biochem, 2005. **138**(1): p. 95-104.

36. Chandra, R., S.A. Endow, and E.D. Salmon, *An N-terminal truncation of the ncd motor protein supports diffusional movement of microtubules in motility assays.* J Cell Sci, 1993. **104**(3): p. 899-906.

37. Hirose, K., et al., *Structural comparison of dimeric Eg5, Neurospora kinesin (Nkin) and Ncd head-Nkin neck chimera with conventional kinesin.* EMBO J, 2000. **19**(20): p. 5308-5314.

38. Sablin, E.P., et al., *Direction determination in the minus-end-directed kinesin motor ncd.* Nature, 1998. **395**(6704): p. 813-816.

39. Foster, K.A., A.T. Mackey, and S.P. Gilbert, *A Mechanistic Model for Ncd Directionality.* J. Biol. Chem., 2001. **276**(22): p. 19259-19266.

Chapter 2: The Tail Domain of the Non-claret Disjunctional Motor Protein Contains a Functional Nuclear Localization Signal

Abstract

The activity of non-claret disjunctional (Ncd), a *Drosophila* meiotic and mitotic motor protein, must be regulated to the M-phase of the cell cycle so as not to interfere with the interphase microtubule (MT) array. Nuclear sequestration may be a potential method of Ncd regulation. To determine the location of a functional nuclear localization signal (NLS) within the Ncd polypeptide, GFP-Ncd fusion proteins containing full length Ncd, individual Ncd domains, or a combination of Ncd domains were constructed. The cellular localization of each fusion protein was observed in transfected Schneider 2 (S2) *Drosophila* cells, as nuclear or cytoplasmic. GFP fusion proteins containing the Ncd tail domain, including GFP-full length Ncd, GFP-Ncd tail domain, and GFP-Ncd tail-stalk domain combination, localized to the nucleus of transfected S2 cells. Consequently, it was determined that a functional NLS is located within the tail domain of the Ncd motor protein. Furthermore, experimentation involving GFP-Ncd tail fusions containing bisections and trisections of the Ncd tail domain indicated that multiple clusters of basic amino acids throughout the tail domain may be essential for nuclear localization.

Introduction

Ncd is an integral member of a team of motor proteins responsible for maintaining the integrity of the mitotic bipolar spindle in *Drosophila* embryos, as well as the organization and stability of meiotic spindles in *Drosophila* oocytes [1, 2]. While Ncd loss of function results in chromosome non-disjunction and consequent aneuploidy [1], uncontrolled activity of Ncd outside of the cell cycle M-phase could result in the detrimental association of Ncd with the interphase MT array. An improper interaction of this nature may result in the paralysis of normal interphase MT functions, such as vesicle transport and organelle placement [3]. Therefore, it is essential that Ncd activity be limited only to the M-phase of the cell cycle. Ncd is retained in the nucleus until prophase [4], indicating that nuclear sequestration may be a mode of regulation to prevent Ncd from interfering with the interphase MT array. Nuclear membrane transport has been well established as a mode for regulating cellular pathways [5].

Active protein transport across the nuclear membrane is reliant upon the presence of a nuclear localization signal (NLS) within the amino acid sequence of the protein being translocated [6]. Typically, NLSs consist of cluster patterns of basic amino acid residues, arginine (R) and lysine (K) [6]. Two common types of NLSs include the SV40 NLS which contains a single basic amino acid cluster, and a bipartite NLS (that is composed of two basic amino acid clusters separated by a ten amino acid residue linker [7, 8]. PSORTII, a sequence analysis web interface program (http://psort.nibb.ac.jp/) predicted a bipartite NLS in Ncd between amino acids 92 and 108, a sequence segment that lies within the tail domain.

In an effort to identify the location of a regulatory NLS in the Ncd protein sequence, GFP-and CFP- Ncd fusion proteins were expressed in Schneider 2 (S2) *Drosophila* cells. Subsequently, the expression and cellular location (nuclear or cytoplasmic) of GFP fusion proteins containing full length Ncd, individual Ncd domains, a combination of Ncd domains, and sequence fragments of the Ncd tail domain were monitored with fluorescent microscopy. GFP and CFP alone are not actively transported across the nuclear membrane; therefore, Ncd sequence fragments that resulted in the active localization of GFP or CFP to the nucleus were considered to contain a putative NLS. Additionally, V5 epitope tagged Ncd and V5 epitope tagged Ncd tail domain were expressed in S2 cells and the cellular location of each protein was determined with immuno-fluorescence.

Methods

Generation of Constructions

The Green Fluorescent protein (GFP) coding sequence was amplified by PCR from the plasmid, pEGFP-Tub (nucleotides 613-1329). Custom designed primers GFPEcoRV and GFPXhoI (Invitrogen), were used as the forward and reverse primers (0.4 µM/reaction), respectively (Table 2.1.). The GFPEcoRV and GFPXhoI primers attached EcoRV and XhoI restriction enzyme sites, respectively, onto the GFP coding sequence. The GFP PCR product was purified using the QIAquick Gel Extraction Kit (Qiagen). Following purification, the GFP PCR product and the *Drosophila* expression plasmid, pMT/V5-His C (Invitrogen), were digested using restriction enzymes, EcoRV

and XhoI and purified using the QIAquick Gel Extraction Kit (Qiagen). Subsequently, the digested GFP fragment and digested pMT/V5-His C were ligated together. After construction, the pMT/V5-His C-GFP plasmid was digested with XhoI and AgeI restriction enzymes and purified using the QIAquick Gel Extraction Kit in preparation for the insertion of the complete Ncd coding sequence or individual Ncd coding sequence regions.

The complete Ncd coding sequence and regions of the Ncd coding sequence (Table 2.2.), including bisections and trisections of the Ncd tail coding sequence (Table 2.3.), were amplified from the plasmid, pMT/V5-His A-Ncd by PCR and inserted into the pMT/V5-His C-GFP plasmid. The forward and reverse primer pairs (Invitrogen) that were used to create each PCR product incorporated a XhoI and an AgeI site, respectively (Tables 2.4. and 2.5.). Ncd 1-700, 1-200, 197-355, 333-700, 1-355, or 197-700 products were purified by a glass milk mediated procedure (Bio 101), and were phosphorylated, according to the Perfectly Blunt Cloning Kit protocol (Novagen). The phosphorylated Ncd PCR products were inserted into Calf Intestinal Alkaline Phosphatase (CIAP) treated pT7Blue-3. Following purification of the pT7Blue-3-Ncd plasmids, the individual Ncd coding sequences were digested from pT7Blue-3 plasmids, using XhoI and AgeI restriction enzymes in preparation for insertion into the expression vector. Alternatively, the amplification of the Ncd tail 1-100, 101-200, 1-67, 68-134, and 135-200 was verified and the PCR products were purified directly from the PCR reaction mixture and digested using XhoI and AgeI. The complete Ncd coding sequence and regions of the Ncd coding sequence were inserted into pMT/V5-His C-GFP for the expression of GFP-Ncd 1-700, 1-200, 197-355, 333-700, 1-355, or 197-700 fusion

proteins, and the expression of GFP-Tail 1-100, 101-200, 1-67, 68-134, and 135-200 fusion proteins.

The Cyano Fluorescent Protein (CFP) coding sequence was amplified from the plasmid, pBSII.ITR.Ik-ECFP (kindly provided by Dr. Edward Wojick, LSU Health Sciences Center), using GFPEcoRV and CFPXhoI primers (Table 2.6.). The CFP PCR product was digested with EcoRV and XhoI restriction enzymes. Likewise, pMT/V5-His C-GFP-Ncd and Ncd-tail plasmids, including pMT/V5-His C-GFP-Tail (full length), were digested with EcoRV and XhoI restriction enzymes to remove the existing GFP coding sequence. Subsequently, CFP was inserted into each Ncd tail plasmid for the expression of CFP-Tail- 1-200, 1-100, 101-200, 1-67, 68-134, 135-200 fusion proteins. As a control, pMT/V5-His C-CFP was constructed from pMT/V5-His C-GFP, using the same cloning method, for the expression of CFP.

Histone 2B protein (H2B) was amplified from pBOS-H2B (BD Biosciences) using primers H2BKpn I and H2BSpe I, which contained KpnI and SpeI restriction enzyme sites, respectively (Table 2.7.). Similarly, the monomeric Red Fluorescent protein (mRFP) was amplified from pRSETB-mRFP (kindly provided by Dr. Roger Tsien, University of California), using primers, mRFPSpeI and mRFPEcoRV, which contained SpeI and EcoRV restriction enzyme sites, respectively (Table 2.8.). Amplified products were purified directly from the PCR reaction and digested with the respective enzymes. In accordance with the restriction enzymes used to digest the H2B PCR product, the pMT/V5-His A *Drosophila* expression plasmid was digested with KpnI and SpeI in preparation for the insertion of the H2B coding sequence. Following insertion of the H2B coding sequence, pMT/V5-His A-H2B was digested with SpeI and EcoRV

restriction enzymes in preparation for the insertion of the mRFP coding sequence. The mRFP coding sequence was inserted into pMT/V5-His A-H2B for the expression of the H2B-mRFP fusion proteins.

In preparation for V5 epitope mediated detection, the full length Ncd and Ncd tail coding sequences were amplified from pMT/V5-His-A-Ncd as before, and were digested along with pMT/V5-His A, by KpnI and XhoI restriction enzymes. Subsequently, full length Ncd and the Ncd tail were ligated into pMT/V5-His-A for the expression of V5 epitope- tagged Ncd 1-700 and Ncd 1-200 proteins.

All PCR reactions were performed, using PFU DNA Polymerase (Stratagene), in 34 cycles of denaturation (94 ^{o}C, 45 s), annealing (55 ^{o}C, 45 s), and extension (72 ^{o}C, 2 min), followed by a final extension (72 ^{o}C, 10 min) after the last cycle. Unless otherwise indicated, PCR and digestion products were separated on 0.8% agarose gels and purified using a glass milk mediated method (Bio 101). Throughout the cloning process Nova Blue *E. coli* cells (Novagen) were transformed via the heat shock method.

Sequence Analysis

Sequencing was performed using PCR amplification with BigDye Terminator Mix followed by analysis on an automated capillary electrophoresis machine, which was performed at the Virginia Bioinformatics Institute. A single base pair deviation was found in the GFP-Ncd 333-700 construction that resulted in a silent mutation ($R^{677}\rightarrow R^{677}$). No sequence deviations were found in the remaining constructions.

Transfection of S2 cells

Schneider 2 (S2) cells were transfected with each pMT/V5-His C-GFP-Ncd plasmid, using Cellfectin (Invitrogen) transfection reagent. The S2 cell cultures were grown in Schneider's Drosophila Medium (Invitrogen) supplemented with 10% fetal bovine serum (Invitrogen), as shaker cultures (150 RPM) incubated at room temperature.

In preparation for transfection, S2 cells were seeded at 1.5 x 10^6 cells/ml into two six-well plates. S2 cells were collected from a culture at 1.3 x 10^7 cells/ml cell density. The cell density was determined using a hemacytometer. Cells were collected and centrifuged at 100 x g for 5 min, and the pellet was resuspended with fresh Schneider's Drosophila Medium to a cell density of 1.5 x 10^6 cells/ml. Transfection experiments involving GFP-Ncd fusions included placing coverslips in the bottom of the cell culture wells prior to seeding the 2 ml of S2 cell resuspension. The cells were allowed to adhere to the coverslips overnight at room temperature.

Subsequently, the Schneider's Drosophila Medium was replaced in each well with a transfection mixture consisting of 2 µg DNA and 10 µg Cellfectin diluted with 1ml of Drosophila Serum Free Media (Invitrogen). Eight different transfection mixtures, each with a separate DNA component, were made. Six transfection mixtures possessed one of the six pMT/V5-His C-GFP-Ncd plasmids. The seventh transfection mixture contained a pMT/V5-His A-GFP plasmid, while the eighth transfection mixture served as a negative control. The cells were allowed to transfect overnight at room temperature.

Following the overnight incubation, the transfection mixtures were aspirated from the cells, and the cells were overlaid with 3 ml fresh Schneider's Drosophila Medium (10% FBS). The cells were then allowed to recover overnight at room temperature. After the recovery period, the plasmids were induced with 1 mM $CuSO_4$ and left to express protein for an additional 24-48 hrs.

Fluorescent Microscopy

Fluorescent microscopy was performed on a Nikon Microphot SA at 60X magnification under oil immersion.

In transfection experiments not involving the expression of H2B-mRFP for DNA localization, 30 µl of Hoechst 33342 (Molecular Probes) was added to a final 1 µg/ml concentration in each culture well and incubated without light for 15 min. Subsequently, the GFP Ncd domain coverslips were removed from the culture wells, washed with 1X PBS and placed on microscope slides. Alternatively, GFP-tail fusions and CFP-tail fusion cell suspensions were placed on acid washed coverslips, covered with 0.5 mg/ml Concanavalin A in water and incubated for 30 min at room temperature. Following incubation, the excess Concanavalin A was removed from the coverslips, and transfected cell suspensions were then overlayed on individual coverslips and incubated for 1 hr at room temperature. Subsequently, the coverslips were placed on microscope slides with structural channels built from double stick tape. The coverslips were sealed with paraffin wax to preserve the cell suspension under the coverslips.

Immunofluorescence experiments were performed by fixing transfected S2 cells with 3.7% paraformaldehyde, washing three times with PBS, and permeabilizing with 0.5% Triton X-100. Anti-V5 epitope antibody was used at the recommended dilution (Invitrogen) of 1:200 in 3% BSA,TBS-0.05% Tween-20. Primary antibody was incubated for 1 hour at RT and cells were washed with PBS-0.1% Tween-20. Secondary, anti-mouse IgG antibody conjugated to Oregon Green was used at a 1:200 dilution in 3% BSA,TBS-0.05% Tween-20.

Table 2.1. GFP custom designed primers (Invitrogen) including EcoRV and XhoI restriction enzyme sites.

PRIMER NAME	PRIMER SEQUENCE (5'→3')	PRIMER DIRECTION
GFPEcoRV	CTA CCG GTC **GAT ATC** ATG GTG AGC AAG GGC	Forward
GFPXhoI	CTC ACG CA**C TCG AG**A TCT GAG TCC GGA	Reverse

***Restriction enzyme site in bold type.**

Table 2.2. Ncd coding sequence regions in each GFP-Ncd construction, and the primer pairs employed to amplify each Ncd coding sequence.

GFP-NCD CONSTRUCTION	NCD CODING SEQUENCE REGIONS	PRIMER PAIR
Ncd 1-700 (full length)	Nucleotides 1-2100	NFX1 DES : NRA700 DES
Ncd 1-200 (tail domain)	Nucleotides 1-600	NFX1 DES : NRA200 DES
Ncd 197-355 (stalk)	Nucleotides 591-1065	NFX197 DES : NRA355 DES
Ncd 333-700 (motor)	Nucleotides 999-2100	NFX333 DES : NRA700 DES
Ncd 1-355 (tail-stalk)	Nucleotides 1-1065	NFX1 DES : NRA355 DES
Ncd 197-700 (stalk-motor)	Nucleotides 591-2100	NFX197 DES : NRA700 DES

Table 2.3. Ncd coding sequence regions in each GFP-Ncd construction, and the primer pairs employed to amplify each Ncd coding sequence.

GFP/CFP-TAIL CONSTRUCTION	TAIL CODING SEQUENCE REGIONS	PRIMER PAIR
Tail 1-300	Nucleotides 1-300	NFX1 DES : Ncdn300AgeI
Tail 301-600	Nucleotides 301-600	Ncdn300XhoI : NRA200 DES
Tail 1-201	Nucleotides 1-201	NFX1 DES : Ncdn200AgeI
Tail 202-402	Nucleotides 202-402	Ncdn200XhoI : Ncdn400AgeI
Tail 403-600	Nucleotides 403-600	Ncdn400XhoI : NRA200 DES

Table 2.4. Ncd custom designed primers (Invitrogen) including XhoI and AgeI restriction enzyme sites.

PRIMER NAME	PRIMER SEQUENCE (5'→3')	PRIMER DIRECTION
NFX1 DES	GAT CAC AGT **CTC GAG** TGG AAT CCC GGC TA	Forward
NFX197 DES	GCT CCC TAC GAC T**CT CGA G**CC CGA TTA CAC GAT	Forward
NRA200 DES	CTT CTC **ACC GGT** TTA GTG GAA GCG GGC CTT	Reverse
NFX333 DES	CAG CTG TTC CAG T**CT CGA G**TG GAG CGC AAA GAG	Forward
NRA355 DES	GGA CTC CAG **ACC GGT** TTA TAT TCG ACA GAA GAC	Reverse
NRA700 DES	GAC TCG AGC **ACC GGT** TTA TTT ATC GAA ATT	Reverse

***Restriction enzyme site in bold type.**

Table 2.5. Ncd Tail custom designed primers (Qiagen) including XhoI and AgeI restriction enzyme sites.

PRIMER NAME	PRIMER SEQUENCE (5'→3')	PRIMER DIRECTION
Ncdn300AgeI	GTT ACC ACG **ACC GGT** TTA GAT GTC GCA AGC GCT	Reverse
Ncdn300XhoI	GTA GCG CTT **CTC GAG** TCA ACG AAC TGC GTG GT	Forward
Ncdn200AgeI	TCC TCC GCG **ACC GGT** TTA CAC CTG GGG CAG ATT	Reverse
Ncdn200XhoI	ACA ATC TGC **CTC GAG** TGC TGG AGC GTC GCG GA	Forward
Ncdn400AgeI	CGC AGG ACG **ACC GGT** TTA CTG GCT GGA AAC AGT	Reverse
Ncdn400XhoI	TCA CTG TTT **CTC GAG** TGC GAC TAG TGC GTC CT	Forward

***Restriction enzyme site in bold type.**

Table 2.6. CFP forward (Invitrogen) and reverse (Qiagen) custom designed primers including EcoRV and XhoI restriction enzyme sites.

PRIMER NAME	PRIMER SEQUENCE (5'→3')	PRIMER DIRECTION
GFPEcoRV	CTA CCG GTC **GAT ATC** ATG GTG AGC AAG GGC	Forward
CFPXhoI	GTC GCG GCC **CTC GAG** CTT GTA CAG CTC GTC	Reverse

***Restriction enzyme site in bold type.**

Table 2.7. H2B custom designed primers (Qiagen) including KpnI and SpeI restriction enzyme sites.

PRIMER NAME	PRIMER SEQUENCE (5'→3')	PRIMER DIRECTION
H2BKpnI	GCA GTC GAC GGT ACC GCC ACC ATG CCA GAG	Forward
H2BSpeI	GCC CTT GCT **ACT AGT** GGT GGC GAC CGG TGG	Reverse

***Restriction enzyme site in bold type.**

Table 2.8. mRFP custom designed primers (Qiagen) includingSpeI and SpeI restriction enzyme sites.

PRIMER NAME	PRIMER SEQUENCE (5'→3')	PRIMER DIRECTION
mRFPSpeI	GAC GAT AAG **ACT AGT** ATG GCC TCC TCC GAG	Forward
mRFPEcoRV	TCA AGC TTC **GAT ATC** TTA GGC GCC GGT GGA	Reverse

***Restriction enzyme site in bold type.**

Results

GFP-Ncd fusion proteins were constructed to contain full length Ncd, individual Ncd domains, tail (1-200), stalk (197-355), or motor (333-700), or combinations of Ncd domains, tail-stalk (1-355) or stalk-motor (197-700) (Figure 2.1). Data gathered from fluorescent microscopy of S2 cells expressing GFP-Ncd fusion proteins, indicates that the Ncd tail domain contains an NLS. Fluorescence associated with GFP-Ncd 1-700 was completely co-localized with the Hoechst DNA stain, which indicated that the GFP-Ncd 1-700 was fully translocated across the nuclear membrane (Figure 2.2). Likewise, the GFP-Ncd 1-200 fusion protein was also fully translocated across the nuclear membrane and co-localized with the Hoechst DNA stain or the H2B-mRFP fusion protein, used to visualize the nucleus (Figure 2.3.). In contrast, GFP-Ncd 197-355 inclusion bodies were formed in the cytoplasm of transfected S2 cells (Figure 2.4), and GFP-Ncd 333-700 localized mostly to the cytoplasm with only diffuse fluorescence within the nucleus (Figure 2.5.).In most cases, the GFP-Ncd 1-355 was completely sequestered in the nucleus, but existed inside the nuclei of transfected cells as inclusion bodies (Figure 2.6.). However, there were also a few instances where S2 cells expressing GFP-Ncd 1-355 failed to localize the protein to the nucleus (Figure 2.7.). In qualitative terms, the occurrence of cytoplasmic localization of GFP-Ncd 1-355 was low. As indicated by DNA staining in the cytoplasm, the cytoplasmic localization of GFP-Ncd 1-355 may be due to the loss of nuclear membrane integrity, which results in the release of nuclear contents into the cytoplasm. Unlike GFP-Ncd 333-700, there was complete exclusion of GFP-Ncd 197-700 from the nucleus, as indicated by the lack of

green fluorescence within the nucleus (Figure 2.8.). Observations of S2 cells expressing GFP alone indicated that GFP passively diffused across the nuclear membrane but was not actively localized to the nucleus, thereby indicating that GFP does not mediate active transport into the nucleus. In summary, GFP-Ncd fusion proteins containing full length Ncd (1-700), the Ncd tail (1-200), or the Ncd tail-stalk (1-355) sequences co-localized with the Hoechst DNA stain or H2B-mRFP in the nucleus, while GFP-Ncd fusion proteins containing the Ncd stalk(197-355), the Ncd motor (333-700), or the Ncd stalk-motor (197-700) sequences localized to the cytoplasm.

An independent assessment of the presence of a NLS within the Ncd tail domain was performed using V5 epitope-tagged full length Ncd (Ncd 1-700) and V5 epitope-tagged Ncd tail (Ncd 1-200) domain (Figure 2.9.). The location of the V5 epitope-tagged fusion proteins was observed by immunochemistry and fluorescent microscopy with respect to DAPI fluorescence used to visualize the nuclei of the S2 cells. The cellular localization of the V5 epitope-tagged proteins were not as clearly defined as the GFP-Ncd 1-700 and GFP-Ncd 1-200 fusion proteins. Typically, Ncd 1-700-V5 appeared to localize to the nucleus or to the nuclear membrane, observed as ring-patterned fluorescence (Figure 2.10.). The nuclear sequestration was not as well defined and compact as that seen by GFP-Ncd 1-700, and Ncd 1-700-V5 proteins that localized to the nuclear membrane did not co-localize with the DAPI-stained DNA. The cellular location of Ncd 1-200-V5 was undetermined with fluorescent microscopy alone. Since the cytoplasmic and nuclear compartments were not well visualized, it could not be determined whether the intense fluorescent ring-like staining occurred along the plasma membrane or the nuclear membrane (Figure 2.10.). For this reason, the cellular

location of Ncd 1-200-V5 was determined with the use of DIC microscopy, which allowed additional visualization of the nucleus. Combination experiments with fluorescent and DIC microscopy indicated that Ncd 1-200-V5 mostly localized to the nuclear membrane, and in a some incidences Ncd 1-200-V5 may have localized to the plasma membrane (Figure 2.11.). It was not determined whether the nuclear membrane staining arose from the presence of fusion proteins along the outside of the membrane or directly inside the nuclear membrane, and the reason for the fluorescent staining along the nuclear and plasma membrane was undetermined. Even with the combination of fluorescent and DIC microscopy, ambiguities in cell compartment visualization persisted, and limitations in identifying the exact location of Ncd 1-200-V5 hindered assignment of cellular localization.

To further define the location of the NLS within the Ncd-tail domain, GFP-Ncd tail fusion proteins, representing bisections or trisections of the Ncd tail (Figure 2.12.), were expressed in S2 cells and the intracellular location of each fusion protein was assessed using fluorescent microscopy. The GFP- Tail 1-100 and 101-200 fusion proteins contained the first half and the second half of the Ncd tail domain sequence, respectively, while the GFP-Tail 1-67, 68-134, and 135-200 fusion proteins contained the first, second and third trisections of the Ncd tail domain sequence, respectively. Using fluorescent microscopy, the location of the fluorescence associated with each fusion protein was evaluated with respect to Hoechst or H2B-mRFP fluorescence localized to the nuclei of the S2 cells (Figures 2.13-2.17.). GFP-Tail 1-100 and GFP-Tail 1-67 fusion proteins located to the cytoplasm of transfected S2 cells expressing each protein. In contrast, the GFP-Tail 101-200, GFP-Tail 68-134, and GFP-Tail 135-

200 fusion proteins localized mainly to the nucleus, with only diffuse localization to the cytoplasm of transfected S2 cells. Qualitatively, greater nuclear sequestration, as indicated by a lower incidence of diffuse cytoplasmic fluorescence, was observed for GFP-Tail 101-200 and GFP-Tail 68-134 than GFP-Tail 135-200.

There were instances of GFP fluorescent bleed-through under the UV light used to excite the Hoechst stain. In order to bypass this issue, and thereby confirm the previous results with a greater signal-to-noise ratio, CFP-Ncd 1-700, CFP-Ncd 1-200, and CFP-Tail 1-100, 101-200, 1-67, 68-134, and 135-200 fusion proteins (Figure 2.18.) were each co-expressed in S2 cells with H2B-mRFP (Figures 2.19.-2.25.). Since there is a significant difference between the peak excitation wavelengths of CFP and RFP, the instance of co-excitation was minimized. As expected, CFP-Tail 1-100 and CFP-Tail 1-67 localized to the cytoplasm. However, in comparison to the GFP and V5-epitope fusion counterparts, CFP-Ncd 1-700 and CFP- Ncd 1-200 showed reduced nuclear sequestration (Figure 2.26.). Furthermore, unlike GFP-Tail 101-200, CFP-Tail 101-200 was completely excluded from the nucleus and formed inclusion bodies, as indicated by the speckled concentration of fluorescence (Figure 2.26.). The nuclear localization of GFP-Tail 68-134 and GFP-Tail 135-200 was also prevented in S2 cells expressing CFP-Tail 68-134 and CFP-Tail 135-200, although passive diffusion may have occurred, as indicated by the slight co-localization with DNA. CFP alone did not localize to the nucleus by means of active transport or passive diffusion (Figure 2.26.).

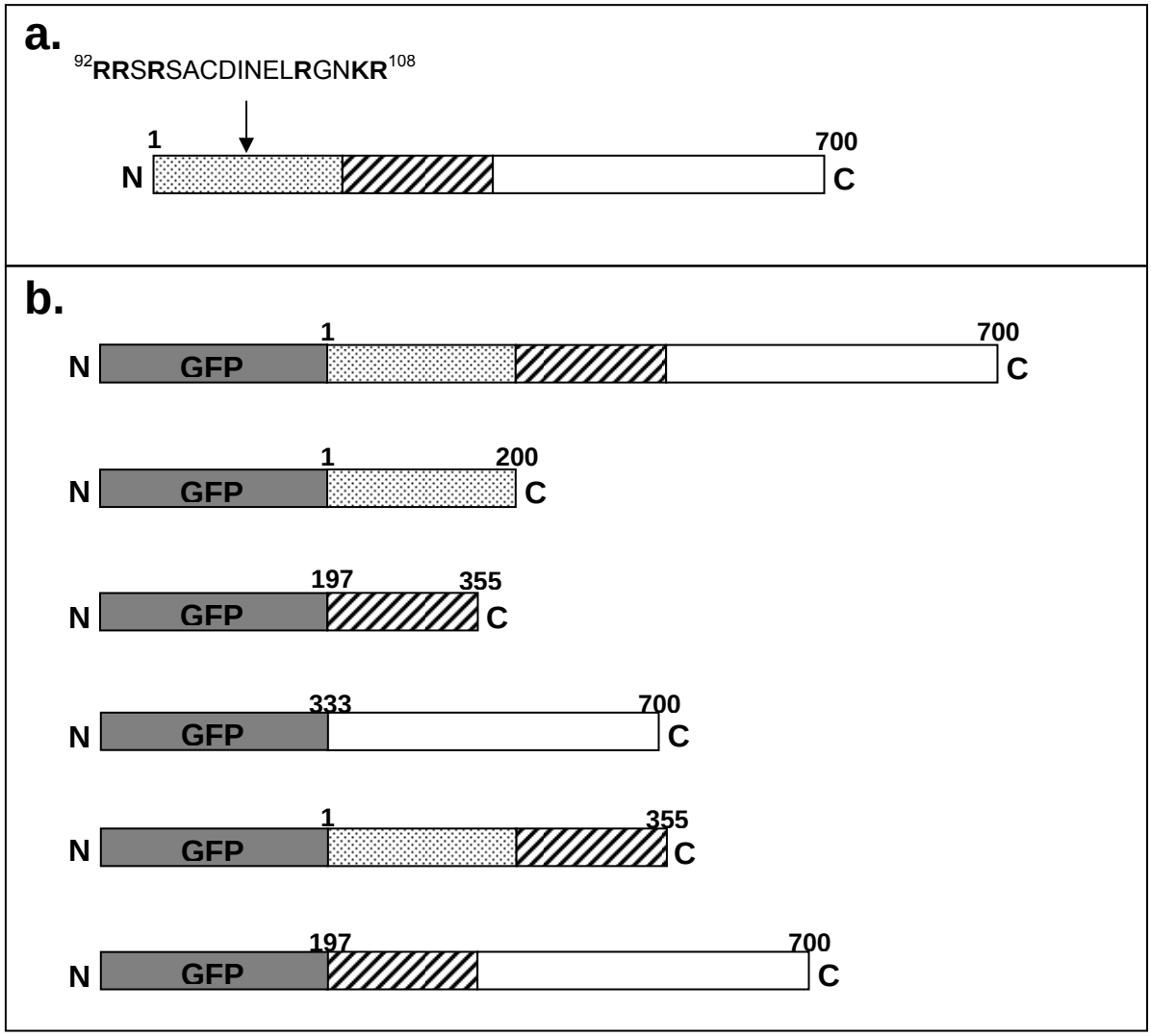

Figure 2.1. Schematic diagram of the Ncd protein sequence and the GFP-Ncd fusion proteins used to determine the location of a putative NLS.

a.) Schematic of the Ncd protein sequence with domains indicated. The tail domain (N-terminus) is designated by a stippled pattern, the stalk domain is designated by diagonal stripes, and the motor domain (C-terminus) is designated in white. A single predicted NLS (AA 92-108), identified using PSORTII sequence analysis program, is also indicated. Basic arginine and lysine residues, in the predicted NLS, are designated in bold print. b.) Schematic of the GFP-Ncd fusion proteins consisting of GFP attached to full length Ncd, Ncd domains, or a combination of Ncd domains. Fusion proteins were expressed with GFP attached at the N-terminus of each Ncd sequence segment.

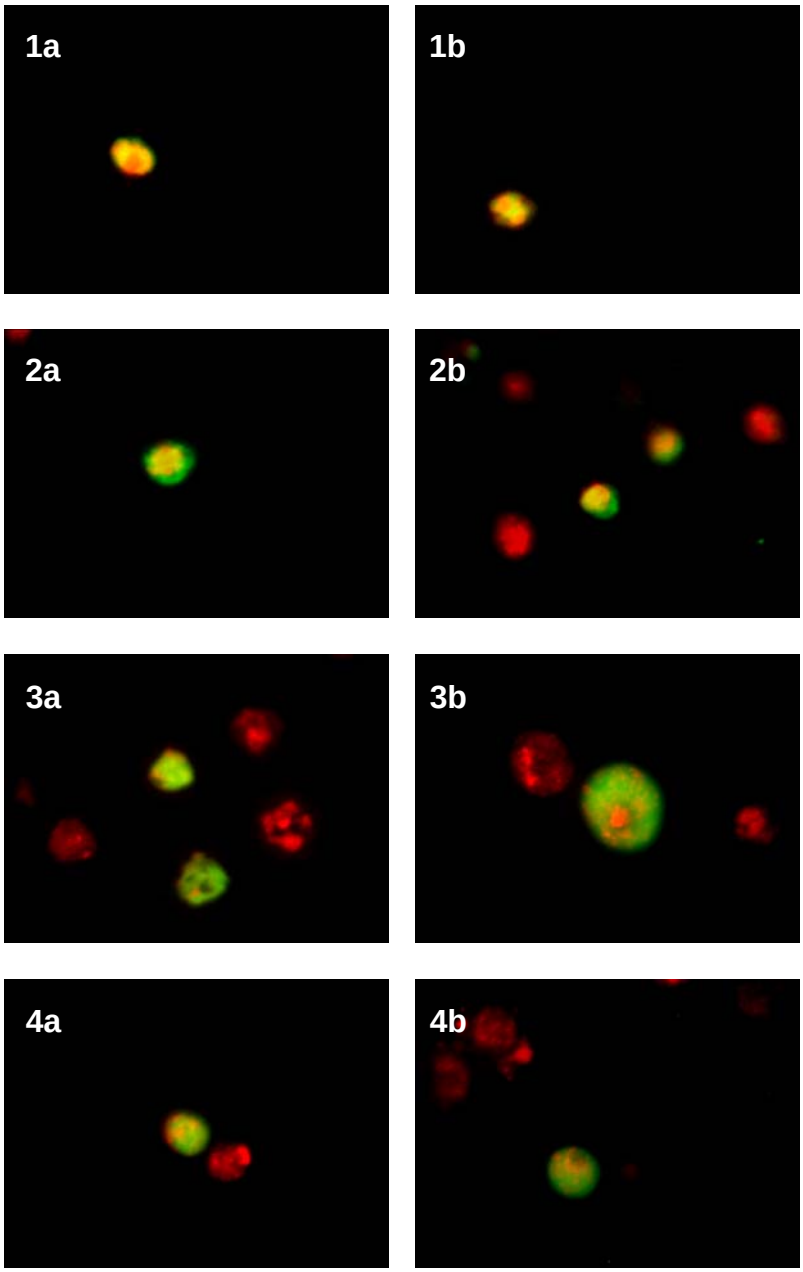

Figure 2.2. GFP-Ncd 1-700 localized to the nuclei of transfected S2 cells.
Images were collected from four separate transfection trials (1-4), and two images (a and b) from each transfection are displayed. The location of DNA is represented in red and the location of GFP-Ncd is represented in green. Co-localization of DNA and GFP-Ncd is represented in yellow. Hoechst stain was used to visualize the DNA.

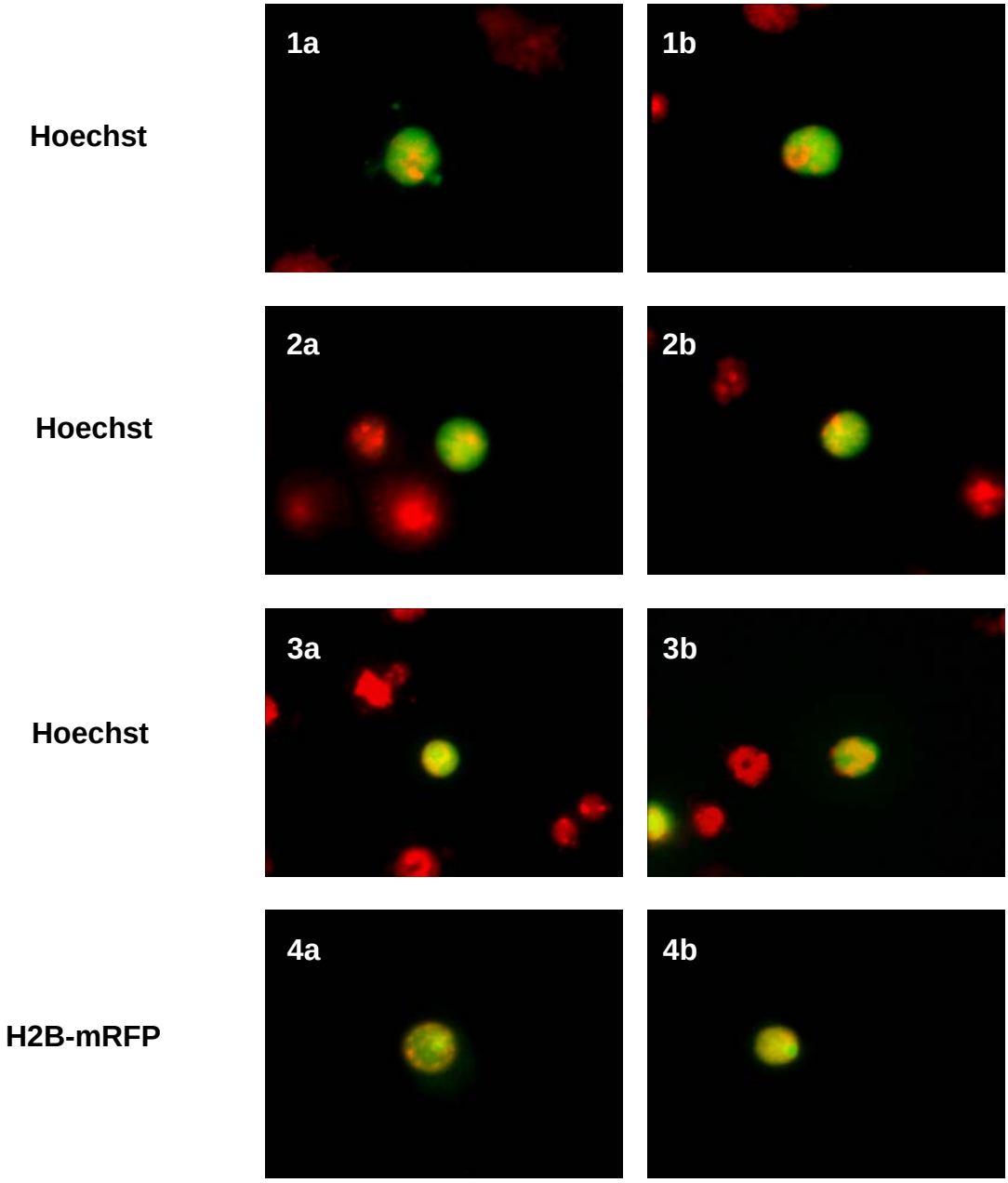

Figure 2.3. GFP-Ncd 1-200 localized to the nuclei of transfected S2 cells.
Images were collected from four separate transfection trials (1-4), and two images (a and b) from each transfection are displayed. The location of DNA is represented in red and the location of GFP-Tail is represented in green. Co-localization of DNA and GFP-Tail is represented in yellow. Hoechst stain or H2B- mRFP fusion protein was used to visualize the DNA as indicated.

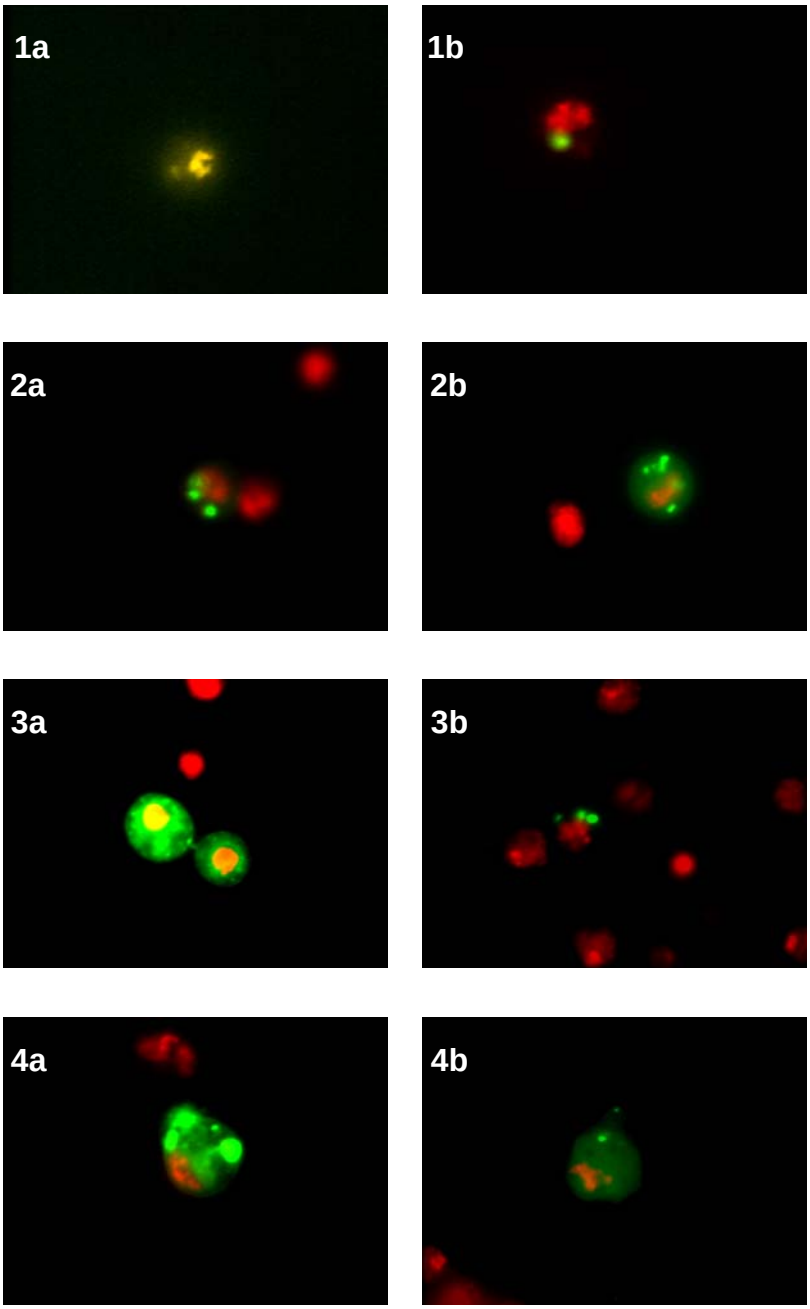

Figure 2.4. GFP-Ncd 197-355 localized to the cytoplasm of transfected S2 cells.
Images were collected from four separate transfection trials (1-4), and two images (a and b) from each transfection are displayed. The location of DNA is represented in red and the location of GFP-Stalk is represented in green. Co-localization of DNA and GFP-Stalk is represented in yellow. Hoechst stain was used to visualize the DNA.

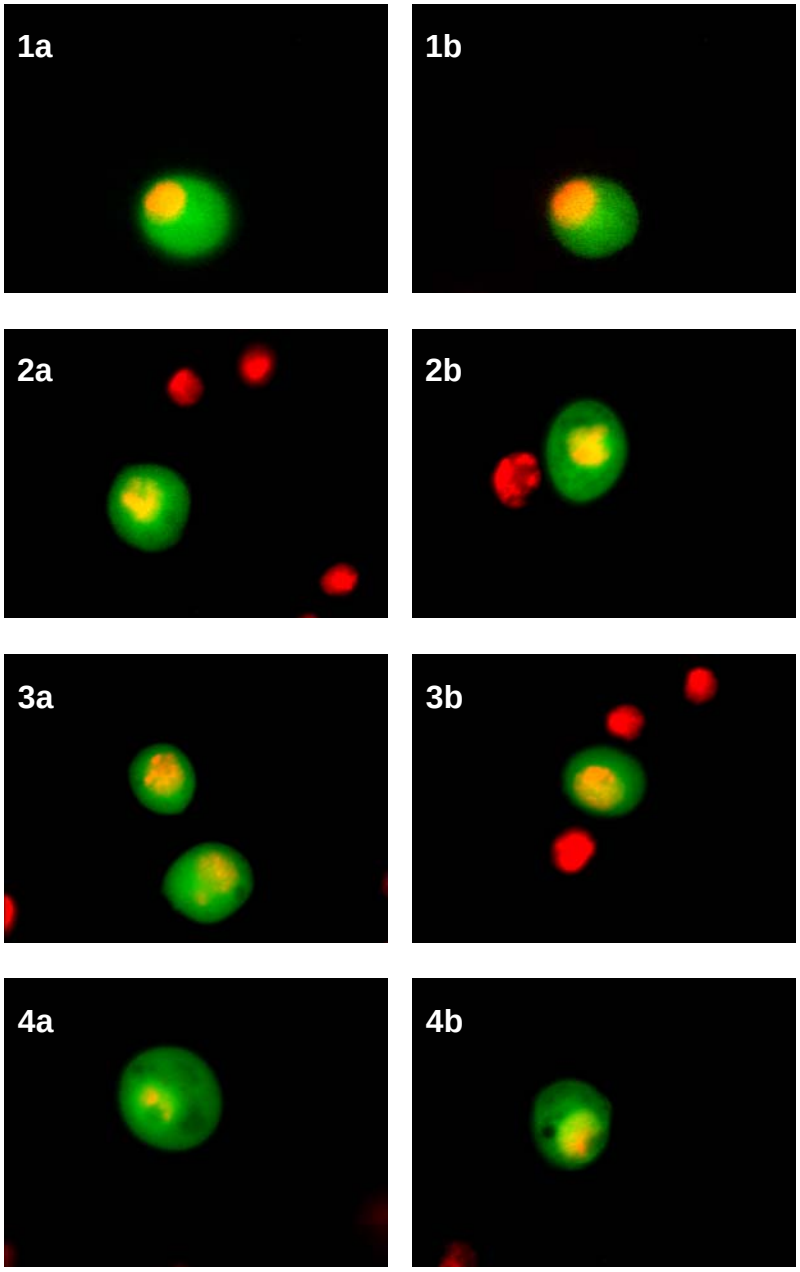

Figure 2.5. GFP-Ncd 333-700 localized to the cytoplasm of transfected S2 cells.
Images were collected from four separate transfection trials (1-4), and two images (a and b) from each transfection are displayed. The location of DNA is represented in red and the location of GFP-Motor is represented in green. Co-localization of DNA and GFP-Motor is represented in yellow. Hoechst stain was used to visualize the DNA.

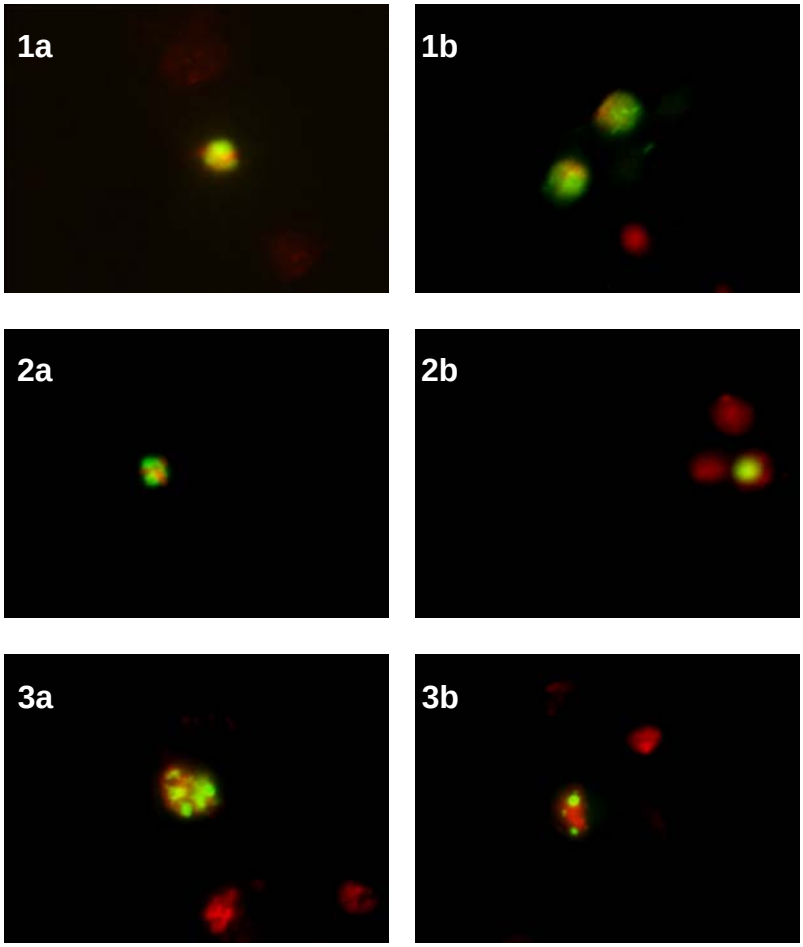

Figure 2.6. GFP-Ncd 1-355 localized to the nuclei of transfected S2 cells.
Images were collected from three separate transfection trials (1-3), and two images (a and b) from each transfection are displayed. The location of DNA is represented in red and the location of GFP-Tail-Stalk is represented in green. Co-localization of DNA and GFP-Tail-Stalk is represented in yellow. Hoechst stain was used to visualize the DNA.

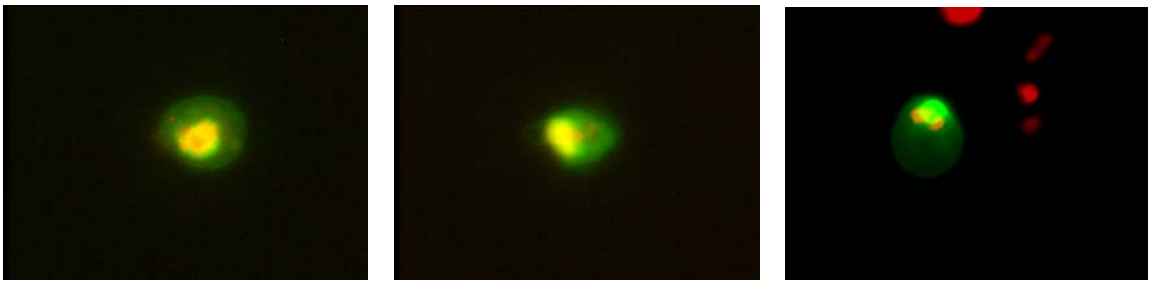

Figure 2.7. GFP-Ncd 1-355 partially localized to the cytoplasm of transfected S2 cells.
The location of DNA is represented in red and the location of GFP-Tail-Stalk is represented in green. Co-localization of DNA and GFP-Tail-Stalk is represented in yellow. Hoechst stain was used to visualize the DNA.

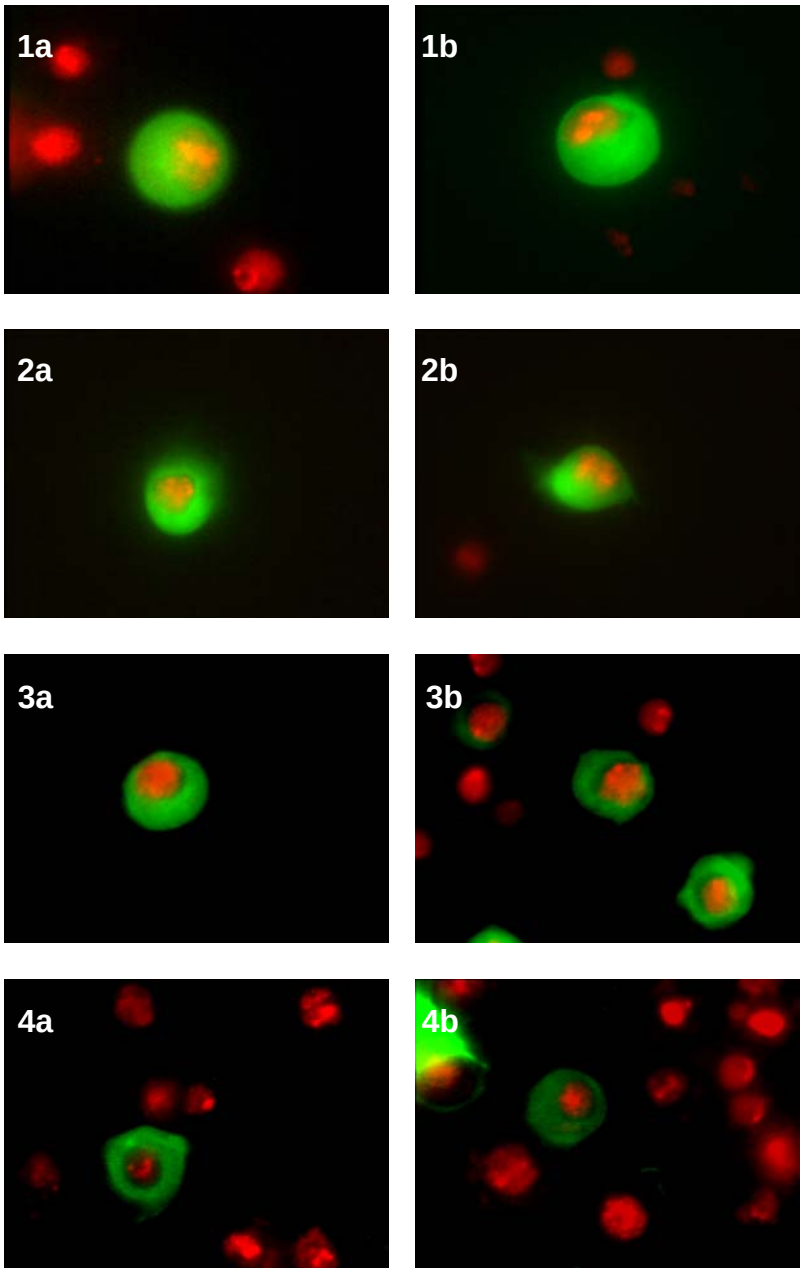

Figure 2.8. GFP-Ncd 197-700 localized to the cytoplasm of transfected S2 cells.
Images were collected from four separate transfection trials (1-4), and two images (a and b) from each transfection are displayed. The location of DNA is represented in red and the location of GFP-Stalk-Motor is represented in green. Co-localization of DNA and GFP-Stalk-Motor is represented in yellow. Hoechst stain was used to visualize the DNA.

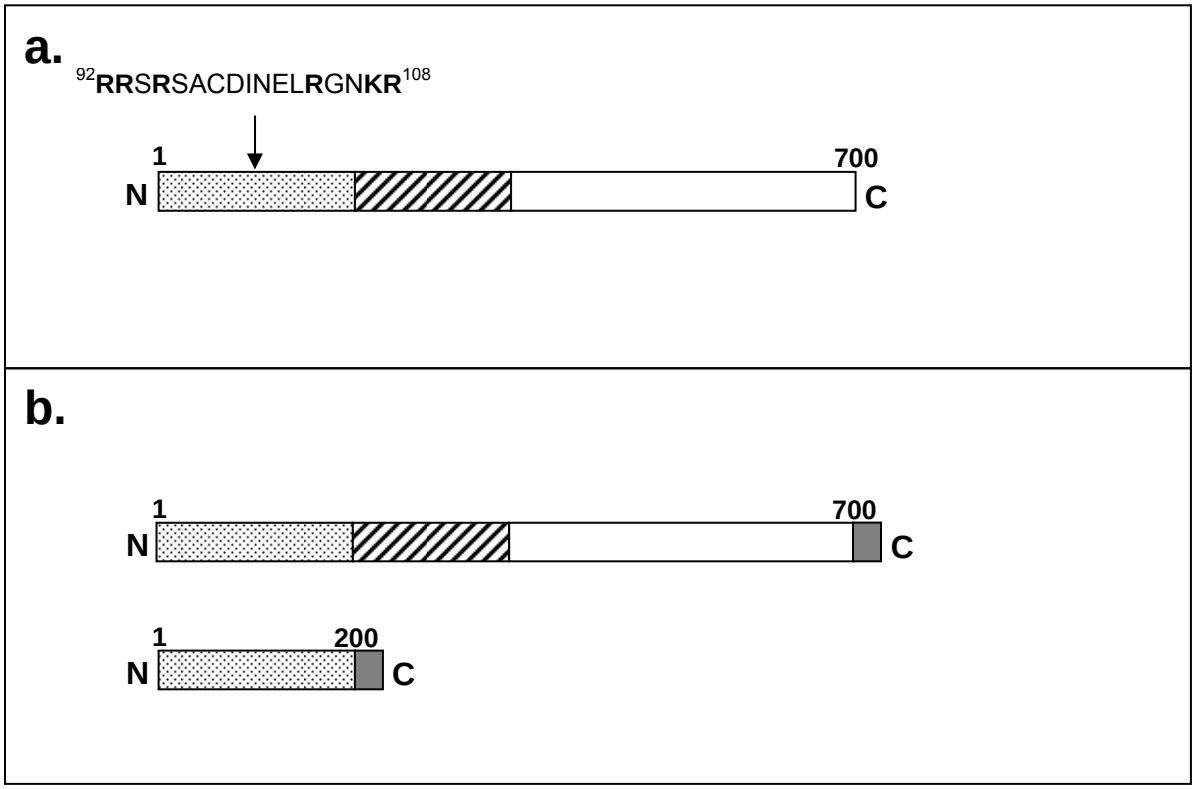

Figure 2.9. Schematic diagram of the Ncd protein sequence and V5 epitope-tagged Ncd and Ncd tail proteins.

a.) Schematic of the Ncd protein sequence with domains indicated. The tail domain (N-terminus) is designated by a stippled pattern, the stalk domain is designated by diagonal stripes, and the motor domain (C-terminus) is designated in white. A single predicted NLS (AA 92-108), identified using PSORTII sequence analysis program, is also indicated. Basic arginine and lysine residues in the predicted NLS are designated in bold print. b.) Schematic of the Ncd +V5 and Tail +V5 fusion proteins, used to further support the hypothesis that the Ncd tail domain is the location of a putative NLS. The V5 epitope (designated in gray) was expressed as a C-terminal tag on full length Ncd and the Ncd tail domain sequence. The V5 epitope tag consisted of a 8 AA linker preceding the 14 AA V5 epitope, in addition to a 3 AA linker and a 6 AA His tag following the V5 epitope tag.

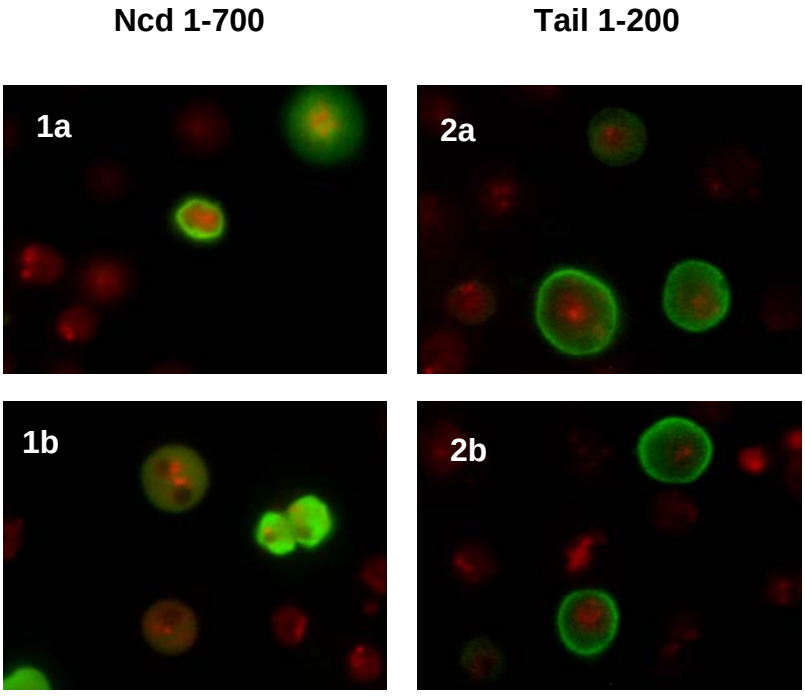

Figure 2.10. Ncd 1-700-V5 localized to the nuclei of S2 transfected cells, while the localization of Ncd 1-200-V5 remained unclear.
1a and 1b) With the exception of one cell (1a, upper right), Ncd 1-700-V5 loosely co-localizes with the DNA. 2a and 2b) An intense ring-like fluorescence appears along what appears to be the plasma membrane, but did not confirm cytoplasmic localization of Ncd 1-200-V5. The location of DNA is represented in red and the location of Ncd 1-700-V5 and Ncd 1-200-V5 is represented in green. Co-localization of DNA and Ncd 1-700-V5 or Ncd 1-200-V5 is represented in yellow. DAPI stain was used to visualize the DNA.

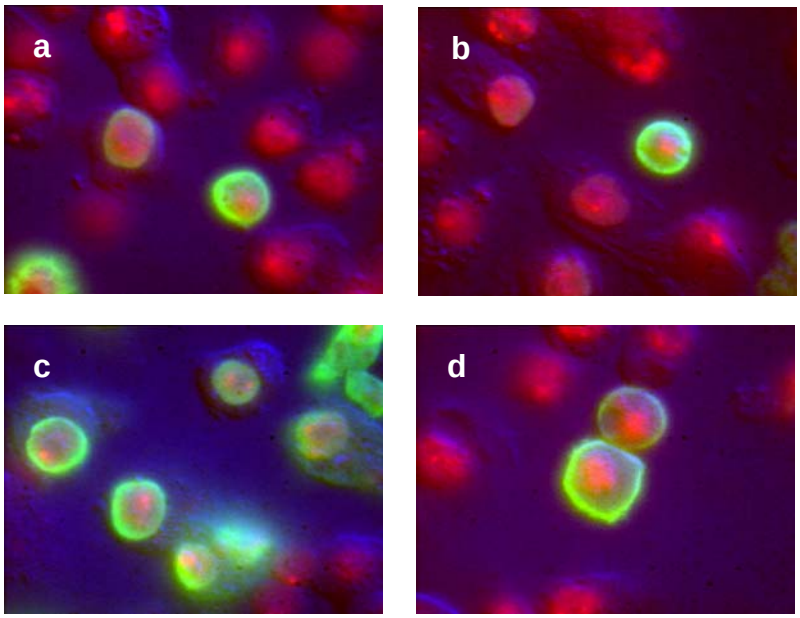

Figure 2.11. Combination experiments with fluorescent and DIC microscopy indicated that Ncd 1-200-V5 typically localized to the nuclear membrane of transfected S2 cells.
a-c) Ncd 1-200-V5 localizes to the nuclear membrane. d) Ncd 1-200-V5 may localize to the plasma membrane. The location of DNA is represented in pink and the location of Ncd 1-200-V5 is represented in green. DAPI stain was used to visualize the DNA.

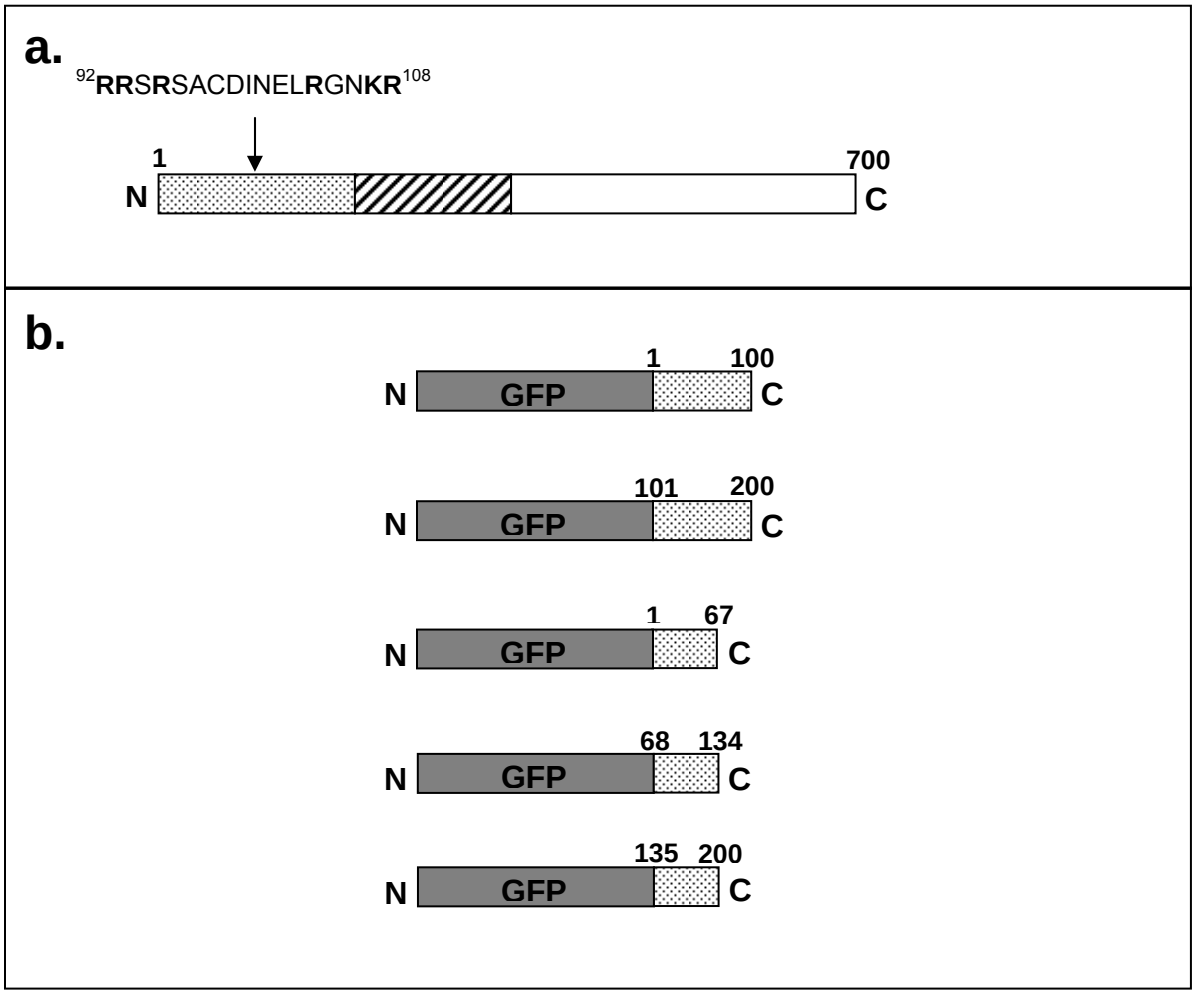

Figure 2.12. Schematic diagram of the Ncd protein sequence and the GFP-Ncd tail fusion proteins used to further define the location of a putative NLS.

a.) Schematic of the Ncd protein sequence with domains indicated. The tail domain (N-terminus) is designated by a stippled pattern, the stalk domain is designated by diagonal stripes, and the motor domain (C-terminus) is designated in white. A single predicted NLS (AA 92-108), identified using PSORTII sequence analysis program, is also indicated. Basic arginine and lysine residues, in the predicted NLS, are designated in bold print. b.) Schematic of the GFP-Ncd tail fusion proteins consisting of GFP attached to AA 1-100, 101-200, 1-67, 68-134, and 135-200. Fusion proteins were expressed with GFP attached at the N-terminus of each Ncd tail sequence segment.

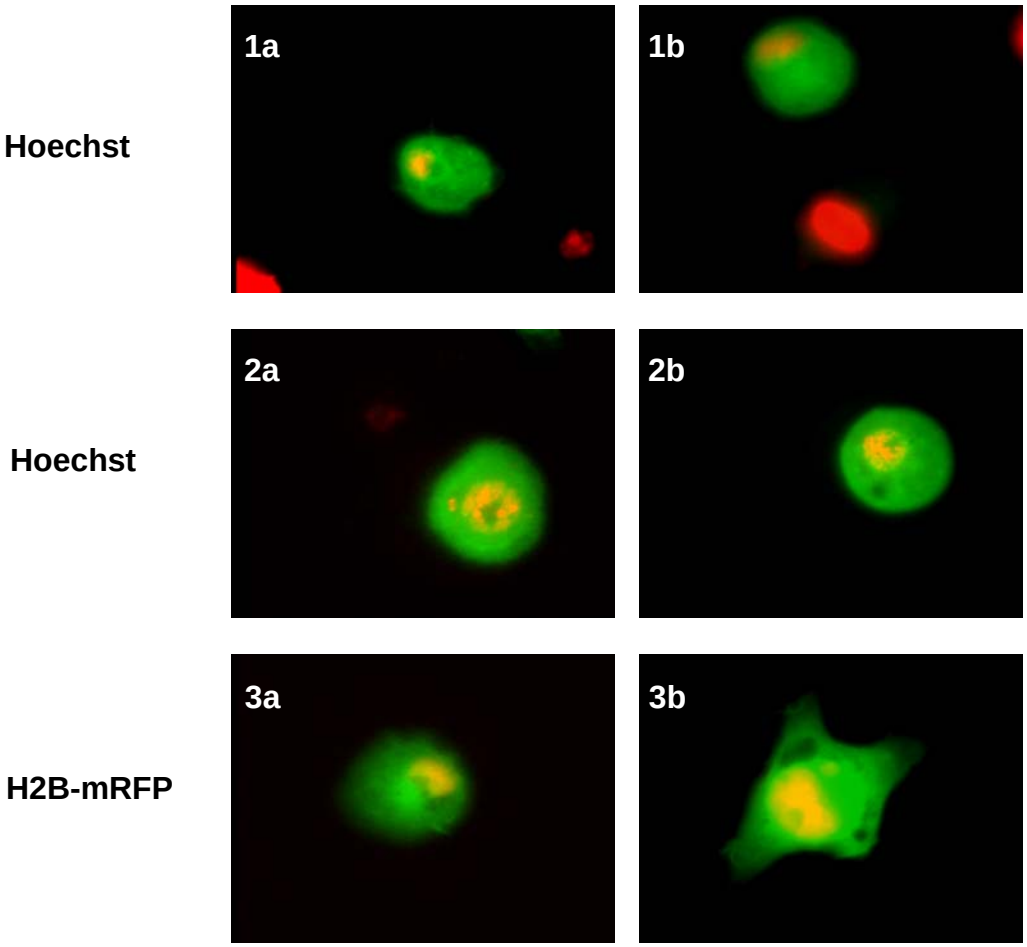

Figure 2.13. GFP-Tail 1-100 localized primarily to the cytoplasm of transfected S2 cells. Images were collected from three separate transfection trials (1-3), and two images (a and b) from each transfection are displayed. The location of DNA is represented in red and the location of GFP-Tail 1-100 is represented in green. Co-localization of DNA and GFP-Tail 1-100 is represented in yellow. Hoechst stain or H2B- mRFP fusion protein was used to visualize the DNA as indicated.

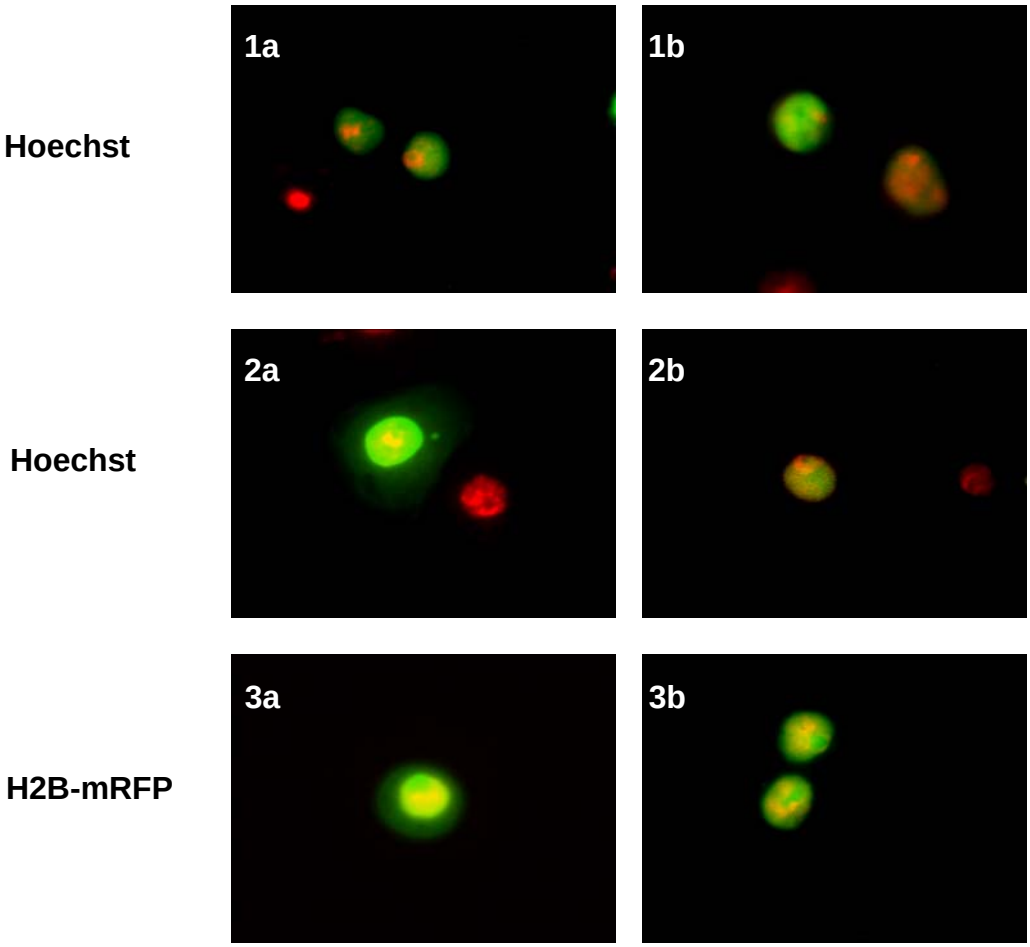

Figure 2.14. GFP-Tail 101-200 localized primarily to the nuclei of transfected S2 cells. Images were collected from three separate transfection trials (1-3), and two images (a and b) from each transfection are displayed. The location of DNA is represented in red and the location of GFP-Tail 101-200 is represented in green. Co-localization of DNA and GFP-Tail 101-200 is represented in yellow. Hoechst stain or H2B- mRFP fusion protein was used to visualize the DNA as indicated.

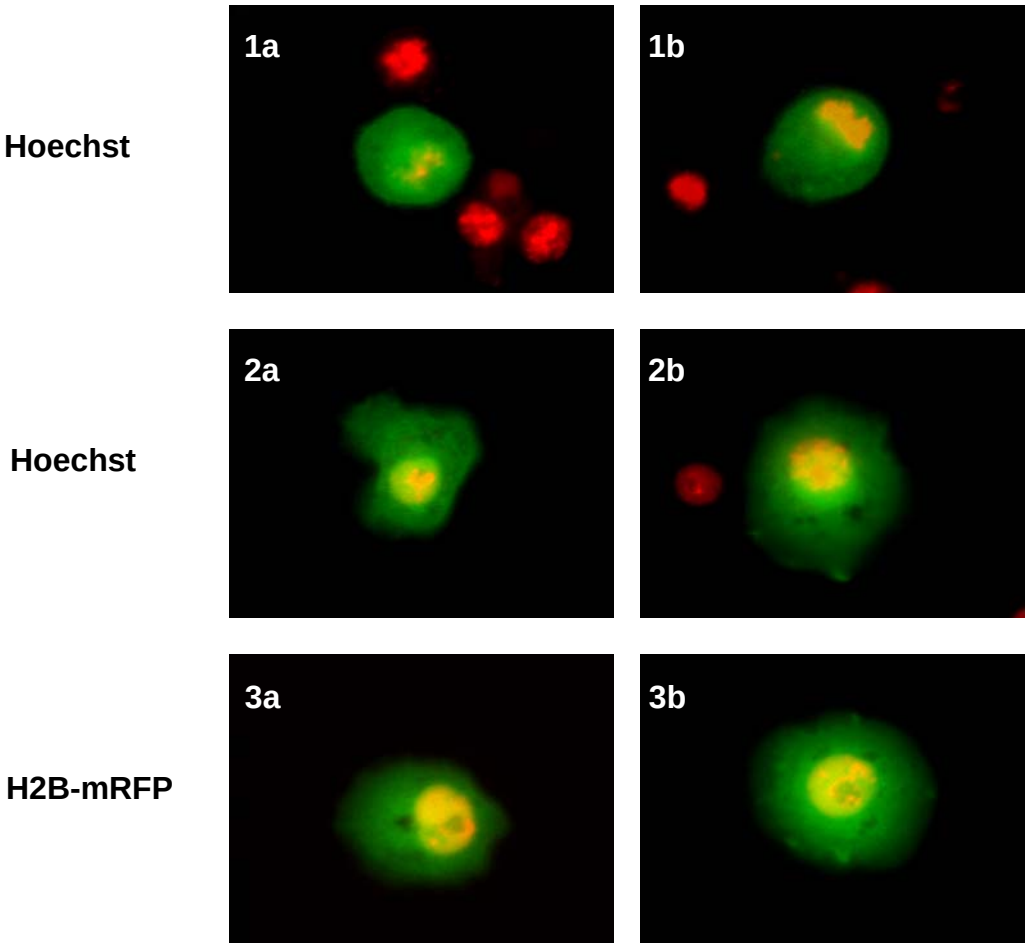

Figure 2.15. GFP-Tail 1-67 localized primarily to the cytoplasm of transfected S2 cells. Images were collected from three separate transfection trials (1-3), and two images (a and b) from each transfection are displayed. The location of DNA is represented in red and the location of GFP-Tail 1-67 is represented in green. Co-localization of DNA and GFP-Tail 1-67 is represented in yellow. Hoechst stain or H2B- mRFP fusion protein was used to visualize the DNA as indicated.

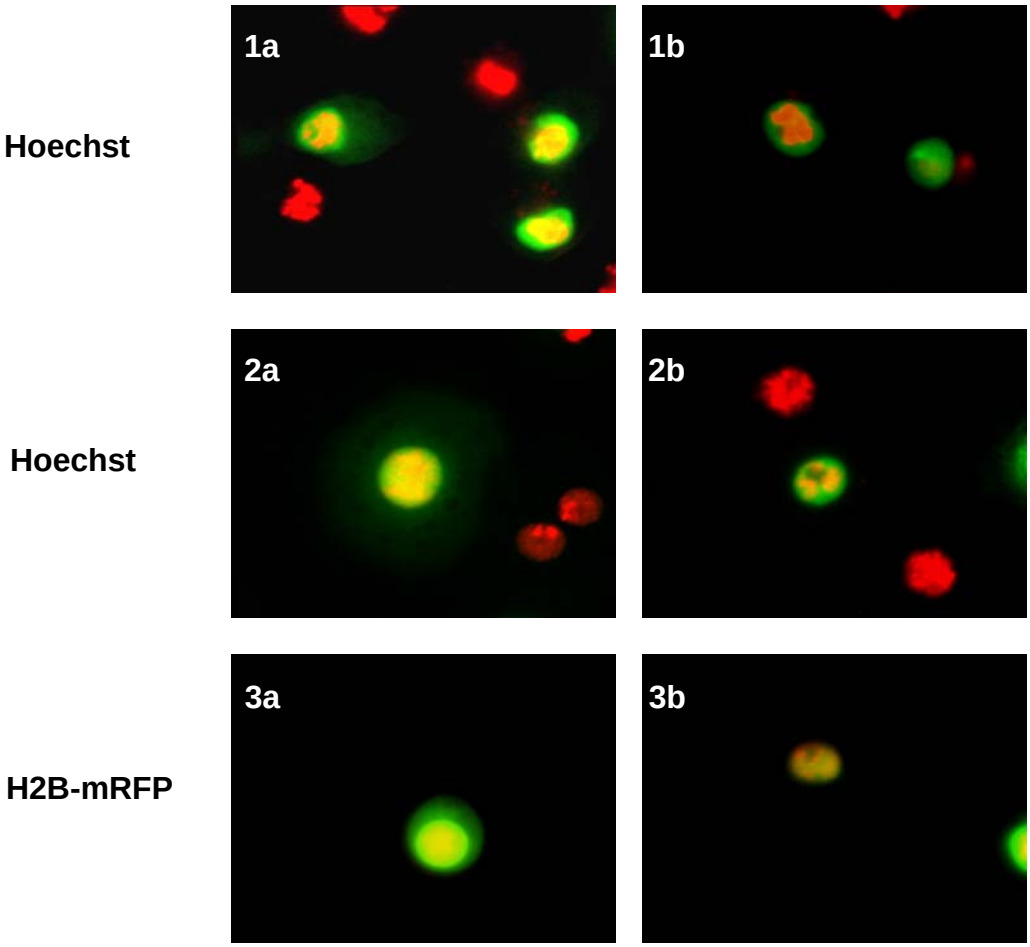

Figure 2.16. GFP-Tail 68-134 localized primarily to the nuclei of transfected S2 cells. Images were collected from three separate transfection trials (1-3), and two images (a and b) from each transfection are displayed. The location of DNA is represented in red and the location of GFP-Tail 68-134 is represented in green. Co-localization of DNA and GFP-Tail 68-134 is represented in yellow. Hoechst stain or H2B- mRFP fusion protein was used to visualize the DNA as indicated.

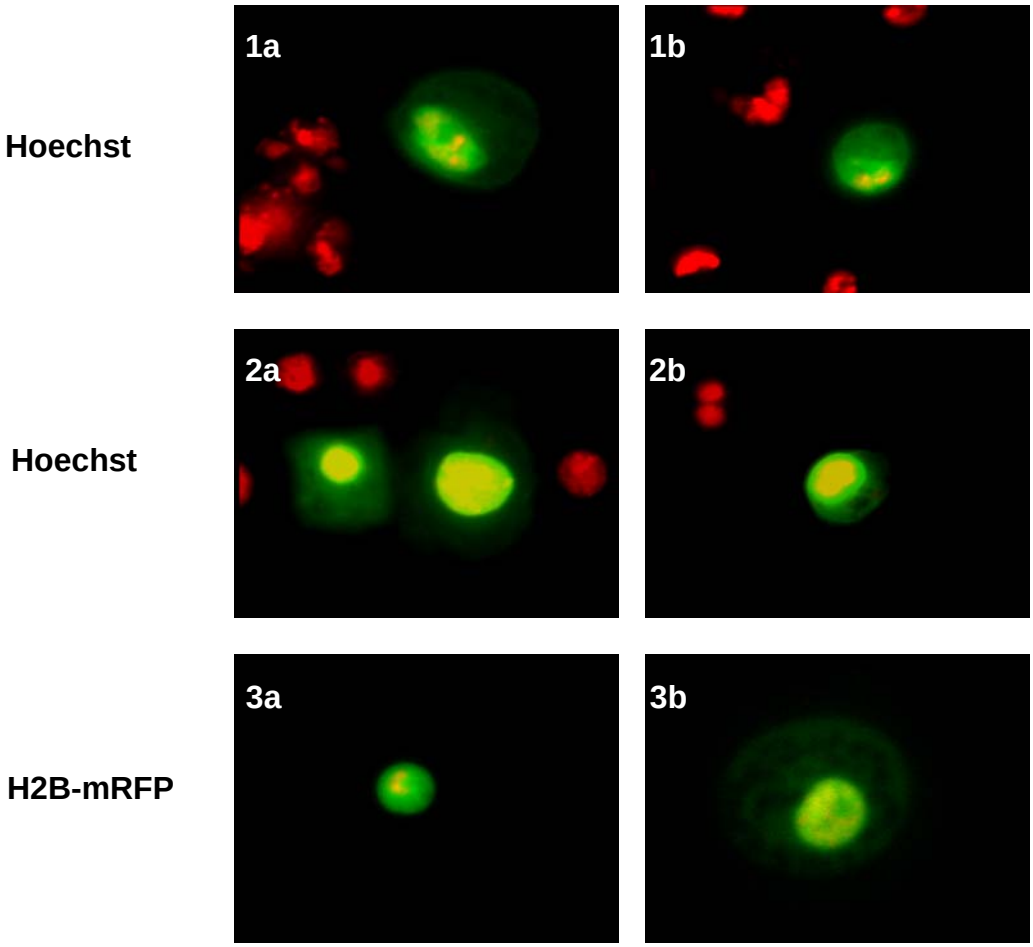

Figure 2.17. GFP-Tail 135-200 localized primarily to the nuclei of transfected S2 cells. Images were collected from three separate transfection trials (1-3), and two images (a and b) from each transfection are displayed. The location of DNA is represented in red and the location of GFP-Tail 135-200 is represented in green. Co-localization of DNA and GFP-Tail 135-200 is represented in yellow. Hoechst stain or H2B- mRFP fusion protein was used to visualize the DNA as indicated.

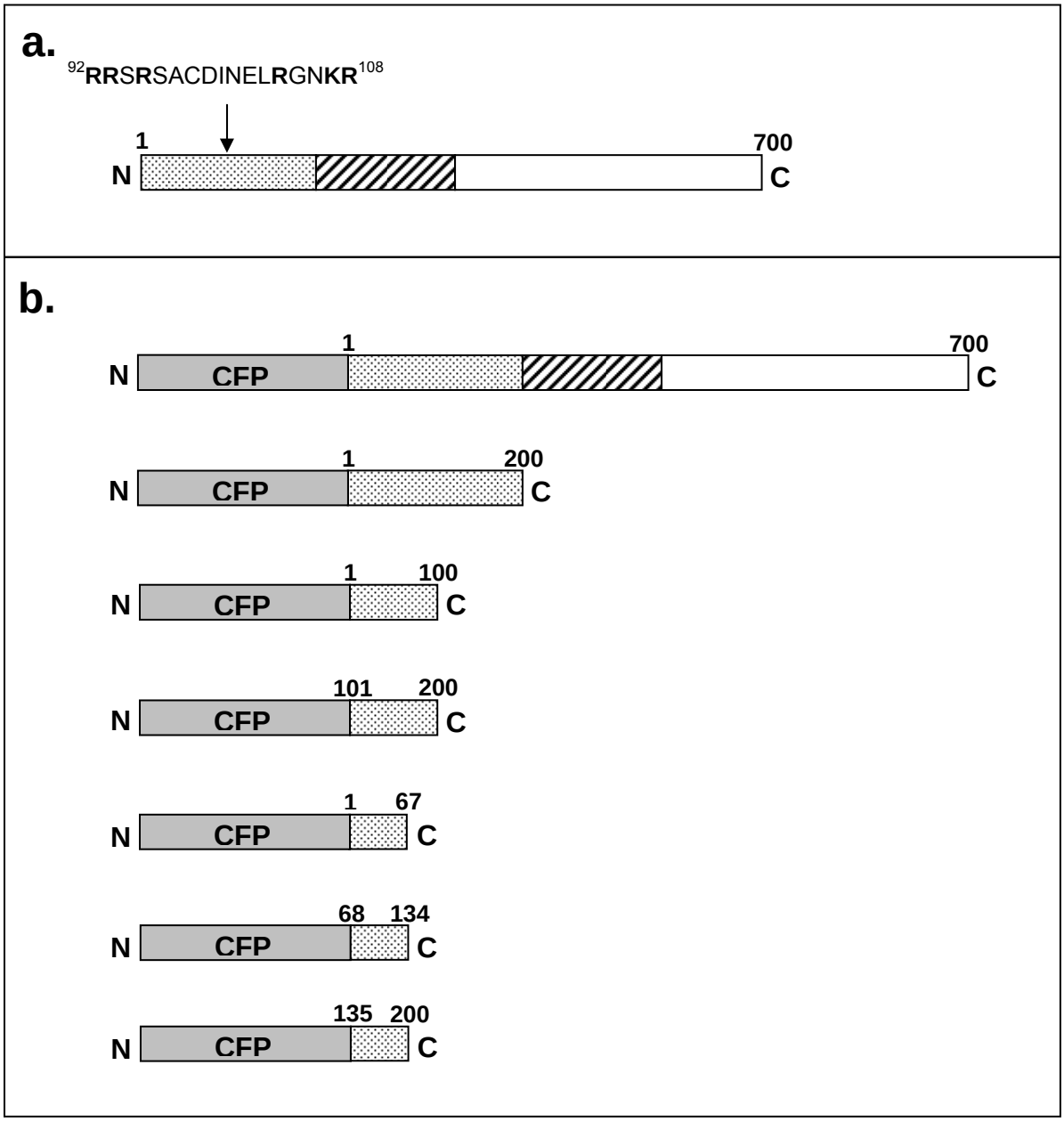

Figure 2.18. Schematic diagram of the Ncd protein sequence and the CFP-Ncd, CFP-Tail, and the CFP-Ncd tail fusion proteins used to further define the location of a putative NLS.
a.) Schematic of the Ncd protein sequence with domains indicated. The tail domain (N-terminus) is designated by a stippled pattern, the stalk domain is designated by diagonal stripes, and the motor domain (C-terminus) is designated in white. A single predicted NLS (AA 92-108), identified using PSORTII sequence analysis program, is also indicated. Basic arginine and lysine residues, in the predicted NLS, are designated in bold print. b.) Schematic of the CFP-Ncd, CFP-Tail, and the CFP-Ncd tail fusion proteins consisting of CFP attached to full length Ncd, the full length Ncd tail, and the Ncd tail

amino acids 1-100, 101-200, 1-67, 68-134, and 135-200. Fusion proteins were expressed with CFP attached at the N-terminus of each Ncd tail sequence segment.

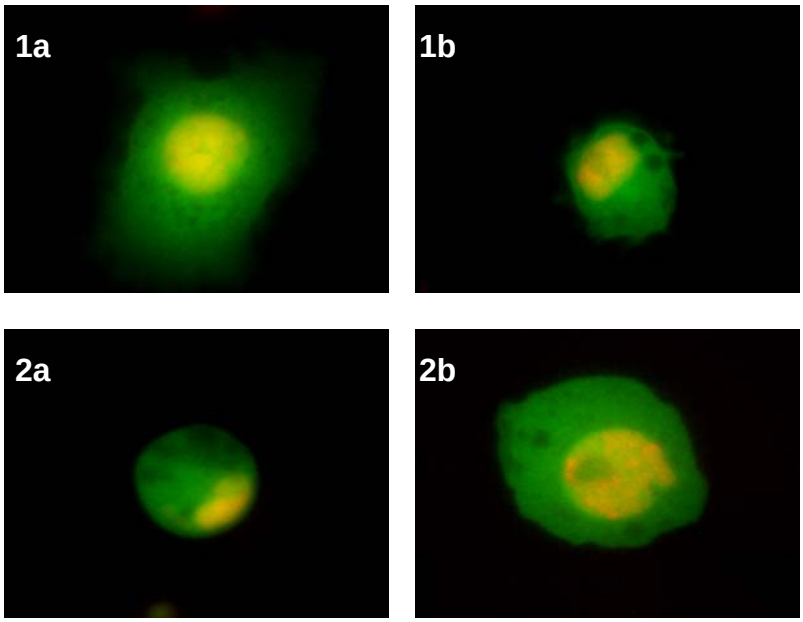

Figure 2.19. CFP-Ncd 1-700 localized to the cytoplasm of transfected S2 cells.
Images were collected from two separate transfection trials (1-2), and two images (a and b) from each transfection are displayed. The location of DNA is represented in red and the location of CFP-Ncd is represented in green. Co-localization of DNA and CFP-Ncd is represented in yellow. H2B- mRFP fusion protein was used to visualize the DNA as indicated.

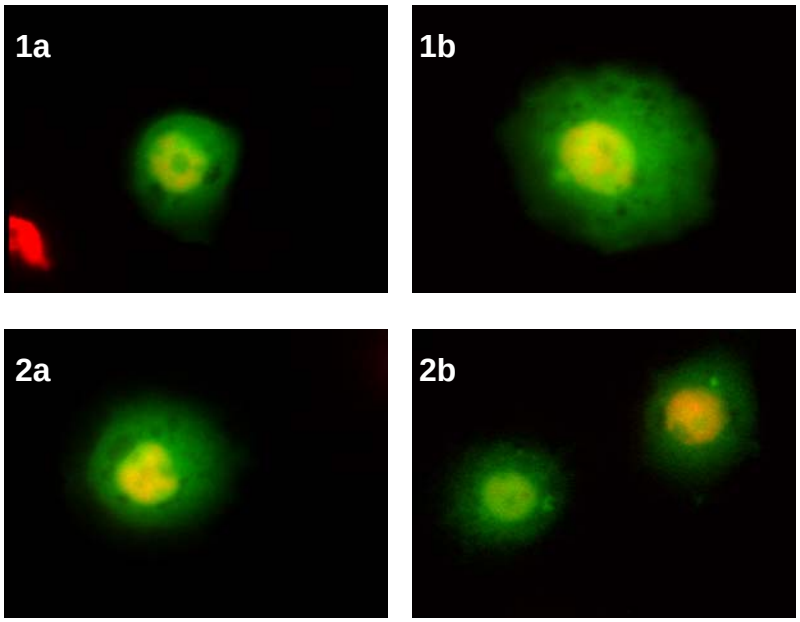

Figure 2.20. CFP-Ncd 1-200 localized to the cytoplasm of transfected S2 cells.
Images were collected from two separate transfection trials (1-2), and two images (a and b) from each transfection are displayed. The location of DNA is represented in red and the location of CFP-Tail is represented in green. Co-localization of DNA and CFP-Tail is represented in yellow. H2B- mRFP fusion protein was used to visualize the DNA as indicated.

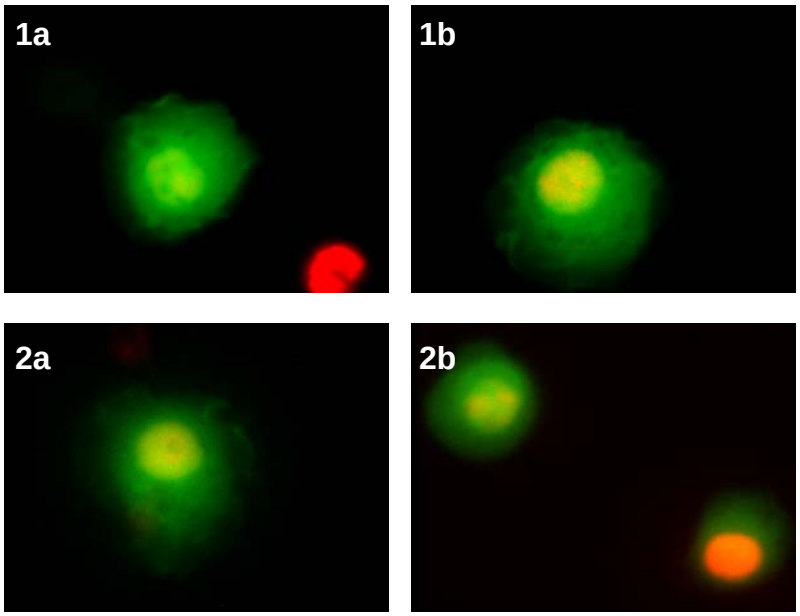

Figure 2.21. CFP-Tail1-100 localized to the cytoplasm of transfected S2 cells.
Images were collected from two separate transfection trials (1-2), and two images (a and b) from each transfection are displayed. The location of DNA is represented in red and the location of CFP-Tail 1-100 is represented in green. Co-localization of DNA and CFP-Tail 1-100 is represented in yellow. H2B-mRFP fusion protein was used to visualize the DNA as indicated.

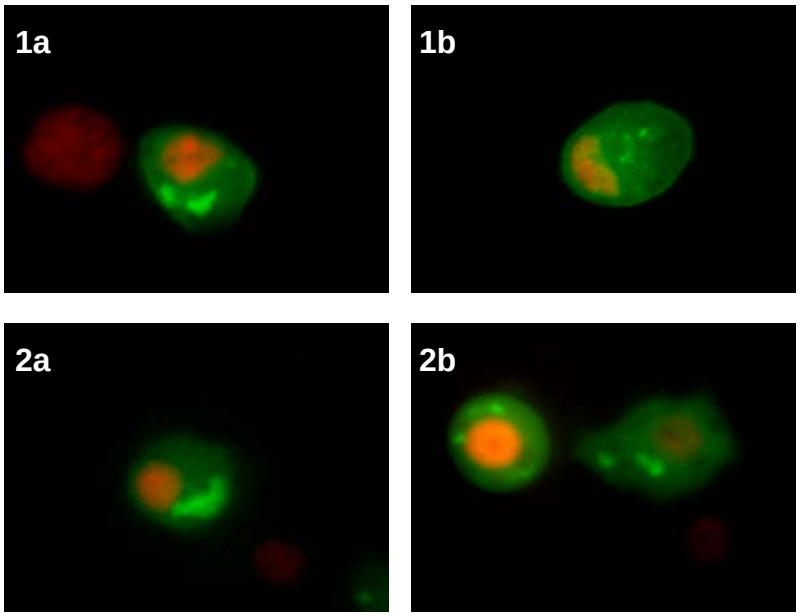

Figure 2.22. CFP-Tail 101-200 localized to the cytoplasm of transfected S2 cells.
Images were collected from two separate transfection trials (1-2), and two images (a and b) from each transfection are displayed. The location of DNA is represented in red and the location of CFP-Tail 101-200 is represented in green. Co-localization of DNA and CFP-Tail 101-200 is represented in yellow. H2B- mRFP fusion protein was used to visualize the DNA as indicated.

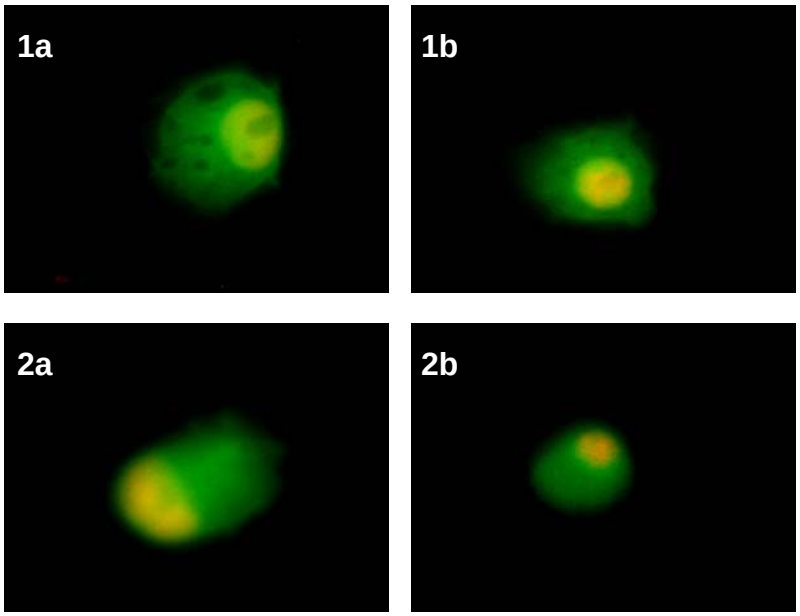

Figure 2.23. CFP-Tail 1-67 localized to the cytoplasm of transfected S2 cells.
Images were collected from two separate transfection trials (1-2), and two images (a and b) from each transfection are displayed. The location of DNA is represented in red and the location of CFP-Tail 1-67 is represented in green. Co-localization of DNA and CFP-Tail 1-67 is represented in yellow. H2B- mRFP fusion protein was used to visualize the DNA as indicated.

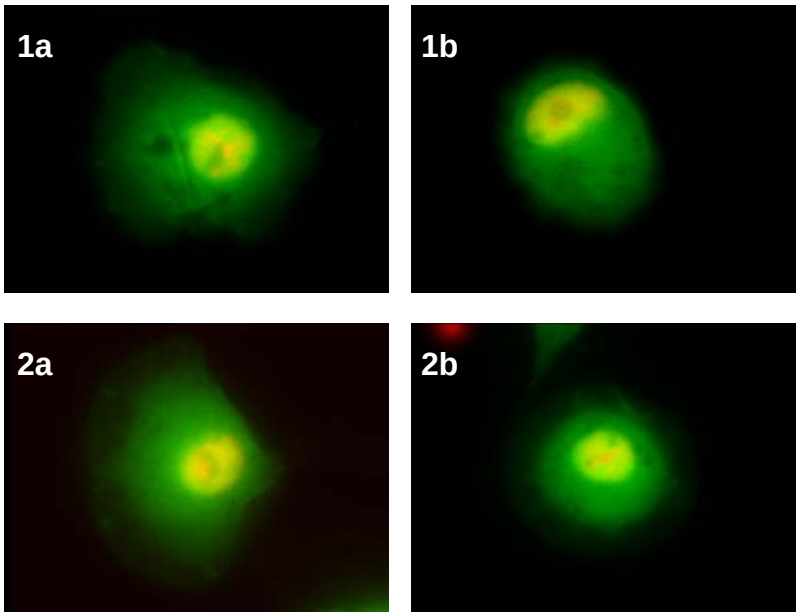

Figure 2.24. CFP-Tail 68-134 localized to the cytoplasm of transfected S2 cells.
Images were collected from two separate transfection trials (1-2), and two images (a and b) from each transfection are displayed. The location of DNA is represented in red and the location of CFP-Tail 68-134 is represented in green. Co-localization of DNA and CFP-Tail 68-134 is represented in yellow. H2B-mRFP fusion protein was used to visualize the DNA as indicated.

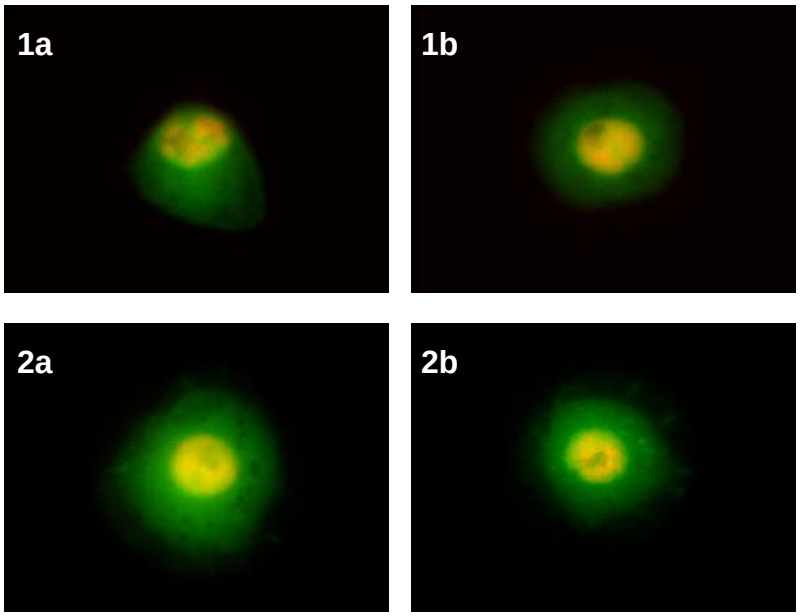

Figure 2.25. CFP-Tail 135-200 localized to the cytoplasm of transfected S2 cells.
Images were collected from two separate transfection trials (1-2), and two images (a and b) from each transfection are displayed. The location of DNA is represented in red and the location of CFP-Tail 135-200 is represented in green. Co-localization of DNA and CFP-Tail 135-200 is represented in yellow. H2B- mRFP fusion protein was used to visualize the DNA as indicated.

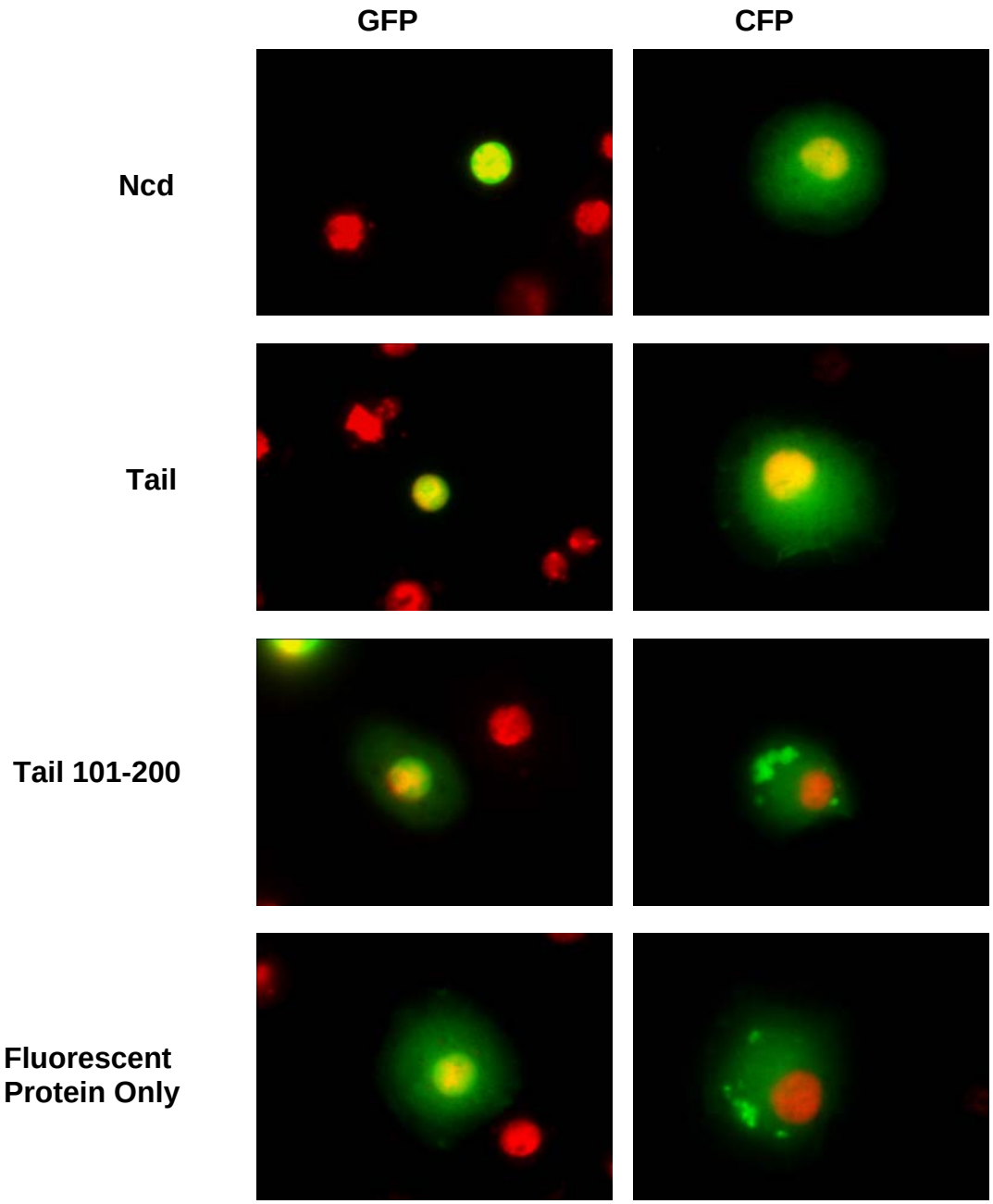

Figure 2.26. CFP-Ncd fusion proteins that contain the entire NLS or portions of the NLS failed to localize to the nuclei of transfected S2 cells.

As compared to GFP-Ncd fusion protein counterparts, CFP-Ncd fusion proteins remain in the cytoplasm regardless of NLS presence. The location of DNA is represented in red and the location of GFP-Ncd and CFP-Ncd fusion proteins are represented in green. Co-localization of DNA and respective fusion proteins is represented in yellow.

Discussion

Only GFP fusion proteins that contained the Ncd tail domain sequence localized to the nuclei of the S2 cells, indicating that a functional NLS exists within the tail domain. Fusion proteins GFP-Ncd 1-700, GFP-Ncd 1-200, and GFP-Ncd 1-355, all of which encompassed the Ncd tail sequence, localized to the nuclei of the S2 cells. In comparison, GFP- Ncd 197-355, GFP- Ncd 333- 700, and GFP- Ncd 197-700, which lacked the predicted NLS, localized to the cytoplasm (Figures 2.2.-2.8.). Proteins larger than 40 kDa are unable to efficiently diffuse across the nuclear membrane. Therefore, larger proteins, like GFP-Ncd 1-700 (~103 kDa) GFP-Ncd 1-200 (~48 kDa), and GFP-Ncd 1-355 (~65 kDa), must be actively transported across the nuclear membrane. Fusion proteins containing the Ncd stalk domain, GFP-Ncd 1-355 and GFP-Ncd 197-355, demonstrated a propensity to form inclusion bodies, most likely through compounded coiled-coiled interactions between stalk domains. As is evident from the nuclear sequestration of GFP-Ncd 1-355 and the cytoplasmic location of GFP-Ncd 197-355, the formation of inclusion bodies did not influence the cellular localization. Additionally, in instances where un-aggregated GFP-Ncd 197-355 was observed, the fusion protein was still localized to the cytoplasm. Interestingly, the GFP-Ncd 197-700 fusion protein, which represents the Ncd stalk-motor domains of the Ncd protein, demonstrated no inclusion body formation. This trend is most likely attributed to the steric hindrance placed on coiled-coiled mediated aggregation by the large, globular motor domain, an effect not achieved by the smaller tail domain in GFP-Ncd 1-355. GFP-Ncd 197-700 (~81 kDa) localized to the cytoplasm and is completely absent from

the nucleus, indicating an inability to passively diffuse through the nuclear pores. In contrast, the smaller protein, GFP-Ncd 333-700 (~66.5 kDa), localized to the cytoplasm and demonstrated a low rate of passive diffusion through the nuclear pores. This indicates that while considerable diffusion may only occur for proteins under 40 kDa, proteins ranging in size up to 66 kDa can achieve baseline diffusion across the nuclear membrane. Therefore, the complete nuclear sequestration, and the consequent lack of cytoplasmic localization, of GFP-Ncd 1-700, GFP-Ncd 1-200, and GFP-Ncd 1-355 fusion proteins is indicative of active transport and retention across the nuclear membrane.

In order to assess the validity of the results obtained using the GFP-Ncd fusion proteins, the presence of a putative NLS within the Ncd tail domain was demonstrated using V5 epitope mediated immuno-fluorescence (Figure 2.9.). In contrast to the 239 amino acid GFP sequence, the 31 amino acid (including the linker regions and the His tag) V5 epitope is a less significant sequence attachment to the Ncd protein sequence. Consequently, the V5 epitope, theoretically, should present less steric hindrance and interfere less with protein folding than the bulkier GFP sequence. This is especially true when considering that the entire Ncd tail domain is only 200 amino acids, and that the GFP sequence composes over half of the GFP-Ncd tail fusion protein. Therefore, it was hypothesized that if a functional NLS was truly located within the Ncd tail domain of the un-fused recombinant Ncd protein, both V5 epitope tagged Ncd and V5 epitope tagged Ncd tail would be translocated over the nuclear membrane and in effect be sequestered in the nucleus of S2 cells. However, the data gathered from immunofluorescence experiments was ambiguous for both Ncd 1-700-V5 and Ncd 1-200-V5 proteins (Figure

2.10.). Ncd 1-700-V5 appeared to localize to the nucleus, but did not always co-localize with the DNA. Instead, at times Ncd 1-700-V5 localized along the nuclear membrane and around the DNA. Immuno-fluorescent staining of Ncd 1-200-V5 occurred in the cytoplasm, mostly as a fluorescent ring along what appeared to be the plasma membrane. However, DIC microscopy, performed in conjunction with fluorescence microscopy to better identify the location of the fluorescence, demonstrated that Ncd 1-200-V5 localized mostly to the nuclear membrane, not the plasma membrane (Figure 2.11.). The fluorescent staining of the nuclear membrane may be a factor of the staining technique (i.e. antibody concentration), a result of V5 epitope-tagged protein over-expression and consequent clogging of nuclear pores, or may be a genuine representation of the Ncd location. Perhaps Ncd is localized and anchored to the nuclear membrane instead of free-floating in the nucleoplasm. Interestingly, at the onset of mitosis, Ncd is released from the nucleus at prophase, as opposed to another *Drosophila* mitotic motor protein, KLP61F, which is released at the onset of prometaphase [4]. It is possible that Ncd is sequestered at the nuclear membrane for the purpose of rapid release at the onset of mitosis. It may also be possible that Ncd contains a nuclear export signal (NES) that permits nuclear release prior to nuclear membrane fenestration.

The cellular localization of the individual GFP-Tail fusion proteins outlines sequence segments within the tail domain that may be essential or important to the nuclear sequestration process. The fusion proteins GFP-Tail 101-200, GFP-Tail 68-134, and GFP-Tail 135-200 localized primarily to the nuclei of transfected S2 cells (Figures 2.14., 2.16.,2.17.). Out of the three nuclear fusion proteins, GFP-Tail 135-200

was the least sequestered. This indicates that basic amino acid residues within segment 101-134 may be essential to nuclear sequestration. GFP-Tail 101-200 and GFP-Tail 68-134 fully sequestered to the nucleus suggesting that a combination of basic amino acid residues within segments 101- 134 and 135-200, respectively, may result in a more efficient nuclear localization for each protein. Furthermore, while fusion proteins GFP-Tail 1-100 and GFP-Tail 1-67 localize to the cytoplasm of S2 cells (Figures 2.13.,2.15.), basic amino acid residues within these sequence segments may ensure complete nuclear sequestration. The belief that nuclear sequestration is supported by residues in both the 1-100 and 101-200 tail segments corresponds with findings by Karabay and Walker [9], which identify two MT binding sites in the tail domain within residue segments 83-100 and 115-187. Like nuclear localization, Ncd tail- MT binding is also mediated by basic amino acid residues, therefore, the basic residues within MT binding site 83-100 may combine with the basic residues within 101-200 to guarantee complete nuclear sequestration. Alternately, given that GFP-Tail 68-134 encompasses the NLS prediction from the PSORT II algorithm between amino acid residues 92-108 and did not wholly localize to the nucleus, this algorithm may have predicted incorrect basic amino acid clusters as a putative NLS. It has been demonstrated that a single basic amino acid cluster, belonging to a bipartite pair, can be functionally rescued by the presence of neutral and acidic amino acids on the N-terminus and C-terminus flanking regions, respectively [8]. This finding was based on the characterization of the c-Myc NLS, AAKRVKLD, which was also shown to confer nuclear localization in the reverse sequence order [10]. Since GFP-Tail 101-200 and GFP-Tail 68-134 demonstrated comparable sequestration (Figures 2.14.,2.16.), and it is

possible that both fusion proteins contain an identical, single, basic amino acid cluster and have been rescued by flanking acidic and neutral amino acids. Furthermore, the partial nuclear localization of GFP-Tail 135-200 may also be attributed to a c-Myc-like NLS. GFP-Tail 135-200 contains the residue cluster, DFKARFH, which is similar to the c-Myc NLS in that an acidic amino acid residue flanks basic amino acid residues [8, 10].

GFP and CFP differ in sequence by only six amino acid residues, therefore, it is surprising that CFP interfered with nuclear sequestration of proteins that were localized to the nucleus as GFP fusions. Unlike the GFP counterparts, CFP-Ncd 1-700, CFP-Ncd 1-200 CFP-Tail 101-200, CFP-Tail 68-134, and CFP-Tail 135-200 were not sequestered to the nucleus (Figure 2.26.). However, fluorescence is present within the nuclei, and considering that CFP-Ncd 1-700 is too large for passive diffusion across the nuclear membrane, there must be a low level of active transport. The presence of CFP inclusion bodies were observed in S2 cells expressing CFP alone and in S2 cells expressing CFP-tail 101-200 (Figure 2.26.). Taken together, the low active transport of CFP-Ncd 1-700 and the presence of CFP inclusion bodies indicates that the interference of nuclear localization may be due to CFP misfolding.

For further exploration of the Ncd NLS, experimentation should include the expression of a GFP-Ncd tail 68-200 fusion protein in S2 cells, and subsequent monitoring of cellular localization with fluorescent microscopy to determine whether complete nuclear sequestration occurs. Additionally, through site- directed mutagenesis, key basic amino acid residues should be mutated to alanine to determine which mutation results in the elimination of nuclear sequestration. Loss of function mutation experiments will pinpoint basic amino acid residues within the Ncd tail protein

sequence that are essential to the nuclear sequestration of Ncd. Additionally, further work with Ncd 1-700-V5 and Ncd 1-200-V5 is merited for both the validation of the aforementioned findings and for the potential exploration of an Ncd NES.

References

1. Hatsumi, M. and S.A. Endow, *The Drosophila ncd microtubule motor protein is spindle-associated in meiotic and mitotic cells.* J Cell Sci, 1992. **103**(4): p. 1013-1020.
2. Chandra, R., et al., *Structural and functional domains of the Drosophila ncd microtubule motor protein.* J. Biol. Chem., 1993. **268**(12): p. 9005-9013.
3. Lodish, H., Berk, A., Zipursky, S.L., Matsudaira, P., Baltimore, D., & Darnell, J.E., *Molecular Cell Biology*. 4th ed. 2000, New York: W.H. Freeman and Company.
4. Sharp, D.J., et al., *Functional Coordination of Three Mitotic Motors in Drosophila Embryos.* Mol. Biol. Cell, 2000. **11**(1): p. 241-253.
5. Makhnevych, T., et al., *Cell Cycle Regulated Transport Controlled by Alterations in the Nuclear Pore Complex.* Cell, 2003. **115**(7): p. 813-823.
6. Görlich, D., et al., *Two different subunits of importin cooperate to recognize nuclear localization signals and bind them to the nuclear envelope.* Current Biology, 1995. **5**(4): p. 383-392.
7. Dingwall, C. and R.A. Laskey, *Nuclear import: A tale of two sites.* Current Biology, 1998. **8**(25): p. R922-R924.
8. Makkerh, J.P.S., C. Dingwall, and R.A. Laskey, *Comparative mutagenesis of nuclear localization signals reveals the importance of neutral and acidic amino acids.* Current Biology, 1996. **6**(8): p. 1025-1027.
9. Karabay, A. and R.A. Walker, *Identification of Microtubule Binding Sites in the Ncd Tail Domain* Biochemistry, 1999. **38**(6): p. 1838-1849.

10. Saphire, A.C.S., S.J. Bark, and L. Gerace, *All Four Homochiral Enantiomers of a Nuclear Localization Sequence Derived from c-Myc Serve as Functional Import Signals.* Journal of Biological Chemistry, 1998. **273**(45): p. 29764-29769.

Chapter 3: The steric effects of dimerization on Ncd tail-microtubule interactions

Abstract

The non-claret disjunctional motor protein (Ncd) tail domain binds microtubules (MTs) as cargo for transport within the cell. Ncd exists *in vivo* as a homodimer, and stoichiometric binding ratio (B_{max}) experiments performed with Ncd monomers do not account for the steric restrictions incurred from Ncd dimerization. To establish a physiologically relevant B_{max} between the Ncd tail domain and MTs, the Ncd tail was expressed with the Ncd stalk domain to promote dimerization. Furthermore, Ncd tail-stalk proteins were expressed as a N-terminal maltose binding protein (MBP) fusion to enhance solubility of the Ncd tail-stalk protein. MT co-sedimentation assays revealed that MBP-Ncd tail-stalk aggregated under binding assay salt concentrations, thereby preventing an accurate B_{max} assessment. Together, ineffective MBP mediated purification and the inability to remove MBP from the Ncd tail-stalk indicated that MBP may have been misfolded, and consequently, encouraged aggregation in lowered salt conditions.

Introduction

While the Ncd motor domain has traditionally been a target of motor protein research because of its sequence homology to kinesin, the tail domain has been less characterized. Experimentation by Walker and Karabay, with monomeric tail proteins

have identified MT binding sites in the Ncd tail domain and have elucidated the role of the Ncd tail in MT assembly and stability [1, 2]. Additionally, a monomeric tail protein, NT6, has been utilized to identify Ncd tail binding sites on α- and β- tubulin [3, 4]. However, since Ncd exists *in vivo* as a homodimer, interactions between the Ncd tail and MTs may be sterically restricted by dimerization [5]. Therefore, the goal of this project was to outline the interaction between the Ncd tail and MTs using Ncd tail-stalk dimers.

In contrast to the Ncd motor domain, the Ncd tail domain sequence is unlike that of most kinesin superfamily members. Instead, the Ncd tail shares chemical and functional similarity with MT associated proteins (MAPs) like tau and MAP2, which, like Ncd, are known to elicit MT assembly and stabilization. Furthermore, like tau and MAP, the Ncd tail is rich in basic residues (17%) and proline residues (11%) [1-3]. MT sedimentation assays performed with monomeric Ncd tail proteins have led to the identification of a conformation-independent MT binding site between residues 83-100 and a conformation-dependent MT binding site between residues 115-187, which most likely combine to form a single binding site [1, 2]. Each MT-binding site contains clusters of basic residues surrounded by several proline residues. Binding stoichiometry (B_{max}) values gathered from MT co-sedimentation assays, performed with NT6, a monomeric Ncd tail fragment that spans both MT binding sites in the tail, has indicated that a 4:1 binding ratio exists between the Ncd tail and the α- and β- tubulin dimer [2-4]. However, although it may be possible for four monomeric Ncd tail proteins to bind all four sites on a tubulin dimer it is unlikely that four Ncd homodimers afford the steric clearance to bind all four sites [3]. Therefore, Ncd tail-stalk proteins are more

physiologically relevant for determining binding stoichiometry between the Ncd tail domain and MTs.

The Ncd tail-stalk sequence was expressed with maltose binding protein 2 (MBP2), an altered version of wild type MBP from *E. coli* [6], at the N-terminus to encourage the proper folding and solubility of bacterially expressed Ncd tail-stalk. Proteins that are over-expressed in *E. coli* cells may form inclusion bodies as a result of high numbers of folding intermediates. Inclusion bodies are typically indicative of misfolded, inactive proteins [7]. The fusion of solubilizing proteins like MBP, glutathione S-transferase (GST), and thioredoxin (TRX) to the protein of study is a common method of preventing inclusion body formation [7, 8]. Furthermore, fusion tags also increase protein yield by deterring proteolysis of folding intermediates [7]. Purified MBP2-Ncd tail-stalk proteins (81.6 kDa) were expressed in preparation for MT co-sedimentation assays to determine the binding stoichiometry value (B_{max}) of the Ncd tail-stalk to each tubulin dimer. However, despite efforts to produce soluble Ncd tail-stalk proteins, MBP2-Ncd tail-stalk proteins aggregated, thereby preventing the accurate determination of the B_{max} between Ncd tail domain and MTs.

Methods

Generation of MBP2-Ncd Tail-Stalk Constructions

The Ncd tail-stalk protein coding sequence was amplified by PCR using the Walker lab Ncd #1 plasmid at 10 ng/µl, PFU DNA Polymerase (Stratagene), and custom

designed primers NR354Sal I and ThNcd0 0.4 μM (Invitrogen). The NR354Sal I primer attached a Sal I restriction enzyme site onto the Ncd tail-stalk protein coding sequence, and amplification with ThNcd0 facilitated blunt end ligation. The PCR reaction was performed in 34 cycles of denaturation (94 ^{o}C, 45 s), annealing (55 ^{o}C, 45 s), and extension (72 ^{o}C, 2 min), followed by a final extension (72 ^{o}C, 10 min) after the last cycle. The Ncd tail-stalk PCR product was purified using Pellet Paint Co-Precipitant (Novagen), and the Ncd tail-stalk PCR product was phosphorylated according to the Perfectly Blunt Cloning Kit (Novagen), with the use of the End Conversion Mix (Novagen). Following purification, the Ncd tail-stalk PCR product was digested with Sal I restriction enzyme (Promega), subsequently, Pellet Paint Co-Precipitant was used to purify the Ncd tail-stalk digested product. The Ncd tail-stalk was then ligated into pMAL-p2X (Amp^{R}) (New England Biolabs) digested with Sal I and Xmn I, resulting in staggered and blunt end ligation points to complement the ligation ends of the Ncd tail-stalk PCR fragment. The Ncd tail-stalk fragment was ligated in translational sequence with the open reading frame of the MBP2 within the pMAL-p2X vector. The insertion of the Ncd tail-stalk resulted in a MBP2-Ncd tail-stalk construction that is translated into a fusion protein consisting of the Ncd tail-stalk fused to the C-terminus of the MBP2. Nova Blue *E. coli* cells (Novagen) were transformed with the pMAL-p2X-Ncd tail-stalk ligation mixture, via heat shock. The pMAL-p2X-Ncd tail-stalk plasmid was purified from an *E. coli* bacteria culture grown at 37^{o}C. The region of the pMAL-p2X-Ncd tail-stalk expression plasmid that encodes the MBP2-Ncd tail-stalk fusion protein was sequenced, no sequence deviation was evident. Sequencing was performed using PCR amplification with BigDye Terminator Mix followed by analysis on an automated

capillary electrophoresis machine, which was performed at the Virginia Bioinformatics Institute.

Expression and Purification of the Ncd tail-stalk Protein

The pMAL-p2X-Ncd tail-stalk plasmid was transformed into pLys *E. coli* cells (Cap^R), via the heat shock method. Subsequently, the cells were plated on an ampicillin-Luria Broth plate. A single colony of cells possessing the pMAL-p2X-Ncd tail-stalk plasmid was used to inoculate 25 ml of Luria Broth, supplemented with ampicillin (AMP) to 100 µg/ml and chloramphenicol (CAP) to 34 µg/ml to select for only the pLys cell type containing the pMAL-p2X-Ncd tail-stalk plasmid. After an overnight incubation at 37 ^oC at 150 RPM, 20 ml of the overnight culture was used to inoculate two 1 L Luria Broth volumes supplemented with AMP and CAP to 100 µg/ml and 34 µg/ml, respectively. The 1 L pLys *E. coli* cultures were incubated at 37 ^oC and 350 RPM for 2.5 hrs, at which time a T_0 sample was taken from each culture flask. Subsequently, protein expression was induced by the addition of IPTG to 0.2 mM to each 1 L pLys *E. coli* culture flask. The cultures were then incubated for 18 hrs at room temperature, after which time a T_{18} sample was collected from each culture. Cells were collected by centrifugation at 7,000 RPM for 20 min at 4 ^oC. The pellets were each resuspended in 80 ml PM/5 buffer and centrifuged again at 4,400 RPM for 15 min at 4 ^oC. This resulted in the collection of four pellets, two from each flask. Each pellet was weighed prior to freezing in liquid Nitrogen and storage at – 80 ^oC. Time samples separated on a 7.5 %

SDS-PAGE gel demonstrate the induced expression of MBP2-Ncd tail-stalk (~85 kDa band) and, as indicated by the manufacturer, a pMAL-p2X protein (25 kDa band).

Pellets of MBP2- Ncd tail-stalk expressing *E. coli* cells were processed to collect and purify MBP2-Ncd tail-stalk. Each pellet was thawed in a 37 ^{o}C water bath and resuspended in a lysis buffer (20 mM phosphate buffer, 1 mM $MgSO_4$, 200 mM NaCl, 1 mM DTT, 2 mM PMSF, 10 mM $MgCl_2$, and 40 µg/ml DNase), 5 ml of lysis buffer per gram weight of the pellet. The pellet was rocked in the lysis buffer for 15 m at room temperature. The cells were then lysed in a French Press, three times at 15,000 psi. The lysate was centrifuged at 11,500 RPM for 30 min at 4 ^{o}C. The supernatant was collected and the pellet was resuspended in PBM 200 buffer (20 mM phosphate buffer, 1 mM $MgSO_4$, 200 mM NaCl). The supernatant was loaded on an equilibrated (PBM 200) 3.0 ml amylose resin column (New England Biolabs), in order to purify MBP2- Ncd tail-stalk proteins by affinity chromatography. The column was washed with 10 column volumes of PBM 200 buffer, and bound protein was eluted from the column with 5 column volumes of PBM 200 buffer supplemented with maltose to 10 mM final concentration. Column samples were analyzed with SDS-PAGE, and eluate samples containing MBP2 -Ncd tail-stalk protein were combined for further purification with ion exchange chromatography. The second and third eluate fractions were combined and diluted 1:3 with PBM buffer (20 mM phosphate, 1 mM $MgSO_4$), and the final volume was loaded onto a 3 ml SP-Sepharose (Pharmacia) resin column, equilibrated with PBM buffer. The column was washed with 30 ml AB buffer (20 mM Pipes, 1 mM $MgCl_2$, 1 mM EGTA, pH 6.9). The proteins were eluted from the column with a 100 mM to 500 mM NaCl step gradient, using 5 column volumes each of four separate buffers

containing 100 mM NaCl, 250 mM NaCl, 350 mM NaCl, or 500 mM NaCl in AB buffer. SDS-PAGE analysis indicated the elution of MBP2-Ncd tail-stalk with 350 mM NaCl. The first three 350 mM NaCl eluates were combined and the protein stock was concentrated with a Centriprep 30 (Amicon). Protein quantification was performed using the Bradford method (BioRad).

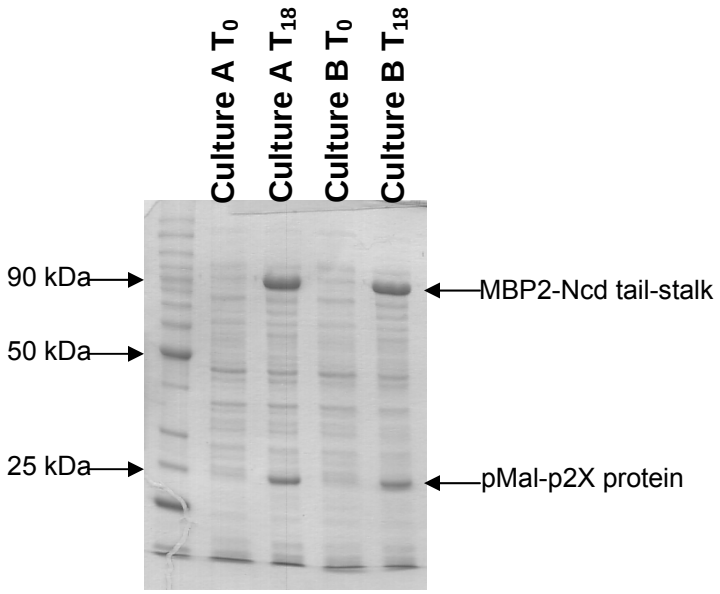

Figure 3.1. IPTG induction of pLys *E. coli* cells containing the pMAL-p2X-Ncd tail-stalk plasmid. Samples from two *E. coli* cultures were taken before induction (T_0) and at 18 hours (T_{18}) after induction. MBP2-Ncd tail-stalk protein migrates at or slightly above the 80 kDa marker band. A pMal-p2X protein, migrating below 25 kDa, is also expressed after induction.

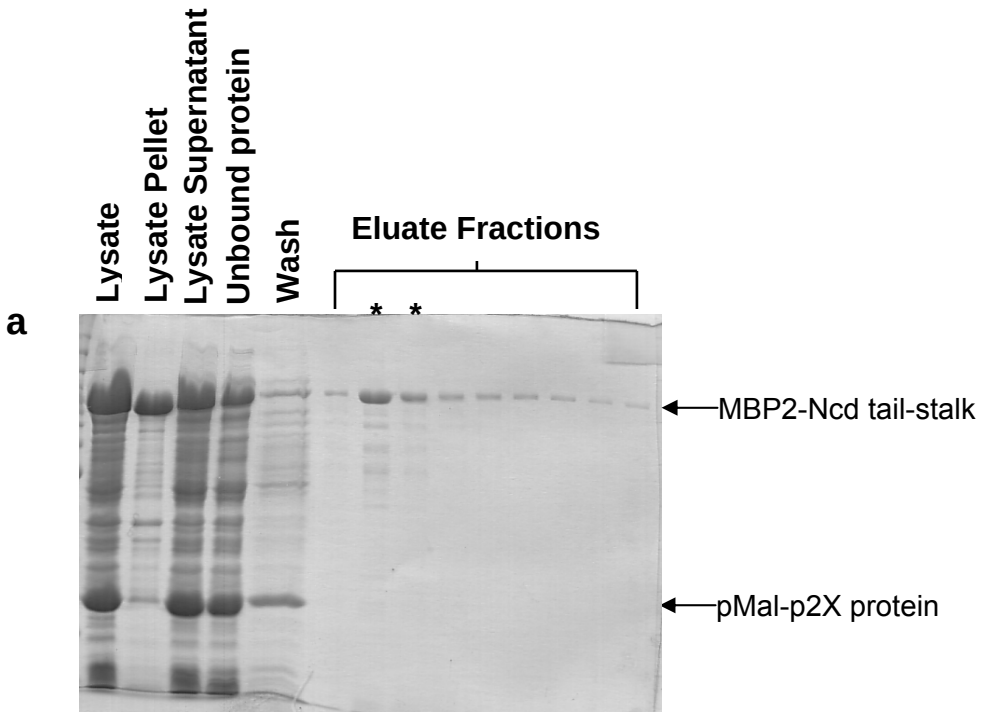

Figure 3.2. Purification of MBP2-Ncd tail-stalk protein by affinity chromatography (a) and subsequent ion exchange chromatography (b,c).

a) Soluble MBP2-Ncd tail-stalk was purified on amylose resin, and the second and third eluate fractions (*) were combined for b and c) purification on S-Sepharose from which MBP2-Ncd tail stalk was eluted within the first three eluate fractions of 350 mM NaCl (*). The eluates were combined and concentrated to a stock concentration of 14.7 µM

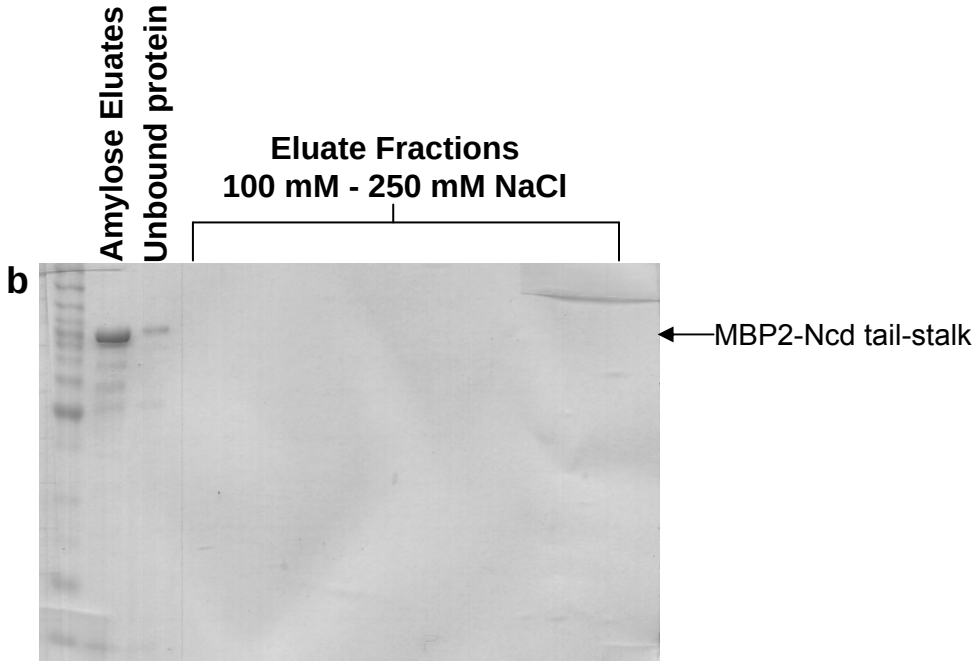
Amylose Eluates
Unbound protein
Eluate Fractions
100 mM - 250 mM NaCl
b
MBP2-Ncd tail-stalk

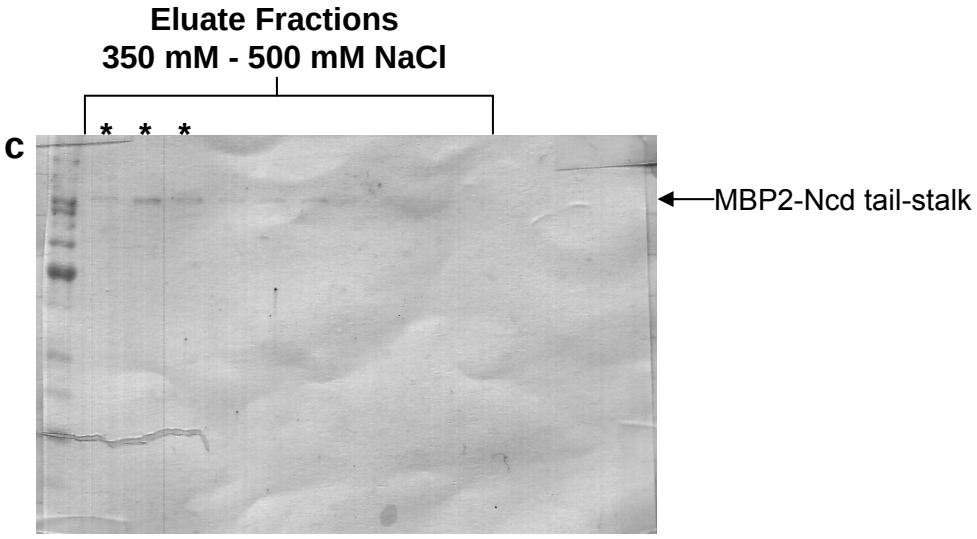
Eluate Fractions
350 mM - 500 mM NaCl
* * *
c
MBP2-Ncd tail-stalk

An alternative method of purification was used to retrieve MBP2- Ncd tail-stalk fusion proteins first, by ion exchange chromatography and secondly, by affinity chromatography. Pellets were lysed in a method identical to the aforementioned purification method, and the lysates were centrifuged as stated above. Following centrifugation, each supernatant was diluted 1:3 with PBM buffer and loaded onto a 3.0 ml SP-Sepharose resin (Pharmacia) column equilibrated with PBM buffer. The SP-Sepharose column was washed with 10 volumes of AB buffer plus 1 mM DTT, and proteins were eluted from the column using 5 column volumes of 250 mM NaCl, 1 mM DTT in AB buffer and 5 column volumes of 500 mM NaCl, 1 mM DTT in AB buffer. SDS-PAGE analysis verified the presence of MBP2-Ncd tail-stalk protein in the 500 mM NaCl elution fraction. In preparation for affinity purification, the 500 mM elution sample was diluted 1:2 with AB buffer plus 1 mM DTT to a salt concentration of 250 mM NaCl. Subsequently, the eluate sample was loaded onto an equilibrated (AB buffer) 3.0 ml amylose resin column. The column was washed with 10 column volumes of AB buffer plus 1 mM DTT, and the proteins were eluted with 5 ml AB buffer supplemented with 50 mM NaCl, 10 mM maltose, and 1 mM DTT. SDS-PAGE analysis indicated that most of the MBP2-Ncd tail-stalk remained unbound to the amylose resin and that the bound MBP2-Ncd tail-stalk was eluted mostly in the third and fourth eluate fractions. To improve the purification yield, unbound MBP2-Ncd tail-stalk from the initial purification was re-loaded onto the amylose resin column and the purification cycle was performed consecutively five times, from which the first purification cycle yielded additional MBP2-Ncd tail-stalk. The resin bed was equilibrated with 10 column volumes of AB buffer between each purification attempt. Eluate fractions containing MBP2-Ncd tail-stalk

were combined and concentrated in a Centriprep 30 (Amicon) **(E30)**. Since a majority of the MBP2-Ncd tail-stalk protein did not bind to the amylose resin, a portion of the unbound MBP2-Ncd tail-stalk was also concentrated in a Centriprep 30 **(FT30)**, and a volume of FT30 was concentrated in a Microcon 10 (Amicon) **(FT10)**. Given that most MBP2-Ncd tail-stalk remained unbound, additional purification procedures included only the ion-exchange chromatography detailed above. All protein quantification was performed using the Bradford method (BioRad).

Taxol Stabilized Microtubules (TMTs)

Lyophilized tubulin (1 mg) was resuspended in 100 µl 1X PM buffer and 1 mM GTP, and incubated at 37 ^{o}C for 20 m. Subsequently, 100 µl 1X PM buffer supplemented with 100 µM taxol was added, from which TMTs were formed at 37 ^{o}C for at least 15 m. Stock tubulin was stored at a 50 µM concentration at -80 ^{o}C.

Microtubule Binding Assays

MT binding assays were performed in AB buffer containing 40 µM taxol and 100 µg/ml bovine serum albumin (BSA) as 150 µl reaction volumes. TMTs, at a concentration of 2.5 µM tubulin, were combined with MBP2-Ncd tail-stalk protein at 0.625 µM, 1.25 µM, 2.5 µM, 5.0 µM, 10.0 µM, or 15.0 µM concentrations (MBP2-Ncd tail-stalk : TMTs ratios of 0.25:1, 0.5:1, 1:1, 2:1, 4:1, and 6:1). Reactions were incubated at 25 ^{o}C for 30 min. Subsequently, 50 µl of the reaction was collected for analysis, and 100 µl of the reaction mixture was overlayed over a 25 % sucrose cushion

plus 40 μM taxol and centrifuged at 100,000 x g for 30 min at 25 ^{o}C in a TLA 45 rotor or a TLA 100.3 K rotor in a Beckman TL-100 ultracentrifuge. After centrifugation, the supernatant was collected from above the sucrose cushion and the pellet was resuspended in 100 μl AB buffer. The initial reaction samples and the supernatant and pellet fractions were analyzed with SDS-PAGE, and the co-sedimentation of the MBP2-Ncd tail-stalk with the TMTs was determined.

Microtubule Bundling Assays

MT binding assays were performed in AB buffer containing 40 μM taxol and 100 μg/ml BSA as 50 μl reactions. Taxol stabilized MTs (TMTs), at a concentration of 2.5 μM tubulin, were combined with MBP2-Ncd tail-stalk protein 2.5 or 5.0 μM concentrations (MBP2-Ncd tail-stalk : TMTs ratios of 1:1 and 2:1). Reactions were performed at 25 ^{o}C for 30 min. Following incubation, coverslips were placed on microscope slides with structural channels built from double stick tape, and the reaction mixtures were dispensed into the channels. The coverslips were sealed with paraffin wax to preserve the suspension under the coverslips, and the MT bundling capability of the MBP2-Ncd tail-stalk protein was determined with video-enhanced DIC microscopy [1].

MBP2-Ncd tail-stalk Digestion

Digestion reactions of MBP2-Ncd tail-stalk, in 250 mM NaCl, were performed with Thrombin or Factor Xa in order to remove the MBP2 domain from the Ncd tail-stalk. Thrombin digestion was performed at room temperature, using 1 u of thrombin per mg of MBP2-Ncd tail-stalk protein. The thrombin enzyme solution was supplemented with 5 mM $CaCl_2$ to enhance enzyme function. Factor X_a digestion was performed at room temperature, using a w/w enzyme to fusion protein ratio of 1%. Time-point samples were taken from the overall reaction volume and were processed with 2X SDS/β-mercaptoethanol buffer in a thermocycler for 5 m at 99 ^{0}C to inactivate the digestive enzymes.

Results

MBP2-Ncd tail-stalk:tubulin co-sedimentation assays

MBP2-Ncd tail-stalk was bacterially expressed (Figure 3.1) in preparation for MT co-sedimentation assays, which were performed to determine the stoichiometric binding relationship between Ncd tail-stalk and MTs. The initial purification of MBP2-Ncd tail-stalk by amylose affinity chromatography followed by SP-Sepharose ion exchange chromatography (Figure 3.2 a-c) yielded protein used in the primary TMT-MBP2-Ncd tail-stalk co-sedimentation experiments performed at 0.25:1, 0.5:1, 1:1, and 2:1 MBP2-Ncd tail-stalk monomer to tubulin dimer ratios (Figures 3.3. and 3.4.). Supernatant and

pellet fractions were analyzed with SDS-PAGE, which demonstrated that the total amount of MBP2-Ncd tail-stalk pelleted with the TMTs at 0.25:1, 0.5:1, 1:1, and 2:1 MBP2-Ncd tail-stalk to tubulin ratios. Control sedimentation reactions were also performed. These included reactions containing TMTs minus MBP2-Ncd tail-stalk (0:1) and reactions containing MBP2-Ncd tail-stalk, at 2.5 μM, minus TMTs (1:0). SDS-PAGE analysis of the TMT control reaction, 0:1, demonstrated that tubulin was present only in the pellet fraction, indicating that the tubulin was present as TMTs. SDS-PAGE analysis showed a faint band representing MBP2-Ncd tail-stalk in the pellet fraction of the MBP2-Ncd tail-stalk control reaction, 1:0 (Figure 3.3.). The presence of this band was attributed to an inadequate separation of the supernatant and pellet fractions. Consequently, sucrose cushions were used in subsequent reactions to prevent this supposed artifact from occurring. However, even in the presence of a 25% sucrose cushion MBP2-Ncd tail-stalk was still detected in the pellet fraction (Figure 3.4.).

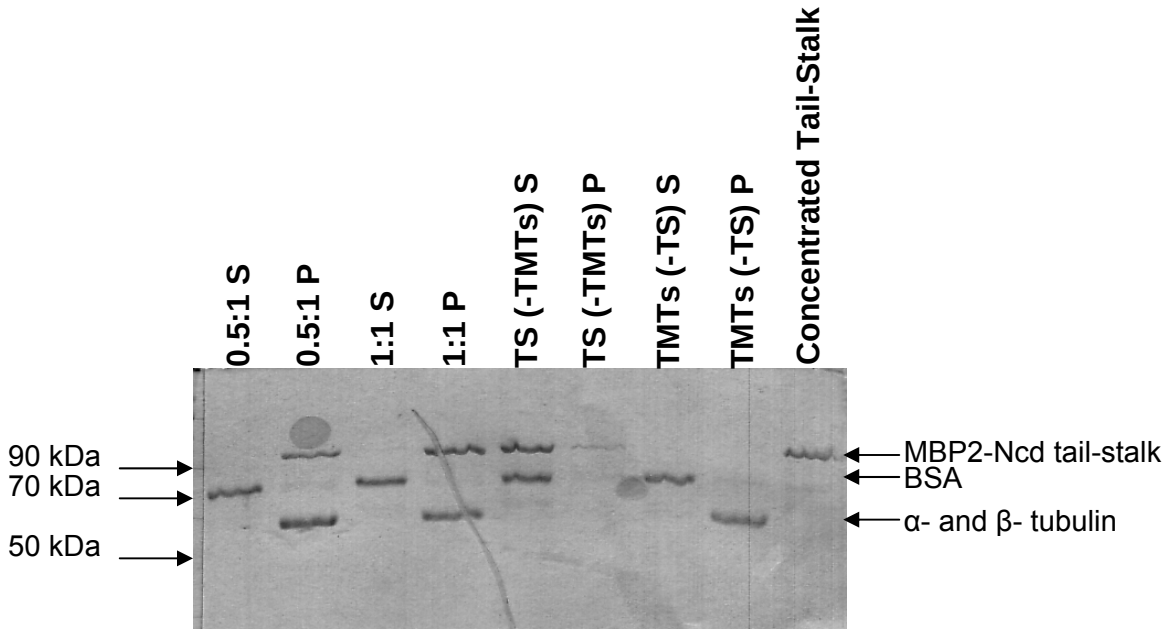

Figure 3.3. MBP2-Ncd tail-stalk co-sediments with the TMTs up to a 1:1 MBP2-Ncd tail-stalk to TMTs ratio.

Co-sedimentation assays were performed with MBP2-Ncd tail-stalk and tubulin at 0.5:1 and 1:1 ratios and SDS-PAGE analysis of supernatant (S) and pellet (P) fractions was performed. Reactions involving MBP2-Ncd tail-stalk alone (TS(-TMTs)) and TMTs alone (TMTs(-TS)) were performed as controls. Residual MBP2-Ncd tail-stalk detected in the tail-stalk (-TMTs) pellet fraction was initially attributed to ineffective pellet-supernatant separation.

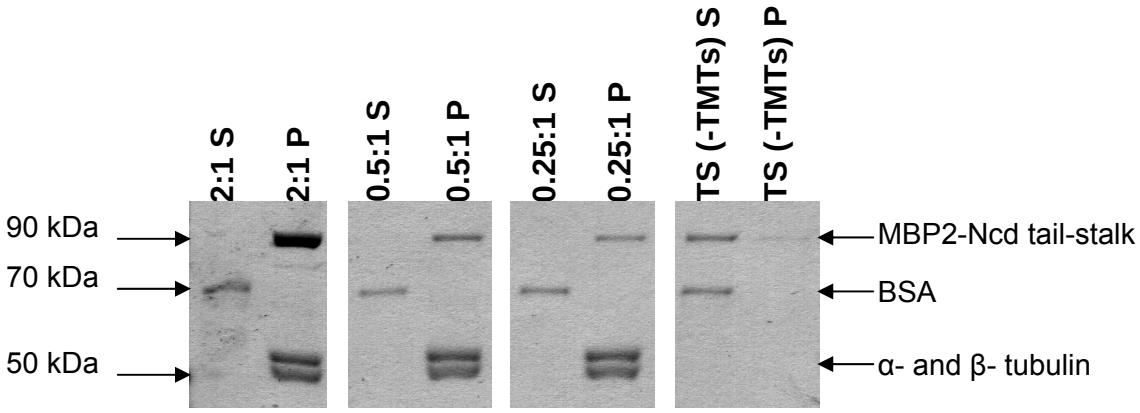

Figure 3.4. MBP2-Ncd tail-stalk co-sediments with the TMTs up to a 2:1 MBP2-Ncd tail-stalk to TMTs ratio.

Co-sedimentation assays performed with MBP2-Ncd tail-stalk and tubulin at 0.25:1, 0.5:1, and 2:1 ratios with the addition of a sucrose cushion. Despite the use of a sucrose cushion, residual MBP2-Ncd tail-stalk was detected in the tail-stalk (-TMTs) pellet fraction.

In an effort to increase protein yield from amylose purification, ion exchange chromatography was used prior to affinity purification (Figure 3.5. a-c). This purification method allowed for the removal of potential interfering proteins prior to amylose affinity purification. Analysis of column fractions indicated a large amount of MBP2-Ncd tail-stalk protein, purified by SP-Sepharose, still remained unbound to the amylose resin. Furthermore, the SP-Sepharose resin alone purified the MBP2-Ncd tail-stalk to a level equal to the purification level achieved by using both the affinity chromatography and ion-exchange chromatography. Therefore, MT co-sedimentation experiments were performed at a 4:1 MBP2-Ncd tail-stalk to tubulin ratio in order to compare the binding of the MBP2- Ncd tail-stalk protein that remained unbound to the amylose resin (FT30) and the bound MBP2- Ncd tail-stalk protein (E30). Secondly, a portion of the FT30 was concentrated (FT10), and the activity of the FT30 and FT10 were compared to determine any effects of concentration. SDS-PAGE analysis showed no difference between the solubility and MT-binding ability of E30 and FT30 or FT10 (Figure 3.6.). Furthermore, FT30 and E30 protein solutions were used in TMT bundling reactions at 1:1 and 2:1 MBP2-Ncd tail-stalk to tubulin ratios. Both FT30 and E30 bundled TMTs to a degree proportional to the amount of MBP2-Ncd tail-stalk in the reaction (Figure 3.7.). Specifically, there was increased bundling activity in the 2:1 bundling reaction as compared to the 1:1 bundling reaction. In consideration of the solubility, binding and bundling similarities, the unbound MBP2-Ncd tail-stalk fractions, FT30 and FT10, and the bound MBP2-Ncd tail-stalk fraction, E30, were used in subsequent MT co-sedimentation reactions without discrimination. In addition, MBP2-Ncd tail-stalk that

was purified only by ion-exchange chromatography was also used in MT co-sedimentation reactions.

MT co-sedimentation experiments were performed at 0.25:1 (data not shown), 0.5:1, 1:1, 2:1, 4:1, and 6:1 MBP2-Ncd tail-stalk to tubulin ratios, and supernatant and pellet fractions were analyzed with SDS-PAGE. Additionally, control co-sedimentation reactions were performed, including reactions containing TMTs minus MBP2-Ncd tail-stalk, and reactions containing MBP2-Ncd tail-stalk, of respective concentrations, minus TMTs. In an effort to achieve better separation of supernatant and pellet fractions, this round of MT co-sedimentation experiments was performed using 100 µl of a 25 % sucrose cushion. Complete co-sedimentation of MBP2-Ncd tail-stalk with TMTs occurred up to a 2:1 ratio, while a portion of MBP2-Ncd tail-stalk remained in the supernatant fraction of the 4:1 and 6:1 ratio co-sedimentation experiment (Figure 3.8.). However, SDS-PAGE analysis of MBP2-Ncd tail-stalk minus TMTs control reactions showed MBP2-Ncd tail-stalk in the pellet fractions. These data indicate the presence of MBP2-Ncd tail-stalk protein aggregates, which in turn indicates that the 2:1 B_{max} is inaccurate. This also implies that the faint bands in the 1:0 control reactions of the initial co-sedimentation experiments were most likely not an artifact of poor supernatant/pellet fractionation, but were a result of MBP2-Ncd tail-stalk protein aggregation. SDS-PAGE analysis of the TMT control reaction, 0:1, demonstrated that tubulin was present only in the pellet fraction, indicating that the tubulin was present as TMTs.

Removal of MBP from Ncd tail-stalk

In an effort to remedy MBP2-Ncd tail-stalk aggregation and to obtain only soluble Ncd tail-stalk, the removal of MBP by endopeptidases, thrombin and Factor Xa, was attempted. Samples of thrombin and Factor Xa digestions were collected at half-hour and one hour time points (T), respectively. Thrombin digestion of MBP2-Ncd tail-stalk resulted in the formation of a prominent 60-65 kDa product (Product A) and a less prominent product migrating below 50 kDa (Product B), both of which became more abundant as a function of time (Figure 3.9a.). While the very faint secondary product may migrate near 40kDa, which is roughly the molecular weight of both MBP and Ncd, the primary product migrates at a much higher molecular weight, indicating that a mostly non-specific digestion occurs within the MBP sequence or the Ncd tail-stalk sequence but not at the thrombin cleavage site between the two. Likewise, non-specific Factor Xa digestion results in the formation of a primary product at 55 kDa (Product A) that is formed almost immediately upon enzyme addition (Figure 3.9b.). Over time, a secondary product migrating below 50 kDa (Product B) forms as the primary product disappears, indicating that a secondary digestion of the primary digestion product occurs (Figure 3.9b.). Similarly to thrombin, Factor Xa produces a product that may migrate near the expected molecular weight of both MBP and Ncd tail-stalk.

To determine whether the Ncd tail-stalk subunit MT-binding activity is preserved, volumes of each thrombin and Factor Xa digestion reaction were used in a TMT co-sedimentation assays. None of the products from either thrombin or Factor Xa

digestion pelleted with TMTs. However, undigested MBP2-Ncd tail-stalk remaining in the one hour thrombin reaction did co-sediment with the TMTs (Figure 3.10.).

Identification of aggregating conditions

While misfolding of MBP may induce aggregation other factors such as, protein stock concentration and salt concentration were also investigated as possible reasons for MBP2-Ncd tail-stalk aggregation. A series of sedimentation reactions, in the absence of TMTs, were performed in varying conditions to access those conditions that encourage aggregation (Figure 3.11.). In order to determine whether discrepancies in buffer preparation were causing aggregation, two preparations of AB buffer were used in separate sedimentation reactions. MBP2-Ncd tail-stalk demonstrated greater aggregation in AB buffer preparation A than in preparation B, although the buffer recipe was followed. Buffer A induced aggregation was alleviated upon salt supplementation at 500mM NaCl, resulting in aggregation levels similar to that of buffer B. Similar trends were exhibited in sedimentation reactions performed with concentrated MBP2-Ncd tail-stalk, however, aggregation in all reactions was more severe than in the unconcentrated counterpart reactions.

Additional co-sedimentation reactions were performed in the absence of TMTs to determine whether aggregation was caused primarily by increased protein concentration or by a decrease in salt concentration (Figure 3.12.). Unconcentrated MBP2-Ncd tail-stalk was centrifuged at co-sedimentation speeds to determine any pelleting of aggregates. The pellet fraction was resuspended in AB plus 500 mM NaCl,

to preserve the buffer conditions of the original protein solution. Interestingly, SDS-PAGE analysis of the pellet fraction showed that aggregates were not present, and protein quantification indicated no significant concentration difference between the un-cleared protein stock solution and the cleared protein stock. Sedimentation assays were performed with the cleared, unconcentrated MBP2-Ncd tail-stalk solution or the cleared, concentrated MBP2-Ncd tail-stalk in the absence of TMTs. The final salt concentrations of the sedimentation assays were 110 mM and 8 mM for the unconcentrated and concentrated MBP2-Ncd tail-stalk assays, respectively. SDS-PAGE analysis showed that in both instances, pelleting of MBP2-Ncd tail-stalk occurred in the absence of TMTs, although the amount of protein was greater in the concentrated MBP2-Ncd tail-stalk pellet fraction. These results indicated that aggregation occurred in response to the conditions of the binding assays and not as a direct result of the protein expression and purification.

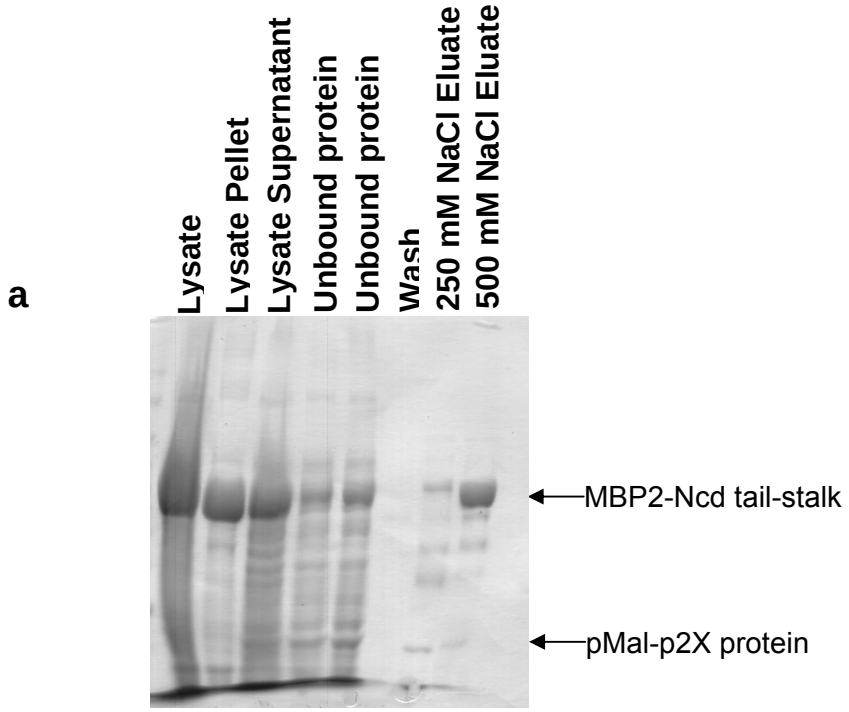

Figure 3.5. Purification of MBP2-Ncd tail-stalk protein by ion exchange chromatography (a) and subsequent affinity chromatography (b,c).

a) Soluble MBP2-Ncd tail-stalk was purified on S-Sepharose resin and eluted with 500 mM NaCl in a single fraction. b) MBP2-Ncd tail-stalk was further purified on amylose resin, eluted in ten fractions from which the third and fourth fractions (+) were combined. c) Unbound MBP2-Ncd tail-stalk (b) was re-purified on amylose resin five times with one unbound, wash, and eluate fraction per purification cycle. Additional purified MBP2-Ncd tail-stalk was obtained in the eluate fraction of the first purification round (*).

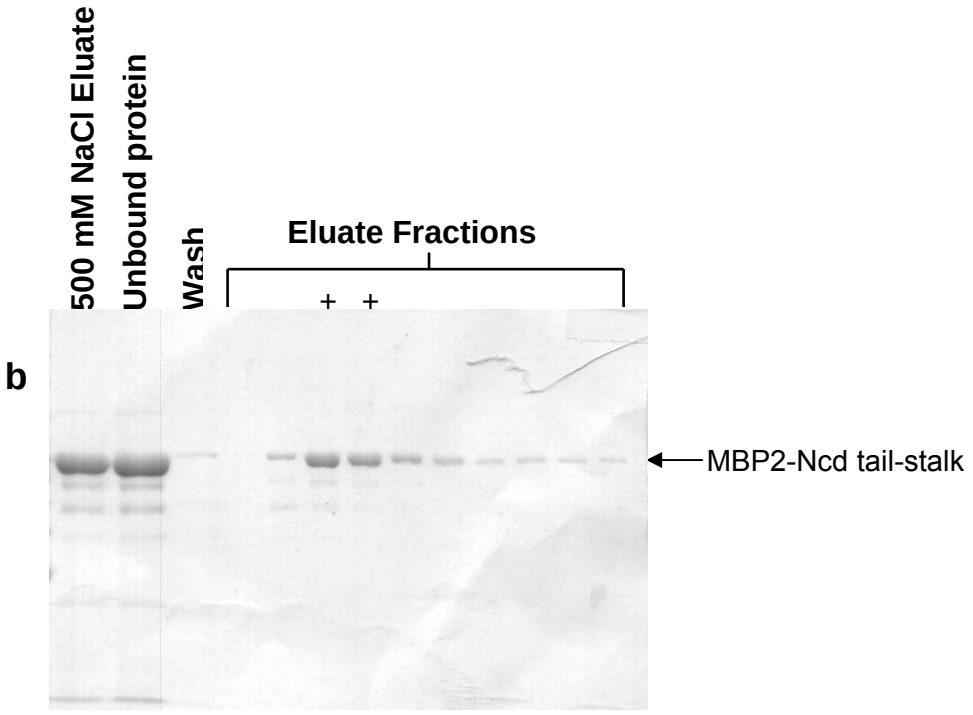
500 mM NaCl Eluate
Unbound protein
Wash
Eluate Fractions
+ +
b
MBP2-Ncd tail-stalk

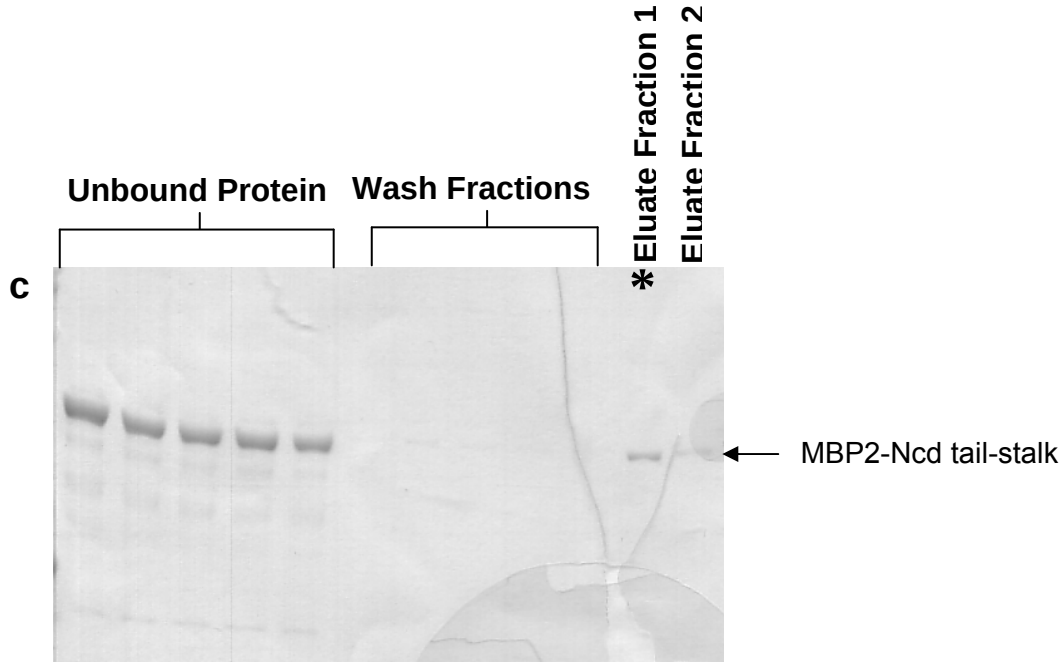
Eluate Fraction 1
Eluate Fraction 2
Unbound Protein
Wash Fractions
*
c
MBP2-Ncd tail-stalk

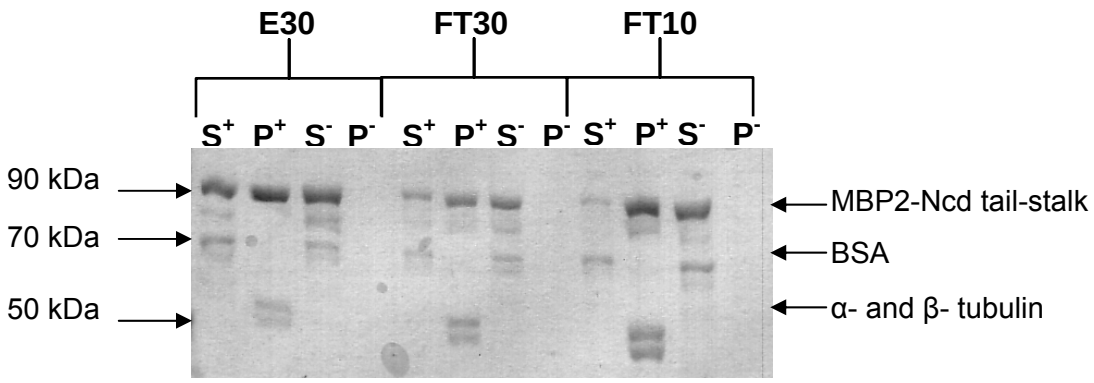

Figure 3.6. Co-sedimentation assays performed with E30, FT30, or FT10 MBP2-Ncd tail-stalk protein preparations indicated that the three preparation were comparable.
Co-sedimentation assays performed at 4:1 and 4:0 MBP2-Ncd tail-stalk monomer to tubulin ratios. SDS-PAGE analysis indicates that all three protein preparations bind tubulin at less than a 4:1 ratio. Since MBP2-Ncd tail-stalk protein remained in supernatant, variations in band intensity are attributed to processing. Supernatant and pellet fractions are labeled S and P, respectively, and the presence or absence of TMTs are denoted as + and -, respectively. Note that the gel is slanted left to right, thereby skewing molecular weight markings on the right side.

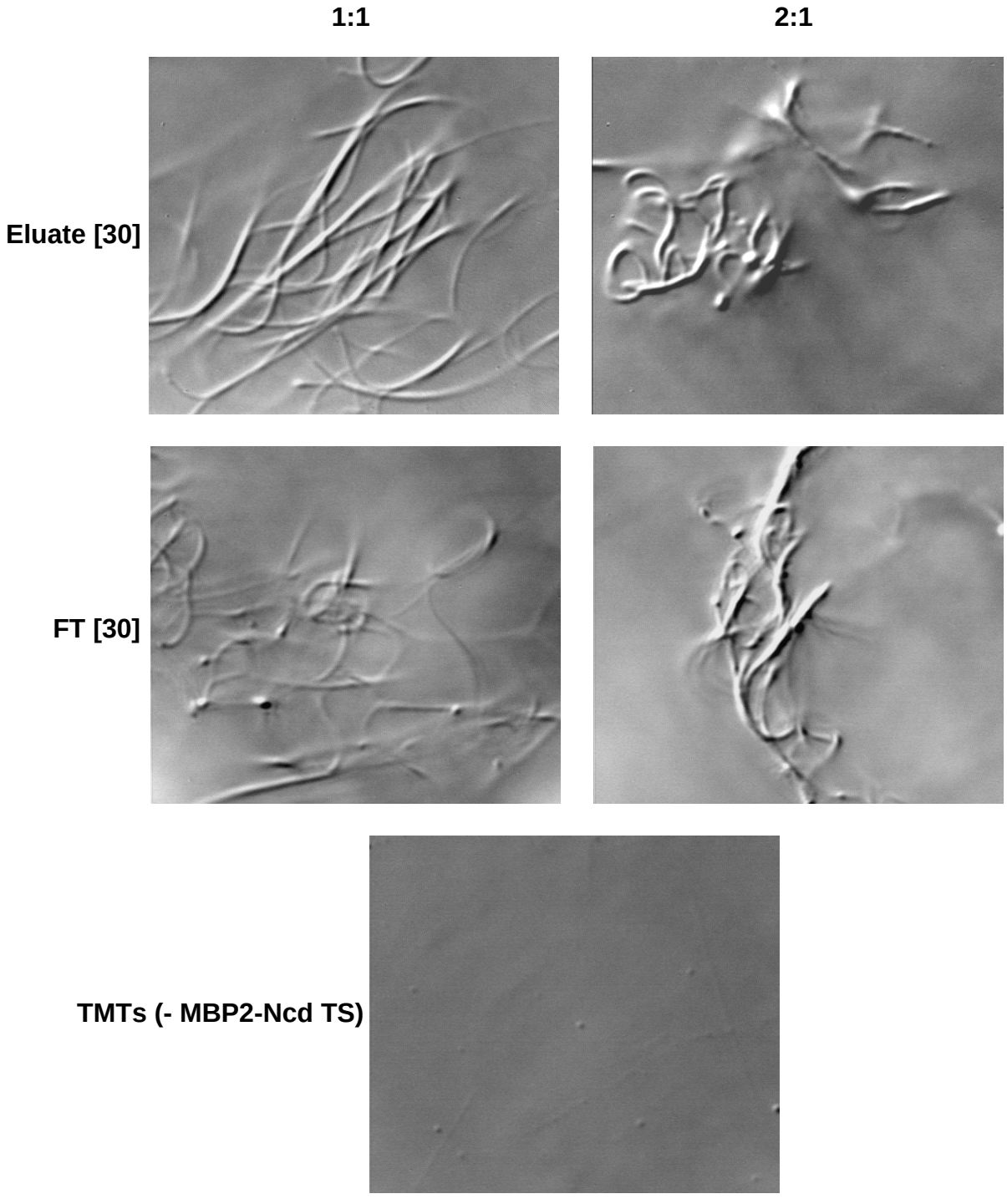
1:1
2:1
Eluate [30]
FT [30]
TMTs (- MBP2-Ncd TS)

Figure 3.7. TMT bundling assays verified the functionality of bound (E30) and unbound (FT30) MBP2-Ncd tail-stalk protein.

TMT bundling was performed at 1:1 and 2:1 MBP2-Ncd tail-stalk to tubulin ratios. Both E30 and FT30 proteins induced TMT bundling at levels directly proportional to the amounts of MBP2-Ncd tail-stalk. E30 and FT30 bundling activities were comparable. TMTs in the absence of MBP2-Ncd tail-stalk showed little bundling activity.

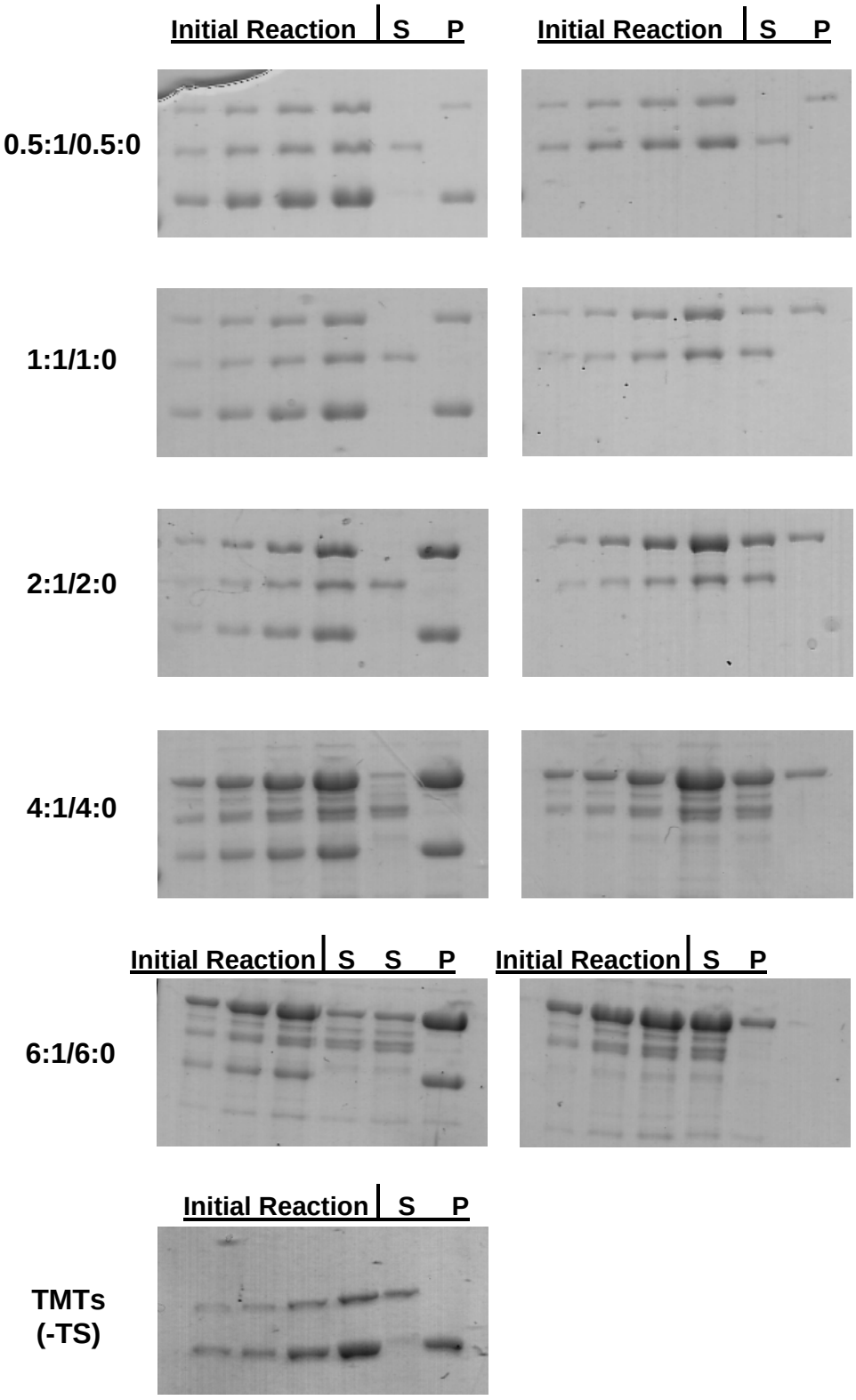
Initial Reaction S P
Initial Reaction S P
0.5:1/0.5:0
1:1/1:0
2:1/2:0
4:1/4:0
Initial Reaction S S P
Initial Reaction S P
6:1/6:0
Initial Reaction S P
TMTs
(-TS)

Figure 3.8. MBP2-Ncd tail-stalk monomers may bind to tubulin at up to a 2:1 ratio but forms aggregates that skew the data.

Co-sedimentation assays performed with MBP2-Ncd tail-stalk and tubulin at 0.5:1, 1:1, 2:1, 4:1 and 6:1 ratios. SDS-PAGE analysis indicates that MBP2-Ncd tail-stalk monomers bind to tubulin at up to a 2:1 ratio, but demonstrated that MBP2-Ncd tail-stalk pellets in the absence of TMTs. Increasing volumes of the total co-sedimentation reaction (Initial Reaction) were loaded for subsequent quantification procedures. Separated supernatant (S) and pellet (P) fractions are denoted.

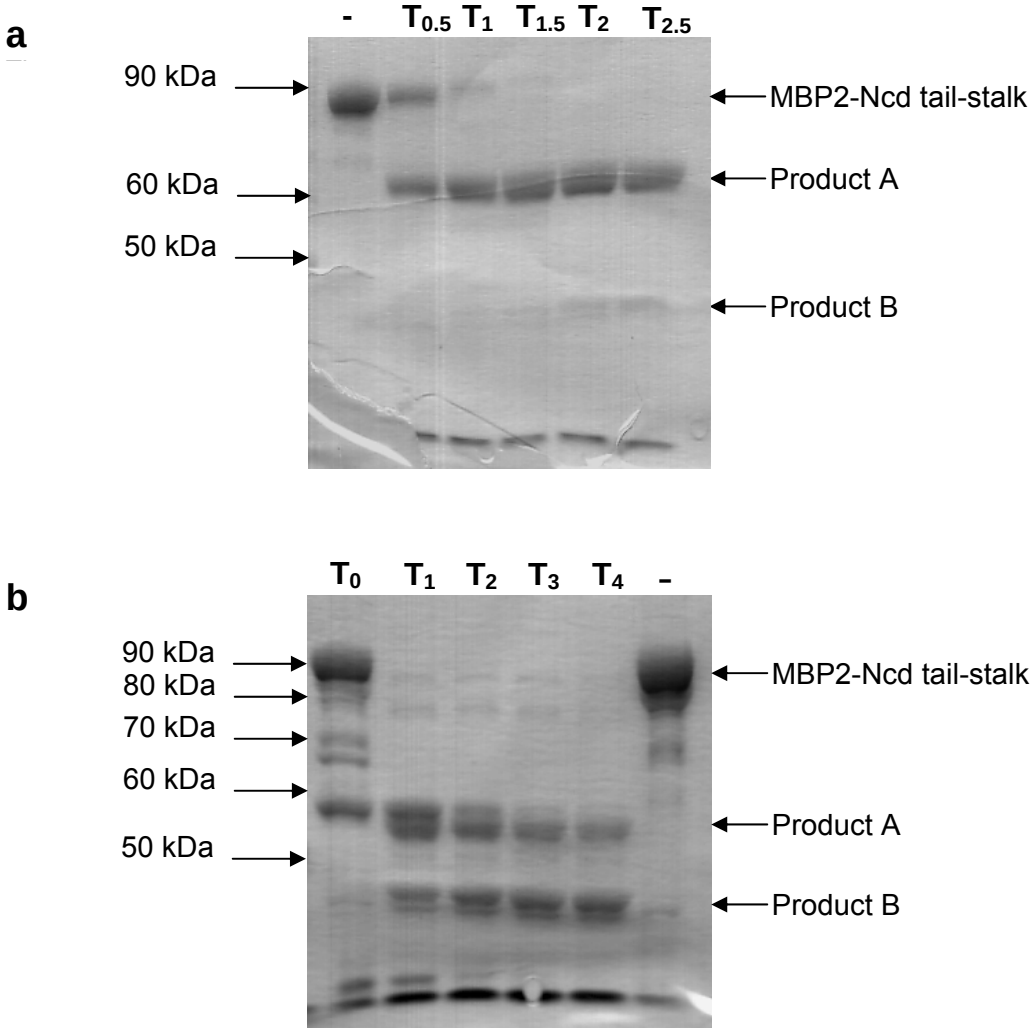

Figure 3.9. Thrombin and Factor Xa mediated removal of MBP from the Ncd tail-stalk does not occur in a site specific manner.

SDS-PAGE analysis of thrombin (a) and Factor Xa (b) time-point samples demonstrated incomplete or non-specific digestion. a) Thrombin digestion results in one product that migrates between 60-65 kDa and a secondary product that migrates below 50 kDa b) Factor Xa digestion results in one product that migrates at 55 kDa (Product A) and another product that migrates below 50 kDa (Product B). Reaction time was measured in hours and is indicated as T. Protein stock without the addition of enzyme was used as a negative control (-).

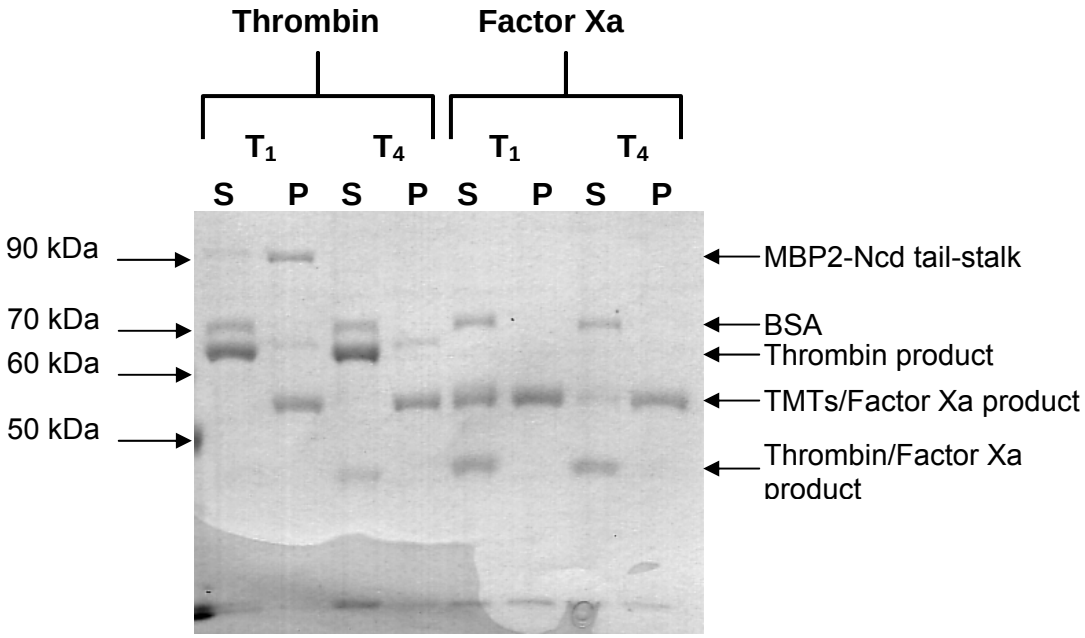

Figure 3.10. MBP2-Ncd tail-stalk digestion products do not retain TMT binding ability. Co-sedimentation assays were performed at a ~4:1 digested MBP2-Ncd tail-stalk to tubulin ratio. SDS-PAGE analysis of the supernatant (S) and pellet (P) fractions from one hour (T_1) and four hour (T_4) enzyme digestions indicate that thrombin and Factor Xa digestive products do not pellet, and thus do not retain the TMT binding ability exhibited by full length MBP2-Ncd tail-stalk.

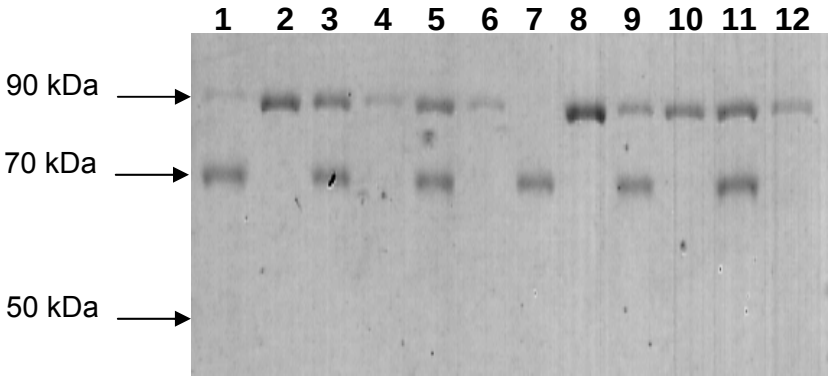

Figure 3.11. Decreased salt concentration and increased protein stock concentration encourage MBP2-Ncd tail-stalk aggregation.

SDS-PAGE analysis was performed on supernatant and pellet fractions from sedimentation assays performed in the absence of TMTs. Lanes 1 and 2- supernatant (1) and pellet (2) of MBP2-Ncd tail-stalk in buffer preparation A; Lanes 3 and 4- supernatant (3) and pellet (4) of MBP2-Ncd tail-stalk in buffer preparation B; Lanes 5 and 6- supernatant (5) and pellet (6) of MBP2-Ncd tail-stalk in buffer preparation A supplemented with 500 mM NaCl; Lanes 7 and 8- supernatant (7) and pellet (8) of MBP2-Ncd tail-stalk [30] in buffer preparation A; Lanes 9 and 10- supernatant (9) and pellet (10) of MBP2-Ncd tail-stalk [30] in buffer preparation B; Lanes 11 and 12- supernatant (11) and pellet (12) of MBP2-Ncd tail-stalk in buffer preparation A supplemented with 500 mM NaCl.

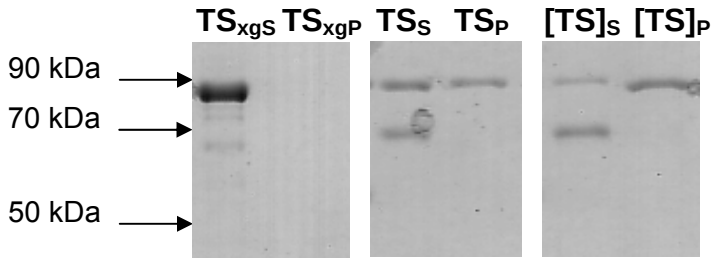

Figure 3.12. MBP2-Ncd tail-stalk aggregation occurs as a function of decreased salt concentration. SDS-PAGE of cleared (xg) MBP2-Ncd tail-stalk that was subsequently used in sedimentation assays in the absence of TMTs. MBP2-Ncd tail-stalk, in 500 mM NaCl, did not pellet under sedimentation centrifugal speeds ($TS_{xgS,}$ TS_{xgP}). Both unconcentrated (TS) and concentrated ([TS]) MBP2-Ncd tail-stalk pelleted in sedimentation assay conditions.

Discussion

Despite efforts to purify soluble Ncd tail-stalk, MBP2-Ncd tail-stalk demonstrated a propensity to aggregate under co-sedimentation assay conditions. Purification methods, protein concentration, and salt concentration were explored as potential factors causing aggregation. The two methods of purification used in this study, in which the order of affinity purification and ion-exchange purification was interchanged, produced protein stock solutions with comparable purity (Figures 3.2. and 3.5.). The amylose binding property of MBP is purported to facilitate affinity purification of the fusion proteins. However, amylose mediated purification resulted in a large amount of unbound MBP2-Ncd tail-stalk (Figures 3.2. and 3.5.), indicating that the MBP domain of some MBP2-Ncd tail-stalk proteins may be misfolded resulting in loss of function. On the contrary, similarity between the solubility and TMT binding properties of E30 and FT30, as indicated by co-sedimentation (Figure 3.6.) and TMT bundling assays (Figure 3.7.), signifies that the most Ncd tail-stalk domains are functional and properly folded.

A preliminary co-sedimentation assay (Figure 3.3.) demonstrated that Ncd tail-stalk monomers bind TMTs up to a 1:1 Ncd to TMTs ratio. MBP2-Ncd tail-stalk detected in the pellet fraction of the tail-stalk control reaction (TS(-TMTs)) was initially attributed to inadequate separation of the supernatant and pellet. Subsequent co-sedimentation assays were performed using a 25% sucrose cushion to facilitate complete separation of the supernatant and pellet. However, the continued fractionation of MBP2-Ncd tail-stalk to the pellet, in the presence of the sucrose cushion, indicated that the fusion protein was aggregating. This trend continued in all

co-sedimentation assays performed, regardless of MBP2-Ncd tail-stalk preparation. (Figures 3.4. and 3.8.). Consequently, although the co-sedimentation assays indicate that Ncd tail-stalk monomers and dimers bind TMTs at a 2:1 and 1:1 ratios, respectively, the accuracy of these results is questionable. Regardless, the resulting 2:1 B_{max} of Ncd tail-stalk monomers, combined with previous findings by Walker and Karabay [2] that a 4:1 B_{max} exists between Ncd tail monomers and tubulin, suggests that upon dimerization, steric hindrance reduces the B_{max} by half. However, MBP2-Ncd tail-stalk aggregation prevented the collection of accurate data to support this idea.

MBPs from many species, including *E. coli*, are extremely efficient solubilizing proteins [7]. MBP has been shown to be more effective than the common solubilizing proteins, GST and TRX [9, 10], and has been shown to solubilize a wide range of fusion partner proteins without interfering with the function of the partner proteins. Specifically, MBP-GFP maintained fluorescence, MBP-α- and β- tubulin preserved heterodimer formation, and the most significant example to this study, *Dictyostelium* EB1 maintained the ability to bind MTs [9, 11, 12]. Since highly soluble proteins do not always confer solubility to insoluble fusion partners, the solubilizing function of MBP may not be solely dependent on the innate solubility of MBP. One theory of MBP solubilizing effect involves MBP behaving as a chaperone to sequester folding intermediates of the partner protein, thereby preventing aggregation [9]. For this reason, it is essential that fusion proteins are expressed with MBP at the N-terminus of the partner protein and that MBP itself folds correctly before the translation of the partner protein is complete [9, 13].

In addition to the purification and solubilizing benefits of the MBP expression system, the successful removal of MBP from fusion partner proteins, tubulin and

nucleotide binding domain, by thrombin and Factor Xa has been documented [10, 14]. Large fusion protein tags may interfere with the function of the studied protein. Often it is necessary to remove the fusion tags to ensure that the studied partner protein is not sterically hindered [8]. This may be particularly true for MBP2-Ncd tail-stalk given that, at 40 kDa, MBP is roughly the same size as the 39 kDa Ncd tail-stalk. However, endopeptidases tasked with the removal of tags often require precisely formulated conditions to ensure cleavage specificity. When these conditions are not met, endopeptidases may cleave proteins incompletely or non-specifically [8]. Both thrombin and Factor Xa have a propensity to target secondary cleavage sites, which leads to partially digested, mixed protein populations [8]. These shortcomings of thrombin and Factor Xa did impact the digestion of MBP2-Ncd tail-stalk. Thrombin digestion resulted in the formation of one product between 60-65 KDa and second product that migrates below 50 kDa. The formation of a 60-65 kDa product is the result of non-specific digestion. Since the thrombin product that migrates below 50 kDa is represented by a consistently weaker signal, it may represent a less dominant non-specific digestion of the full fusion protein or it may be a secondary product that results from further digestion of the primary digestive product. Similarly, Factor Xa digestion of MBP2-Ncd tail-stalk results in the formation of a 55 kDa product that is further digested to 50 kDa, evidenced by the indirect relationship between the signal intensities of each product as a function of time. TMT binding assays performed with both thrombin and Factor Xa digestion reactions in place of undigested MBP2-Ncd tail-stalk showed that none of the digestive products pelleted with the TMTs indicating that the digestive products did not retain the TMT binding ability conferred by the Ncd tail (Figure 3.10.). Conversely, undigested

MBP2-Ncd tail-stalk remaining in the one hour thrombin reaction pelleted with the TMTs, indicating that the increased salt concentration in the digestion reaction did not inhibit interactions between Ncd tail-stalk and TMTs. The non-specific digestion of MBP2-Ncd tail-stalk by thrombin and Factor Xa may have directly disrupted TMT binding by the destruction of the Ncd tail domain, or indirectly by cleaving MBP in a way that resulted in MBP interference with the MT binding region of the Ncd tail domain. Variation in protein expression conditions may influence fusion protein folding and, consequently, MBP removal. This is suggested by the ability of MacDonald et al. [14] to remove MBP from tubulin proteins with the use of Factor Xa, and the inability of Hollomon et al. [11] to do the same.

Variations in buffer preparation were shown to play a role in aggregation, as seen by the increased MBP2-Ncd tail-stalk pelleting in buffer A reactions versus buffer B reactions. This indicated that salt was a factor in the aggregation process, and that even a small decrease in salt concentration was sufficient to alter the extent of aggregation. Furthermore, reactions involving concentrated MBP2-Ncd tail-stalk showed increased aggregation (Figure 3.11.). MBP2-Ncd tail-stalk stored in AB buffer supplemented with 500 mM NaCl did not aggregate, as demonstrated by the absence of MBP2-Ncd tail-stalk in the pellet fraction of the stock solution (Figure 3.12.). The decrease in NaCl concentration to 110 mM that occurred upon diluting the stock protein solution in the sedimentation assay reaction, encouraged aggregation. Accordingly, the addition of smaller volumes of concentrated MBP2-Ncd tail-stalk to the reaction volumes exacerbated the aggregation seen with the unconcentrated MBP2-Ncd tail-stalk (Figure 3.12.). This trend is observed in the comparison of E30, FT30, and FT10 (Figure 3.6.)

where fractionation of MBP2-Ncd tail-stalk between the supernatant and pellet is roughly equal in E30 and FT30, and is biased towards the pellet in the FT10 reaction. Interestingly, the absence of MBP2-Ncd tail-stalk in the pellet fractions of the tail-stalk control (TS(-TMTs)) reactions involving MBP2-Ncd tail-stalk from all three preparation indicates no aggregation occurred.

Taken together, the inefficient binding of MBP2-Ncd tail-stalk to the amylose resin, the incomplete or non-specific digestion of MBP2-Ncd tail-stalk by thrombin and Factor Xa, and finally, the tendency of MBP2-Ncd tail-stalk to aggregate all indicate that MBP may be misfolded. Despite the proclaimed purification benefits, it has been acknowledged that MBP fusions do exhibit poor binding to amylose resins [13]. The maltose binding domain is a hydrophobic cleft much like that of the *E. coli* chaperone GroEL and, like that chaperone, MBP may sequester folding intermediates of the fusion partner in the cleft to prevent protein aggregation. In doing so it may also prevent MBP from binding the amylose resin. However, studies involving site-directed mutagenesis of cleft amino acids did not affect the solubility of fusion proteins indicating that MBP may not promote solubility through the hydrophobic cleft [13]. Instead, MBP may simply be unable to bind amylose resin due to misfolding of maltose binding domain. Furthermore, misfolding of MBP can potentially block or affect the formation of the thrombin and Factor Xa site in the linker region between MBP and Ncd tail-stalk. Given the MT binding ability of Ncd tail-stalk, MBP misfolding is a likely candidate for aggregation of MBP2-Ncd tail-stalk. Despite high solubility, MBP has been shown to consistently form temporary insoluble aggregates during the folding process. These aggregates form independently of protein concentration, and quickly renature to the

correct folding without the aide of chaperones [15]. This may indicate that, when fused to the Ncd tail-stalk, MBP renatures into a close form of the native conformation, but one that is unstable in low salt conditions. However, the possibility that MBP2-Ncd tail-stalk aggregation was solely a product of non-specific interactions between fusion proteins, as a result of low salt conditions in the binding assays, can not be discounted.

Future work should include experimenting with the conditions of MBP2-Ncd tail–stalk expression, including culture growth temperatures and IPTG concentrations [7, 8]. In addition, potential renaturation of misfolded MBP should be explored as a mode to facilitate the removal of MBP. It is also necessary to experiment with the salt concentrations in binding assays in order to determine the optimal conditions that promote specific binding between the Ncd tail domain and TMTs, while preventing aggregation. Lastly, while the solubility and functionality of Ncd tail-stalk indicates proper folding of the MT binding domain, the conformation outside the MT binding domain should be examined in order to further elucidate the origin of aggregates.

References

1. Karabay, A. and R.A. Walker, *The Ncd Tail Domain Promotes Microtubule Assembly and Stability.* Biochemical and Biophysical Research Communications, 1999. **258**(1): p. 39-43.
2. Karabay, A. and R.A. Walker, *Identification of Microtubule Binding Sites in the Ncd Tail Domain* Biochemistry, 1999. **38**(6): p. 1838-1849.
3. Karabay, A. and R.A. Walker, *Identification of Ncd tail domain-binding sites on the tubulin dimer.* Biochemical and Biophysical Research Communications, 2003. **305**(3): p. 523-528.
4. Wendt, T., et al., *A Structural Analysis of the Interaction between ncd Tail and Tubulin Protofilaments.* Journal of Molecular Biology, 2003. **333**(3): p. 541-552.
5. Chandra, R., et al., *Structural and functional domains of the Drosophila ncd microtubule motor protein.* J. Biol. Chem., 1993. **268**(12): p. 9005-9013.
6. Inc., N.E.B. *http://www.neb.com/nebecomm/products/faqproductE8000.asp*. 2009 [cited].
7. Sorensen, H. and K. Mortensen, *Soluble expression of recombinant proteins in the cytoplasm of Escherichia coli.* Microbial Cell Factories, 2005. **4**(1): p. 1.
8. Stevens, R.C., *Design of high-throughput methods of protein production for structural biology.* Structure, 2000. **8**(9): p. R177-R185.
9. Kapust, R.B. and D.S. Waugh, *Escherichia coli maltose-binding protein is uncommonly effective at promoting the solubility of polypeptides to which it is fused.* PRS, 1999. **8**(08): p. 1668-1674.

10. Wang, C., et al., *Expression and purification of the first nucleotide-binding domain and linker region of human multidrug resistance gene product: comparison of fusions to glutathione S-transferase, thioredoxin and maltose-binding protein.* Biochem. J., 1999. **338**(1): p. 77-81.

11. Hollomon, D.W., et al., *Fungal beta -Tubulin, Expressed as a Fusion Protein, Binds Benzimidazole and Phenylcarbamate Fungicides.* Antimicrob. Agents Chemother., 1998. **42**(9): p. 2171-2173.

12. Rehberg, M. and R. Graf, *Dictyostelium EB1 Is a Genuine Centrosomal Component Required for Proper Spindle Formation.* Mol. Biol. Cell, 2002. **13**(7): p. 2301-2310.

13. Jeffrey, D.F., B.K. Rachel, and S.W. David, *Single amino acid substitutions on the surface of Escherichia coli maltose-binding protein can have a profound impact on the solubility of fusion proteins.* Protein Science, 2001. **10**(3): p. 622-630.

14. MacDonald, L.M., et al., *Characterization of factors favoring the expression of soluble protozoan tubulin proteins in Escherichia coli.* Protein Expression and Purification, 2003. **29**(1): p. 117-122.

15. Ganesh, C., et al., *Reversible formation of on-pathway macroscopic aggregates during the folding of maltose binding protein.* Protein Science, 2001. **10**(8): p. 1635-1644.

Chapter 4: A summary of experiments aimed at characterizing the cargo binding and regulatory function of the Ncd tail domain.

Summary

Non-claret disjunctional (Ncd) motor protein is essential to maintaining the integrity of mitotic bipolar spindles in *Drosophila* embryos, and is essential to the organization and stability of meiotic spindles in *Drosophila* oocytes [1, 2]. Ncd is composed of three functional domains, specifically a N-terminal tail domain, a stalk domain, and a C-terminal motor domain [2]. This work was aimed at characterizing the regulatory function and microtubule (MT) binding properties of the Ncd tail domain. Data gathered during the course of this project indicate that the Ncd tail domain contains a NLS necessary for nuclear sequestration of Ncd during interphase, thereby regulating its function to M-phase. Additionally, a project aimed at establishing the stoichiometric binding ratio (B_{max}) between the Ncd tail-stalk and the tubulin dimer suggested that the Ncd homodimer binds to the tubulin dimer at less than a 4:1 ratio.

While loss of Ncd function in the cell cycle M-phase results in chromosome non-disjunction [1], uncontrolled activity of Ncd outside of M-phase could result in a detrimental association of Ncd with the interphase MT array that interferes with normal interphase MT function. It is essential that Ncd activity be limited only to the M-phase of the cell cycle. Ncd is retained in the nucleus until prophase [3], indicating that nuclear sequestration may be a mode of regulation to prevent Ncd from interfering with the interphase MT array. Nuclear membrane transport has been well established as a mode for regulating cellular pathways [4].

Active protein transport across the nuclear membrane is reliant upon the presence of a nuclear localization signal (NLS) within the amino acid sequence of the protein being translocated [5]. To locate the presence of a NLS in the Ncd motor protein GFP-Ncd fusion proteins were constructed to contain full length Ncd, individual Ncd domains, or combinations of Ncd domains. GFP-Ncd constructions containing the tail sequence, specifically, full length Ncd (Ncd 1-700), Ncd tail (Ncd 1-200), and a Ncd tail-stalk combination (Ncd 1-355) constructions, localized to the nucleus of transfect S2 cells. In comparison, GFP constructions composed of the stalk domain (Ncd 197-355), the motor domain (Ncd 333- 700), and the combination of the stalk-motor domains (Ncd 197-700) localized to the cytoplasm of the S2 cells. Data from this work demonstrated that the tail domain contains a NLS, therefore, the role of the Ncd tail domain can be expanded to a regulatory level.

In an effort to further define essential NLS residues within the tail domain, GFP-Tail fusion proteins were constructed containing bisections or trisections of the Ncd tail domain. The fusion proteins GFP-Tail 101-200, GFP-Tail 68-134, and GFP-Tail 135-200 localized primarily to the nuclei of transfected S2 cells. In contrast, GFP-Tail 1-100 and GFP-Tail 1-67 localized primarily to the cytoplasm. The low level of nuclear localization observed by GFP-Tail 1-100 and GFP-Tail 1-67 was attributed to passive diffusion through the nuclear pores, facilitated by the small size of the fusion proteins. Out of the three nuclear localizing fusion proteins, GFP-Tail 135-200 was the least sequestered. This indicates that basic amino acid residues within segment 101-134 may be essential to nuclear sequestration. Furthermore, while fusion proteins GFP-Tail 1-100 and GFP-Tail 1-67 localized to the cytoplasm of S2 cells, basic amino acid

residues within these sequence segments may be required to complete nuclear sequestration of GFP-Tail 101-200, GFP-Tail 68-134, and GFP-Tail 135-200. The belief that nuclear sequestration may be supported by residues in both the 1-100 and 101-200 tail segments corresponds with findings by Karabay and Walker [6], which identify two MT binding sites in the tail domain within residue segments 83-100 and 115-187. It is possible that basic residues within MT binding site 83-100 may combine with the basic residues within 101-200 to guarantee complete nuclear sequestration. Alternately, given that GFP-Tail 68-134 encompasses the NLS prediction from the PSORT II algorithm between amino acid residues 92-108 and did not wholly localize to the nucleus, this algorithm may have predicted incorrect basic amino acid clusters as a putative NLS. Since GFP-Tail 101-200 and GFP-Tail 68-134 demonstrated comparable sequestration, it is possible that both fusion proteins contain an identical, single, basic amino acid cluster and have been rescued by flanking acidic and neutral amino acids [7].

Unlike the highly characterized Ncd motor domain [8], the tail has only recently been shown to fulfill a more dynamic role than that of simply binding MTs as cargo. Ncd tail monomers were demonstrated to initialize MT polymerization even during depolymerizing conditions, including lowered temperatures and high Ca^{2+} concentrations [9]. Furthermore, the Ncd tail domain has been shown to mediate diffusional movement along MTs, thereby aiding to the overall movement of Ncd [10]. However, to fully characterize the role of the Ncd tail in this new capacity, a firm understanding of Ncd tail-mediated MT binding must first be achieved. Past research by Karabay and Walker established a 4:1 B_{max} between Ncd tail monomers and tubulin

dimers [6]. However, considering that Ncd exists *in vivo* as a homodimer and that dimerization may restrict the number of Ncd monomers bound to MTs, this study aimed to establish the B_{max} between Ncd tail dimers and the tubulin dimers. Binding assays performed with Ncd tail-stalk proteins and taxol stabilized MTs (TMTs) resulted in a 2:1 Ncd monomer to TMTs ratio, or a 1:1 Ncd dimer to TMTs ratio. However, MBP2-Ncd tail-stalk was detected in the pellet fraction of the co-sedimentation control performed without MTs, indicating that a fraction of MBP2-Ncd tail-stalk was present as aggregates. Consequently, although the co-sedimentation assays indicated that Ncd tail-stalk monomers and dimers bind TMTs at a 2:1 and 1:1 ratios, respectively, the accuracy of these results is questionable. Regardless, the resulting 2:1 B_{max} of Ncd tail-stalk monomers, combined with previous findings by Karabay and Walker [6] that a 4:1 B_{max} exists between Ncd tail monomers and tubulin, suggests that upon dimerization, steric hindrance may reduce the B_{max} by half. However, MBP2-Ncd tail-stalk aggregation prevented the collection of accurate data to support this idea.

The poor binding of MBP2-Ncd tail-stalk to amylose resin and MBP2-Ncd tail-stalk aggregation in binding assays, in comparison to the preserved MT binding function mediated by the Ncd tail-stalk portion of MBP2-Ncd tail-stalk, indicates that MBP may be misfolded. Attempts to remove MBP2 through thrombin and Factor Xa digestion resulted in non-specific digestion of MBP2-Ncd. Thrombin digestion resulted in the formation of one product between 60-65 kDa and second product that migrates below 50 kDa. The formation of a 60-65 kDa product is the result of non-specific digestion. Since the thrombin product that migrates below 50 kDa is represented by a consistently weaker signal, it may represent a less dominant digestion of the full fusion protein or it

may be a secondary product that results from further digestion of the primary digestive product. Similarly, Factor Xa digestion of MBP2-Ncd tail-stalk results in the formation of a 55 kDa product that is further digested to a molecular weight below 50 kDa. To determine whether the product migrating below 50 kDa represented the Ncd tail-stalk (39 kDa) and MBP (42 kDa), TMT binding assays were performed with both thrombin and Factor Xa digestion reactions in place of undigested MBP2-Ncd tail-stalk. None of the digestive products pelleted with the TMTs indicating that the digestive products did not retain the TMT binding ability conferred by the Ncd tail. The non-specific digestion of MBP2-Ncd tail-stalk by thrombin and Factor Xa may have directly disrupted TMT binding by the destruction of the Ncd tail domain, or indirectly by cleaving MBP2 in a way that resulted in MBP2 interference with the MT binding region of the Ncd tail domain.

The inefficient binding of MBP2-Ncd tail-stalk to the amylose resin, the incomplete or non-specific digestion of MBP2-Ncd tail-stalk by thrombin and Factor Xa, and finally, the tendency of MBP2-Ncd tail-stalk to aggregate all indicate that MBP may be misfolded. Furthermore, analysis of the MBP2 Ncd tail-stalk sock solution and experimentation with the salt concentration in binding assays revealed that aggregation occurred upon dilution of protein stock solution in the binding assay solution, which was accompanied by decrease in NaCl concentration. Taken together, this indicates that MBP2 may be folded in manner that promotes aggregation in low salt conditions.

In conclusion, the Ncd tail domain has versatile function that encompasses a regulatory role and is dependent on MT binding. Continued exploration of the Ncd NLS and Ncd tail-mediated MT binding is essential to fully characterizing the function of the

Ncd tail domain. NLS experimentation should be extended to include the expression of a GFP-Ncd tail 68-200 fusion protein in S2 cells, and subsequent monitoring of cellular localization with fluorescent microscopy to determine whether complete nuclear sequestration occurs. Additionally, through site-directed mutagenesis, key basic amino acid residues should be mutated to alanine to determine which mutation results in the elimination of nuclear sequestration. Further exploration of the B_{max} between the Ncd dimer and MTs can include continued work with MBP-Ncd tail-stalk through quantification of aggregated protein for analysis in binding assay ratios. Also, bacterial cell growth and protein expression conditions can be varied to determine optimal, non-aggregation prone expression of recombinant MBP2-Ncd tail-stalk [11, 12]. Lastly, experimentation with binding assay salt concentrations can be performed to determine conditions that promote specific binding between the Ncd tail domain and TMTs, while preventing aggregation.

References

1. Hatsumi, M. and S.A. Endow, *The Drosophila ncd microtubule motor protein is spindle-associated in meiotic and mitotic cells.* J Cell Sci, 1992. **103**(4): p. 1013-1020.
2. Chandra, R., et al., *Structural and functional domains of the Drosophila ncd microtubule motor protein.* J. Biol. Chem., 1993. **268**(12): p. 9005-9013.
3. Sharp, D.J., et al., *Functional Coordination of Three Mitotic Motors in Drosophila Embryos.* Mol. Biol. Cell, 2000. **11**(1): p. 241-253.
4. Makhnevych, T., et al., *Cell Cycle Regulated Transport Controlled by Alterations in the Nuclear Pore Complex.* Cell, 2003. **115**(7): p. 813-823.
5. Görlich, D., et al., *Two different subunits of importin cooperate to recognize nuclear localization signals and bind them to the nuclear envelope.* Current Biology, 1995. **5**(4): p. 383-392.
6. Karabay, A. and R.A. Walker, *Identification of Microtubule Binding Sites in the Ncd Tail Domain* Biochemistry, 1999. **38**(6): p. 1838-1849.
7. Makkerh, J.P.S., C. Dingwall, and R.A. Laskey, *Comparative mutagenesis of nuclear localization signals reveals the importance of neutral and acidic amino acids.* Current Biology, 1996. **6**(8): p. 1025-1027.
8. Wendt, T., et al., *A Structural Analysis of the Interaction between ncd Tail and Tubulin Protofilaments.* Journal of Molecular Biology, 2003. **333**(3): p. 541-552.

9. Karabay, A. and R.A. Walker, *The Ncd Tail Domain Promotes Microtubule Assembly and Stability.* Biochemical and Biophysical Research Communications, 1999. **258**(1): p. 39-43.

10. Fink, G., et al., *The mitotic kinesin-14 Ncd drives directional microtubule-microtubule sliding.* Nat Cell Biol, 2009. **11**(6): p. 717-723.

11. Sorensen, H. and K. Mortensen, *Soluble expression of recombinant proteins in the cytoplasm of Escherichia coli.* Microbial Cell Factories, 2005. **4**(1): p. 1.

12. Stevens, R.C., *Design of high-throughput methods of protein production for structural biology.* Structure, 2000. **8**(9): p. R177-R185.